

1983

The cathodic electrodisposition of polymer latexes

Andrew J. Hadley
Lehigh University

Follow this and additional works at: <https://preserve.lehigh.edu/etd>

 Part of the [Chemical Engineering Commons](#)

Recommended Citation

Hadley, Andrew J., "The cathodic electrodisposition of polymer latexes" (1983). *Theses and Dissertations*. 5164.
<https://preserve.lehigh.edu/etd/5164>

This Thesis is brought to you for free and open access by Lehigh Preserve. It has been accepted for inclusion in Theses and Dissertations by an authorized administrator of Lehigh Preserve. For more information, please contact preserve@lehigh.edu.

THE CATHODIC ELECTRODEPOSITION OF
POLYMER LATEXES

by

J. Andrew Hadley

A Research Report Presented to the
Graduate Committee of Lehigh University
in Candidacy for the Degree of
Master of Science

Lehigh University

1983

The Cathodic Electrodeposition of
Polymer Latexes

by
J. Andrew Hadley

A Research Report Presented to the
Graduate Committee of Lehigh University
in Candidacy for the Degree of

Master of Science

Table of Contents

1. Introduction	11
1.1 Historical	11
1.2 Background	15
1.3 Statement of Problem	22
2. Experimental	23
2.1 Materials	23
2.2 Electrodeposition Apparatus and Procedure	25
3. Experimental Results and Discussion	34
3.1 Polyurethane Acrylic Latex System Development	34
3.1.1 Introduction	34
3.1.2 Latex Preparation and Characterization	35
3.1.2.1 Preparation	35
3.1.2.2 Characterization	43
3.2 Electrodeposition Behavior	47
3.3 Kinetics of Electrodeposition	71
3.3.1 Introduction	71
3.3.2 Film Growth Results and Discussion	81
3.4 Mechanism of Electrodeposition	102
3.4.1 Introduction	102
3.4.2 Results and Discussion	113
3.4.2.1 Film Characterization	114
3.4.2.2 Induction period	118
4. Conclusions	120
5. Recommendations for Future Work	124
References	126
I. Mathematical Analysis of Flocculation Mechanism	132
II. Mathematical Analysis of Accumulation Mechanism	136

List of Figures

Figure 1-1:	Anodic Electrodeposition Process	17
Figure 1-2:	Cathodic Electrodeposition Process	19
Figure 2-1:	Particle Size Distribution, Commercial Resin Emulsion, Sample 1. Emulsifier Concentration = 1.00 %, based on water.	27
Figure 2-2:	Particle Size Distribution, Commercial Resin Emulsion, Sample 2. Emulsifier Concentration = 0.30 %, based on water.	28
Figure 2-3:	Particle Size Distribution, Commercial Resin Emulsion, Sample 3. Emulsifier Concentration = 0.20 %, based on water.	29
Figure 2-4:	Schematic of Electrodeposition Unit	31
Figure 3-1:	Particle size analysis for polyurethane acrylic latex.	44
Figure 3-2:	Dynamic mechanical spectroscopy results; polyurethane acrylic latex.	46
Figure 3-3:	Current - time curves for the electrodeposition of polyurethane acrylic latex, varying applied voltage.	48
Figure 3-4:	Scanning electron micrograph of polyurethane acrylic latex deposited at 200 V. Magnification = 2000X.	50
Figure 3-5:	Scanning electron micrograph of polyurethane acrylic latex deposited at 75 V. Magnification = 100X.	51
Figure 3-6:	Polyurethane acrylic latex, deposition at 160 V., live entry vs. dead entry.	53
Figure 3-7:	Current - time curves, commercial solubilized resin, varying applied voltage.	55
Figure 3-8:	Current - time curves for the electrodeposition of polyurethane acrylic latex; multiple depositions from the same bath.	63
Figure 3-9:	Scanning electron micrograph of polyurethane acrylic latex deposited at 200 V.; fourth use of bath.	64
Figure 3-10:	Film mass versus applied voltage, polyurethane acrylic latex.	68
Figure 3-11:	Film mass versus applied voltage, commercial resin solution.	70
Figure 3-12:	Film mass versus charge passed; polyurethane acrylic latex.	72
Figure 3-13:	Film mass versus charge passed; commercial resin system, 15% solids, varying applied voltage.	73
Figure 3-14:	Film mass versus deposition time; polyurethane acrylic latex deposited at 160 V.	82

Figure 3-15:	Film mass versus square root of deposition time; polyurethane acrylic latex deposited at 160 V.	83
Figure 3-16:	Ln{film mass} versus deposition time; polyurethane acrylic latex deposited at 160 V.	84
Figure 3-17:	Current - time curves for the electrodeposition of ammonium stabilized solubilized and latex systems on Bonderite steel [58].	88
Figure 3-18:	Film mass versus deposition time and square root of deposition time; polyurethane acrylic latex deposited at 160 V.	90
Figure 3-19:	Film mass versus deposition time; polyurethane acrylic latex deposited at 50 V.	92
Figure 3-20:	Film mass versus deposition time, commercial resin in solubilized form.	95
Figure 3-21:	Film mass versus square root of deposition time, commercial resin in solubilized form.	96
Figure 3-22:	Film mass versus deposition time; V-50 stabilized polyurethane acrylic latex deposited at 160 V.	98
Figure 3-23:	Film mass versus square root of deposition time; V-50 stabilized polyurethane acrylic latex deposited at 160 V.	99
Figure 3-24:	Film mass versus deposition time; commercial resin emulsion sample I-3 deposited at 160 V.	100
Figure 3-25:	Film mass versus square root of deposition time; commercial resin emulsion I-3 deposited at 160 V.	101
Figure 3-26:	Schematic of the fixed and fluid layers expected with the accumulation mechanism of electrodeposition.	107
Figure 3-27:	Potential energy curve for a colloidally stable system.	109
Figure 3-28:	Summation of repulsive, attractive and pressure forces acting on the particles.	110
Figure 3-29:	Film mass as a function of waiting time; polyurethane acrylic latex deposited at 160 V.	115
Figure 3-30:	Film mass as a function of waiting time; polyurethane acrylic latex deposited at 50 V.	116


List of Tables

Table 2-1:	Physical Properties and Formulations of Commercial Resin Samples.	26
Table 3-1:	Polyurethane Acrylic Latex Recipe	36
Table 3-2:	Polyurethane acrylic latex polymerization process and recipe variations.	42
Table 3-3:	Effect of applied voltage on coulombic efficiency; polyurethane acrylic latex.	57
Table 3-4:	Effect of applied voltage and bath conductivity on polyurethane acrylic latex electrodeposition performance.	58
Table 3-5:	Effect of applied voltage on coulombic efficiency; commercial resin system.	59
Table 3-6:	Coulombic efficiency vs. number of depositions; polyurethane acrylic latex.	66
Table 3-7:	The effect of electrodeposition and bath parameters on the critical time.	113


CERTIFICATE OF APPROVAL

This research report is accepted and approved in partial fulfillment of the requirements for the degree of Master of Science in Chemical Engineering.

Professor in Charge:


12/12/1983

Department Chairman:


12/14/83

Acknowledgements

The author wishes to express his gratitude and thanks to:

Dr. Mohamed S. El-Aasser under whose direction this work was completed, and who supplied encouragement, advice, and guidance throughout.

Dr. John W. Vanderhoff for his assistance and direction.

Mr. Ken Earhart for his often unsolicited and always helpful suggestions.

Mrs. Olga Shaffer and Ms. Colleen Dolan for their excellent TEM and SEM support.

The Emulsion Polymers Institute of Lehigh University for financial support of the project.

Mr. and Mrs. Alexander Kowalski, the authors parents, for their continued encouragement and advice.

ABSTRACT

With the development of cathodic electrodeposition as a commercially important coating process, considerable research on various aspects of the process has been initiated. However, the majority of this work has been performed using "solubilized" resins which undergo charge destruction at the cathode to form smooth, thin, insulating films. While the theoretically predicted electrical efficiency of deposition from a latex system is considerably higher than that of solubilized resins, little research has been performed on the fundamental aspects of the cathodic electrodeposition of latexes.

In this study, a cationic polyurethane acrylic latex was developed for use in the cathodic electrodeposition process. The latex exhibited unique physical properties, including a broad glass transition and high damping over a wide temperature range, indicating a structure similar to that observed with latex interpenetrating polymer networks. The glass transition began at approximately -20°C ., so films cast from the latex were tough, flexible, and coalesced easily at room temperature.

Using the polyurethane acrylic latex developed and, for comparison, a commercially available solubilized resin, fundamental aspects of the cathodic electrodeposition of latexes were examined. Experimental data showed that the current - time behavior of the

latex and solubilized systems was similar, with the current cut-off for the solubilized systems generally occurring more rapidly, resulting in thinner films deposited with this system (0.3 - 1.0 mil) than with the latex (1.0 - 15.0 mil). Proper optimization of the bath conductivity and deposition voltage were found to be essential to the electrodeposition performance of the polyurethane acrylic latex, whereas the performance of the solubilized resin system was not as sensitive to these parameters. As predicted, the coulombic efficiency of deposition was observed to be much higher with the latex system (100 - 500 mg./coul.) than that obtained with the solubilized system (20 - 40 mg./coul.). The film thickness was found to decrease with increasing voltage for the latex system, while the film thickness increased with increasing voltage with the solubilized system. This opposite trend indicated different film characteristics and a different deposition mechanism for the two systems. The initially deposited latex film was conducting, and only became insulating upon desorption and redispersion of the surfactant back into the electrodeposition bath.

Examination of the constant voltage electrodeposition kinetics of the polyurethane acrylic latex stabilized with an adsorbed quaternary ammonium surfactant showed a two - stage film growth process. These two stages represented the periods of growth when the film was conducting and insulating, respectively. In the first stage, a linear dependence of the film growth on the deposition time

was observed, while in the second stage a linear dependence on the square root of the deposition time was found. The kinetics of deposition for the commercial resin at constant voltage showed single stage growth, dependent on the square root of deposition time, thus indicating that an insulating film governed the growth rate during the entire deposition process with this system. An examination of the constant voltage electrodeposition kinetics of a polyurethane acrylic latex sample stabilized by charged groups able to undergo charge destruction at the cathode was made, and behavior similar to that experienced with the commercial solubilized resin was observed. The two - stage film growth kinetics observed with the polyurethane acrylic latex stabilized by adsorbed quaternary ammonium surfactant were therefore more a result of the inability of the surfactant to experience charge destruction (either electrochemical or acid - base) at the cathode than the particulate nature of the latex system.

An attempt was made to describe the electrodeposition mechanism in terms of flocculation and accumulation theories. The accumulation mechanism proposes an analogy between electrodeposition and particle sedimentation, and predicts the formation of a two - layer deposited film, comprised of a fluid layer of concentrated latex, and a fixed layer of irreversibly coagulated polymer. This two - layer film was observed during the electrodeposition of the polyurethane acrylic latex, indicating that the accumulation

mechanism governed film formation with this system. Mathematical models developed to describe the electrodeposition process for the proposed mechanisms indicated that the induction time (that period during which no deposition takes place) should be affected differently by various electrodeposition parameters, depending on which mechanism was predominant. Attempts to measure the induction period during constant voltage electrodeposition of the polyurethane acrylic latex, and thereby specify the mechanism precisely, were unsuccessful. While the accumulation mechanism was clearly indicated by the observed film characteristics, occurrence of the flocculation mechanism could not be conclusively ruled out.

1. Introduction

1.1 Historical

In its basic form the technology of organic coating application to metallic substrates is very old; as much as 500 years ago significant efforts were being made to develop durable varnish binders, and paint-making was moving from the mortar - and - pestle production of the artist's supply to a larger production basis, resulting in widespread commercial use [6]. Since that time there has been a continued effort to improve both the corrosion protection performance of organic coatings and the procedures used to apply these coatings. While the industrial production of coatings grew to substantial proportions in the nineteenth century, it is only in the past sixty years that extensive scientific attention has been focused on paint technology. During this period significant advances have been made, particularly in the techniques of application that have become available. Various solutions to the problem of how to achieve rapid application of high quality coatings have been developed, including dip coating, rolling, powder coating, spraying, and electrostatic coating. Among the more recent developments in the technology of coatings application, having reached commercial importance only within the past twenty years, is electrodeposition. In this process, an organic coating is applied from an aqueous medium to a conductive substrate. Deposition is brought about by the application of a direct current, hence the

process is primarily electrochemical in nature, in direct contrast to customary coating methods where only mechanical forces are at work. Under the influence of the applied current, charged polymeric molecules or particles migrate electrophoretically to the electrode of opposite charge (anode for negatively charged particles and cathode for positively charged particles). At the electrode the polymer is destabilized or coagulated and deposited on the electrode, forming a paint film; this organic film becomes insulating, thus the electrodeposition process is self-limiting.

The fundamental process of electrophoretic migration of colloidal particles was observed by Ruess as early as 1809 [8]. Pelton and Linder [9] recorded the first observation of an electrodeposit being formed upon the application of a current in 1905 at the University College in London. An early patent for the painting of conductive substrates was granted to Davey, of General Electric Co., who described a process for the making and application of "japan" [13]. However, practical work on the development of electrophoresis as a means of applying organic coatings is generally considered to have begun with experiments carried out in the U.S. between 1923 and 1933. In the earliest of these experiments, Sheppard and Eberlin [44, 45] examined the anodic electrodeposition of natural rubber latex, and suggested several possible applications, including molded articles, covering and impregnation of fabrics, and the production of leather substitutes. In 1933 Beal

described the "anode process", a term chosen to designate "...the production, directly from (natural) rubber latex, rapidly and in one application, of articles and coatings of the highest grade of unmasticated rubber." [3]. Clayton [12] patented a process in the U.K. in 1936 for the interior coating of cans with an oleoresinous lacquer by anodic electrodeposition, and a paper describing the technology of this process was published by Sumner [49] in 1940. In 1938 Turner and Coler [52] examined the electrodeposition of natural rubber latexes on a mercury pool anode, and further experimental work on the anodic electrodeposition of synthetic rubber latexes was reported by Fink and Feinleib [16, 17] in 1945-1948. Early work in India on the topic of electrodeposition is indicated by patents issued there in 1946 dealing with improvements in the electrodeposition of rubber [26].

Unfortunately, none of these early applications progressed to pigmented resin coating systems, and the rate of formation of an adequate film in the early electrodeposition systems proved to be too slow for a high - speed commercial operation [50]. Thus by the end of World War II most of the industrial processes based upon the principle of electrodeposition had been abandoned.

Following World War II, the huge demand for metallic consumer goods in the U.S. (primarily automobiles and appliances), coupled with the development of various synthetic resins suitable for use in

aqueous - based paints and increasing labor costs, led producers to search for new ways to apply corrosion protective coatings. Also, the occurrence of several serious fires in car factories, all centered around the large dip coating tanks then in use, resulted in increasing pressure to develop alternative coating materials and methods. Researchers at Ford Motor Co. in 1959 became concerned with the problem of "solvent wash" and began to search for a way to apply paint to hidden surfaces and complicated workpieces without the need for involved labor or a solvent - based paint [9]. By 1963 this group had developed a coating composition and an electro-dip priming process that was commercially acceptable, and had begun disclosing the information to a number of leading paint manufacturers [43]. During the past twenty years electrodeposition has grown into a widely practiced application technique; currently approximately 64 electrodeposition tanks are in operation in the U.S. automotive industry, with the result that roughly two-thirds of the automobiles produced in the U.S. are electrocoated [60]. In addition, numerous electrodeposition units are in operation in other manufacturing areas, coating items ranging from farm implements to air conditioners and microwave ovens.

Along with the previously mentioned benefits of organic solvent - free coating and the ability to coat recessed areas, the electrodeposition process has additional advantages which have made it particularly attractive in a number of applications [23, 59]:

- Upon application the coating remains in place; thus there are no runs, sags, solvent washing, or "fatty" edges, and very uniform coverage of the workpiece results.
- Complete mechanization of the process is possible, resulting in lowered labor costs over a manual operation.
- Very good corrosion resistance is observed due to the uniform coverage and absence of film pores.
- The electrocoating bath is formulated at approximately 15% solids, so the rheology of the paint (pumping, agitation) is not a significant problem.
- The counter ion required for polymer stabilization in the aqueous system does not generally deposit with the film (unlike conventional aqueous coatings), resulting in improved film properties.

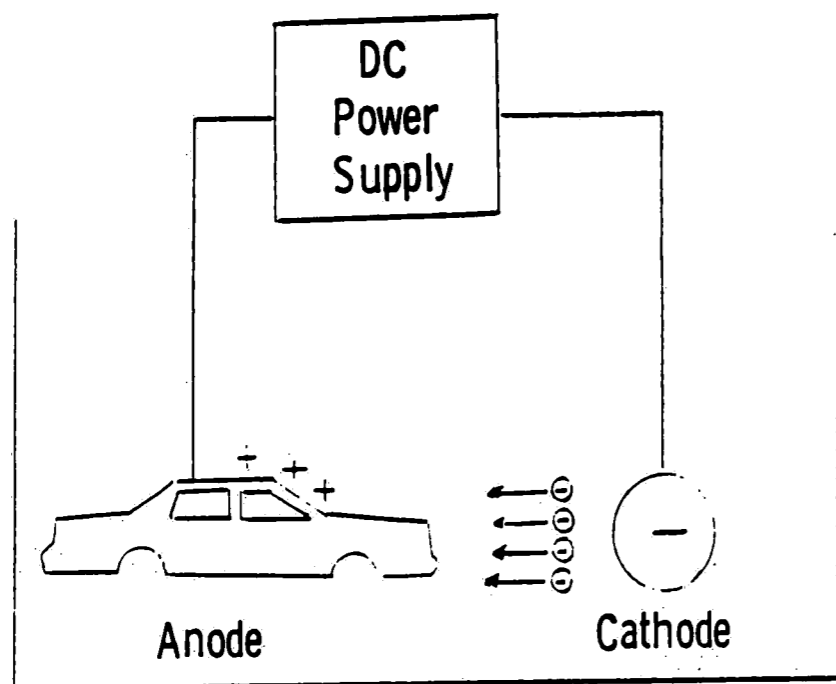
It should be noted that the electrodeposition process does have several disadvantages, including high initial capital costs, strict limitations on coating bath formulation latitude, little masking of substrate surface defects (no "filling"), inability to coat non-conductive objects, and limitations on the film build possible (generally not greater than 15 mil.) [59].

1.2 Background

In the electrodeposition process, a metallic workpiece is placed into a conductive bath and, upon the application of a specific voltage or current, is coated with an insulating film. Thus the electrodeposition process may be viewed as occurring in several distinct stages, including transport of the polymer particles or macro-ions to the workpiece, deposition of the

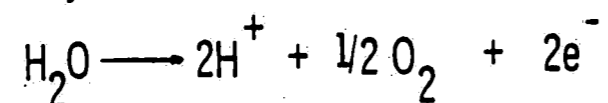
particles onto the object, and growth of the paint film with the coincident insulation of the coated electrode. These various stages may be further considered in terms of specific mechanisms; convection, electrophoresis, electrolysis, coagulation, electroosmosis (the movement of the liquid phase away from the deposited film under the influence of the applied field), and diffusion may all play an important part in the formation of an electrodeposited film. Any analysis of the electrodeposition process must ultimately give consideration to each of these effects.

In anodic electrodeposition, the workpiece is made the anode; consequently the polymer molecules to be deposited must have a negative charge. A schematic of the anodic electrodeposition process is presented in Figure 1-1 (after Wessling [57]). As indicated, the major reactions occurring in anodic electrodeposition are electrolysis of water, oxidation of the anode, and subsequent destabilization and deposition of the resin. The resins utilized in anodic electrodeposition have generally been characterized as carboxyl - containing macro-ions, or polyelectrolytes [4]. These polyelectrolytes are hydrophobic in nature, and are stabilized in the aqueous paint bath due to partial neutralization of the carboxylic acid functional groups by amines or KOH [23]. As anodic electrodeposition was the first commercially successful electrocoating process, the early research concerning the fundamental aspects of the electrodeposition process centered around

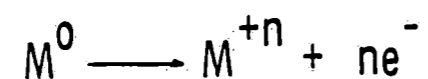


Major Reactions at the Anode:

1) Electrolysis of Water



2) Oxidation of the Anode (Workpiece)



3) Destabilization and Deposition of the Resin

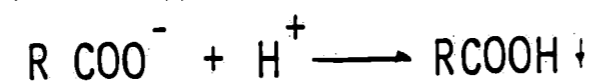
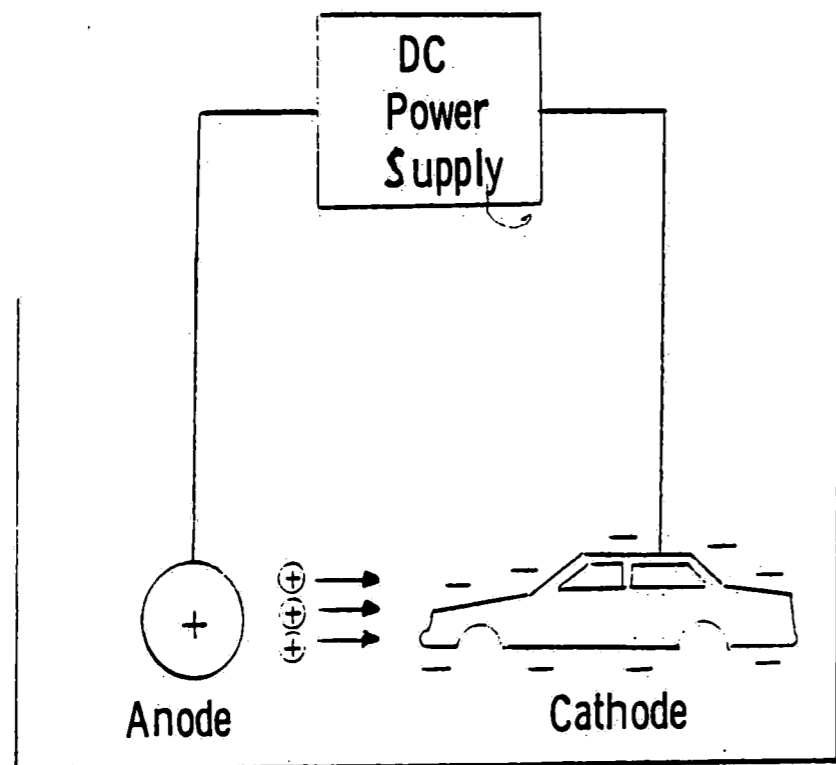


Figure 1-1: Anodic Electrocoat Deposition Process

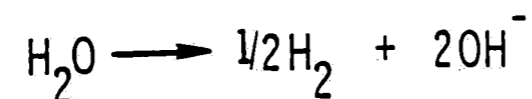
anionic systems. The mechanism of deposition at the anode has been examined by a number of workers [43, 23, 61, 5, 40], and it is generally agreed that deposition takes place primarily by an acid-base charge destruction mechanism (reaction 3, Figure 1-1). In addition to the neutralization of ionized carboxyl groups by protons, Beal [3], Phillips and Damm [37], and Olsen [35] provided experimental evidence indicating that destabilization of the anionic resins by metallic cations generated at the anode (reaction 2, Figure 1-1) is an important deposition mechanism.

While anodic electrodeposition was developed first, primarily due to the availability of anionic paint systems, by 1965 experiments were being carried out on the suitability of cationic resins for electrodeposition. In the cathodic electrodeposition process, the workpiece is made the cathode, and the polymer molecules must carry a positive charge; early efforts to develop cathodic electrodeposition were hindered by the unavailability of cationic resins that were stable (retained charge) at a pH of greater than 6. The cathodic electrodeposition process is outlined in Figure 1-2. As suitable cationic resins became available in the early 1970's, cathodic electrodeposition quickly became recognized as the more desirable electrocoat process for a number of reasons. In cathodic electrodeposition deposition of the paint takes place in a reducing atmosphere (as opposed to the oxidizing atmosphere present in anodic systems), and passivating layers on the



Major Reactions at the Cathode

- 1) Electrolysis of Water



- 2) Deposition of the Resin

Figure 1-2: Cathodic Electrodeposition Process

substrate are not attacked in the alkaline medium surrounding the cathode; both of these factors would be expected to lead to improved corrosion protection [40]. In addition, oxidation of the workpiece does not take place, leading to reduced metal dissolution and a subsequent reduction in both staining of the coating and corrosion of the coated piece. While early workers anticipated no metal dissolution and greatly improved corrosion protection performance with the cathodic system, Murphy [34] and Anderson [2] demonstrated that some dissolution does take place at the cathode, and postulated a mechanism for the alkaline oxidation of metals involving the formulation of soluble metallic oxyanions at the cathode during deposition. However, these and other researchers did observe that the corrosion protection performance of cathodically deposited films (as measured by salt spray and weatherometer exposure tests) was considerably improved over that of films deposited anodically. Upon recognition of the advantages offered by the process, many installations switched from anodic to cathodic coating; today 98% of the automotive coating tanks in operation in the U.S. are cathodic.

Along with the development of commercial cationic electrodeposition systems, fundamental research programs were initiated concerning the mechanism of deposition and other aspects of the cathodic process [60, 59, 42, 38, 7]. However, these studies were carried out with cationic polyelectrolyte resins similar in nature (solubilized) to those used in anodic systems. These

cationic resins were stabilized by the addition of carboxylic acids [29] and consequently were easily destabilized in the alkaline region surrounding the cathode, resulting in a smooth uniform film. However, these macro-ions are both relatively low in molecular weight and high in charge - to - mass ratio, leading to a low electrical efficiency and the requirement of a post-deposition curing reaction. It has long been recognized that the electrical efficiency of deposition from a latex system would be expected to be significantly higher than that from a solubilized polyelectrolyte system [18]. In addition, a latex could be deposited at a high molecular weight without affecting the rheology of the coating bath, thus eliminating the need for a curing reaction following deposition. However, with the exception of the early work on the fundamental aspects of the anodic electrodeposition of natural rubber latex, little research has been undertaken in this area. Wessling, et al, have reported various aspects of the electrodeposition of cationic latexes, including the effect of the surfactant structure on the deposition behavior [57, 58, 56]; the kinetics of the electrodeposition process were not examined. Recent work by Humayun [25] in this laboratory on the electrodeposition of cationic epoxy latexes has indicated that the kinetics and mechanism of deposition from an ammonium stabilized latex differ considerably from those proposed for typical solubilized cationic macro-ion systems.

1.3 Statement of Problem

The objectives of this research project were to develop a latex system suitable for use in the cathodic electrodeposition process, and using this system, to examine some of the fundamental aspects of the electrodeposition of latexes. Included in these objectives were analysis of the mechanism and kinetics of deposition, and a comparison of the electrodeposition behavior of the latex to that of a commercial solubilized resin system.

2. Experimental

2.1 Materials

Several different electrodeposition resins were used in the various experiments performed in this study. A significant portion of the experimental work was devoted toward the development and characterization of a cationic polyurethane - acrylic latex system suitable for use in the cathodic electrodeposition process, therefore the preparation and properties of this latex will be discussed in detail in the "Results and Discussion" section.

In addition to the primary latex system, electrodepositions were carried out using a commercially - available "solubilized" resin. This resin was received from the manufacturer as a 60% non-volatile organic solution, and was composed of an amine - modified epoxy/isocyanate blend. The aqueous electrodeposition solution was prepared by adding 2% acetic acid (based on resin solids) to 20% of the final deionized water, followed by addition of the feed resin with vigorous agitation. Subsequently, the remaining 80% of deionized water was added with continued agitation following which the solution was vacuum stripped at 50 °C in a Buchler rotary evaporator to remove the organic solvent and adjust the solids to the desired level. No surfactant was added during the preparation of the "solubilized" resin; stabilization of the polymer in the aqueous system was a result of protonation of the amino-functional

groups bound to the resin molecules in the presence of the acetic acid ("solubilizer") [29].

Electrodeposition samples were also prepared from the commercial feed resin using a cationic surfactant (hexadecyl trimethyl ammonium bromide) and no acidic solubilizer, resulting in latexes with well-defined particle size and stabilized primarily by the adsorbed surfactant. These latexes were prepared by a direct emulsification process using a mixed emulsifier system [53]. Prior to emulsification, the commercial feed resin was diluted to 40% N.V. with a mixture of toluene and xylene (toluene:xylene = 2.2:1) in order to reduce the solution viscosity and lower the relative proportion of the more water-miscible solvents. Hexadecane was added to the diluted feed resin solution at a level such that the weight ratio of surfactant to hexadecane in the final latex was 2:1. The HDTMAB emulsifier (0.2 - 1.0%, wt. percent based on water) was dissolved in deionized water held at 30 °C. The feed resin solution containing the hexadecane was then added to the surfactant solution with vigorous agitation and held at 30 °C for another 30 minutes. The resulting crude emulsion was sonified in 500 ml. portions for 3 minutes using a Branson Ultrasonic Cell Disrupter, and homogenized by passing through a Manton-Gaulin Submicron Disperser at a pressure of 5000 psig. To insure efficient dispersion the emulsions were homogenized three times. Following emulsification the latex was vacuum stripped at 50 °C in a Buchler rotary evaporator and samples

taken to determine solids content.

The physical properties and formulations of the commercial resin electrodeposition samples are outlined in Table 2-1. The commercial feed resin emulsions all appeared stable with no coagulum evident during emulsification or stripping. Upon standing for 5 weeks a very thin layer of polymer was visible at the bottom of the storage bottles, and the solids had dropped slightly (e.g. from 15.2% to 14.3% for Sample I-3), indicating that a small amount of settling and coagulation had occurred.

The emulsion samples were examined with the transmission electron microscope (using the cold stage to prevent deformation of the particles under the electron beam) and a particle size analysis made. The results of this analysis are presented in Figures 2-1 - 2-3. It should be noted that, within experimental error, the particle size did not vary greatly with varying surfactant concentration, and in all cases the particle size distribution (as indicated by the polydispersity index, PDI) was fairly broad.

2.2 Electrodeposition Apparatus and Procedure

The electrodepositions were performed at room temperature in a rectangular plexiglas cell of dimensions 2.7 cm. x 3.8 cm. x 9.0 cm. Two carbon anodes were connected in parallel, and these were placed at either end of the cell, separated by a distance of 6.0 cm.

Table 2-1: Physical Properties and Formulations of Commercial Resin Samples.

SAMPLE	O/W RATIO (prior to stripping)	Surfactant (wt. % B.O.W.)	pH	CONDUCTIVITY (μ S/cm)	SOLIDS (following stripping)
Solubilized Resin	0.25/1	(0.50% acetic acid "solubilizer")	6.4	1590	15%
Emulsion I-11	0.33/1	1.00% HDTMAB	7.7	811	15%
Emulsion I-21	0.33/1	0.30% HDTMAB	7.5	516	15%
Emulsion I-3	0.33/1	0.20% HDTMAB	7.8	460	15%

SAMPLE LATEX I-1

$D_n = 207.5$	PDI = 1.756
$D_w = 364.3$	$D_{min} = 33.2$
$N = 968$	$D_{max} = 674.1$
$D_v = 257.9$	$D_a = 233.3$
$S_d = 106.7$	STEP = 22.1
$D_q = 404.2$	$D_s = 315.2$

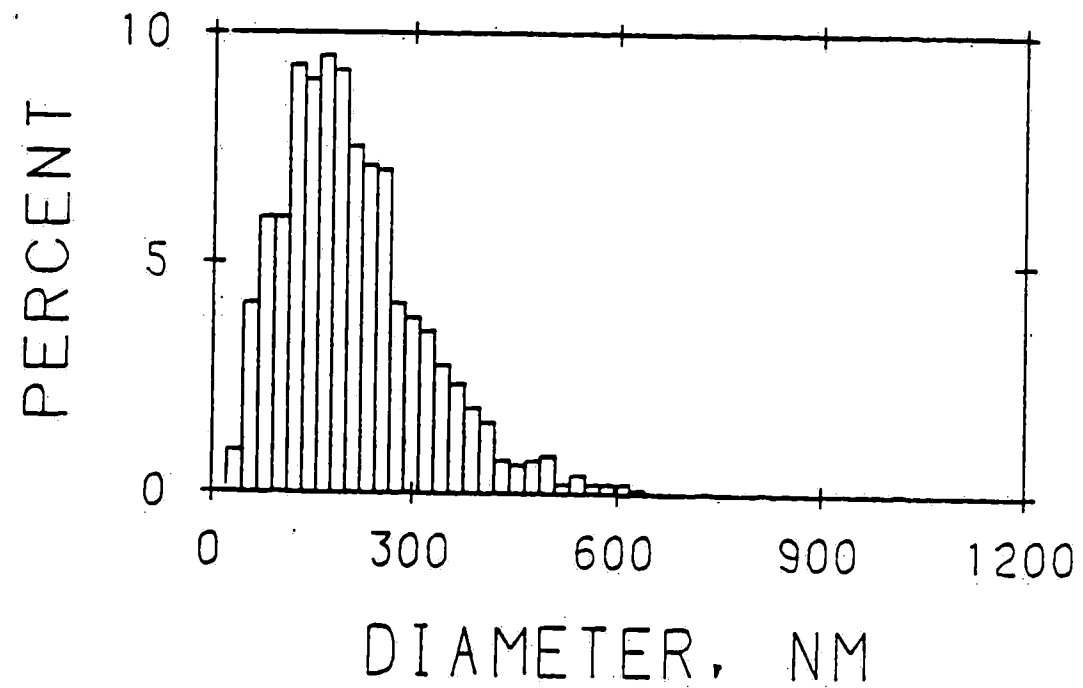


Figure 2-1: Particle Size Distribution, Commercial Resin Emulsion, Sample 1. Emulsifier Concentration = 1.00 %, based on water.

SAMPLE LATEX I-2

$D_n = 162.7$	PDI = 3.197
$D_w = 520.2$	$D_{min} = 56.0$
$N = 719$	$D_{max} = 1137.7$
$D_v = 229.6$	$D_a = 190.2$
$S_d = 98.6$	STEP = 37.3
$D_q = 690.5$	$D_s = 334.6$

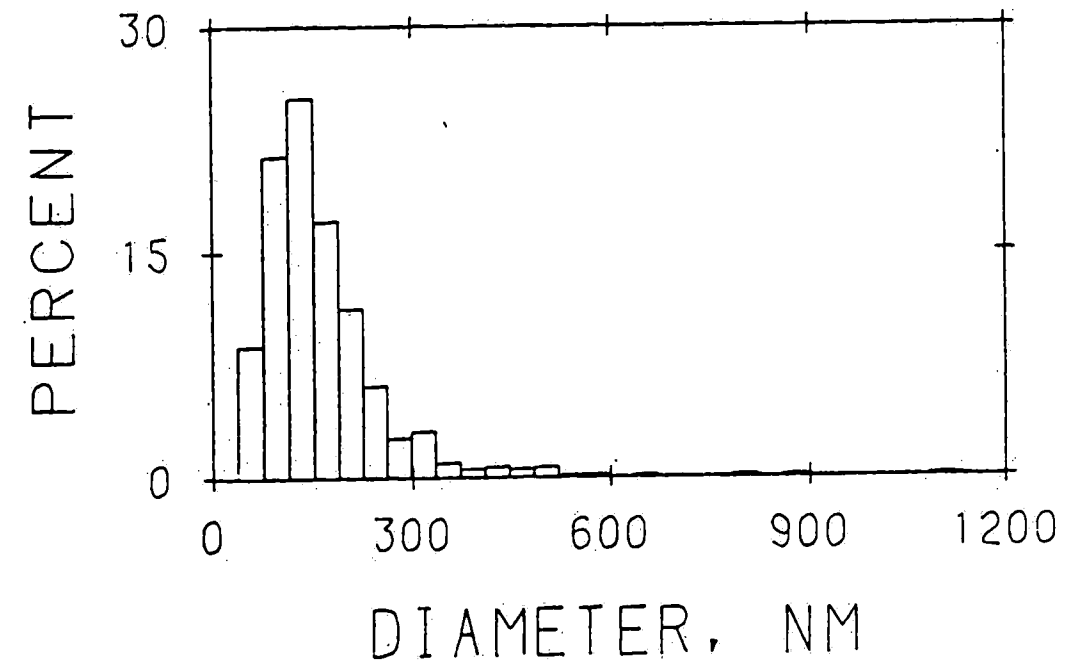


Figure 2-2: Particle Size Distribution, Commercial Resin Emulsion, Sample 2. Emulsifier Concentration = 0.30 %, based on water.

SAMPLE LATEX I-3

D_n = 182.1	PDI = 2.815
D_w = 512.7	D_{min} = 75.0
N = 723	D_{max} = 1225.0
D_v = 241.3	D_a = 205.7
S_d = 95.8	STEP = 50.0
D_q = 693.3	D_s = 331.9

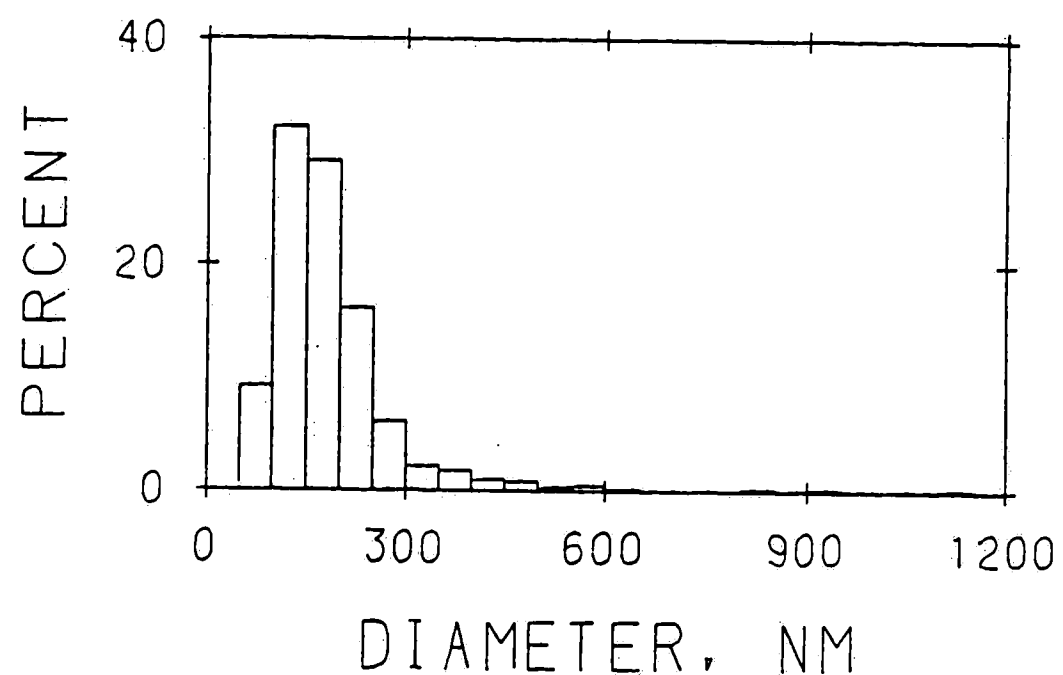
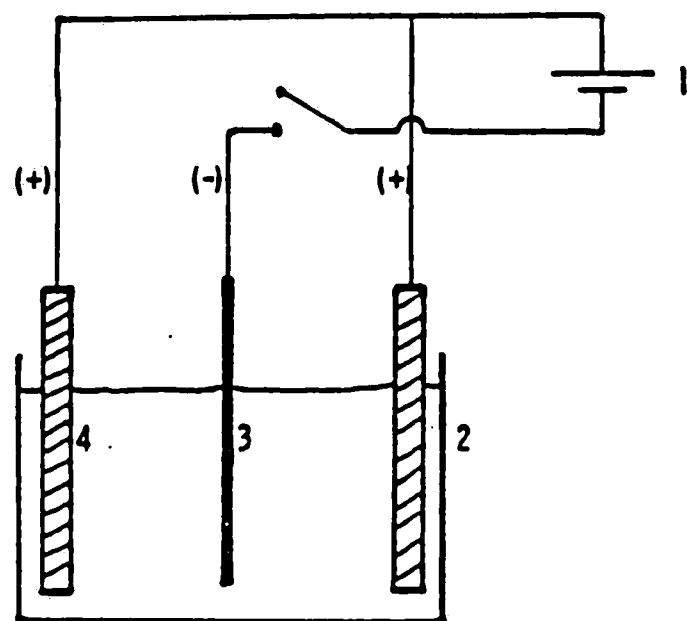


Figure 2-3: Particle Size Distribution, Commercial Resin Emulsion, Sample 3. Emulsifier Concentration = 0.20 %, based on water.

Carbon was used for the anode material in order to prevent dissolution of this electrode during deposition, thus avoiding contamination of the bath with metallic cations. The cathode sample bars upon which depositions were made were Q-Panel, type QD standardized samples of smooth (mill rolled), cold rolled, low carbon steel, with nominal dimensions 15.5 cm. x 2.2 cm. x 0.051 cm. During electrodeposition the sample bar was lowered into the bath midway between the anodes using a motor drive, at a speed of 3 feet per minute.

The power supply for the electrodepositions was a PPG Elcoat laboratory unit capable of providing 750 Volts D.C. and 10 Amperes; the design of the unit was such that only constant applied voltage depositions could be performed. A schematic of the electrodeposition unit is shown in Figure 2-4. Included in the circuit were a Keithley autoranging digital voltmeter to facilitate accurate setting of the applied voltage, and a strip chart recorder to measure the current passing through the electrodeposition cell as a function of time. In addition, an external switch was included in the electrodeposition circuit which permitted the power supply to be turned on without current flowing through the electrodeposition cell. This served two purposes; it provided a means of allowing the power supply to stabilize at the desired voltage setting prior to deposition (preventing voltage fluctuations during deposition), and it enabled the cathode sample to be placed in the bath without



- 1 - 750 Volt, 10 Amp DC Power Supply
- 2 - Rectangular Plexiglas Cell
- 3 - Q - Panel (Type QD) Steel Cathode Sample Bar
- 4 - Carbon Anodes

Figure 2-4: Schematic of Electrodeposition Unit

deposition occurring while the power supply stabilized.

Electrodeposition was typically performed by turning on the power supply and setting the desired voltage, with the external switch in the "off" position. The cathode bar was weighed on a Mettler balance, then connected to the electrodeposition circuit and lowered into the bath ("dead entry"). The run was begun by starting the strip chart recorder, then moving the external switch to the "on" position. No agitation of the bath was provided during deposition. After the desired electrodeposition time, the switch was again moved to the "off" position and the cathode sample bar raised from the bath with the motor drive. Following deposition the sample was dip rinsed with deionized water, dried to a constant weight in a vacuum oven at room temperature, and reweighed to determine the total deposited film mass. The area under the current - time curve obtained from the strip chart recorder was integrated using a Carl Zeiss MOP-3 analyzer in order to calculate the amount of charge passed during deposition. Finally the film area and thickness were measured.

A second type of electrodeposition run was performed by placing the external switch in the "on" position prior to lowering of the sample into the bath. While this "live entry" type of deposition was not as useful in determining the kinetics of electrodeposition as the "dead entry" discussed above, it is the type of deposition

commonly performed commercially, and hence was useful for comparison purposes.

Electrodepositions were generally performed from 15% solids dispersions, with applied voltages in the range 30 - 300 Volts, resulting in initial field strengths in the bath of 10 - 100 Volts/cm. The coated area of the cathode samples was approximately 12 cm.², and the initial current was on the order of 0.5 A., thus the maximum current density was roughly 40 mA/cm.². Samples were coated from very short times (<1.0 sec.) up to >60 sec. depending on the current cut-off behavior. Film thicknesses typically ranged from 0.5 - 30.0 mil.

3. Experimental Results and Discussion

3.1 Polyurethane Acrylic Latex System Development

3.1.1 Introduction

Previous research was performed in this laboratory on the electrodeposition behavior of cationic Epon 1001 latexes, and mixtures of cationic epoxy - curing agent (Epon 1001 + Emerez 1511) latexes [25]. While the work done with the Epon 1001 latex prepared by direct emulsification proved useful in elucidating some of the fundamental aspects of the cathodic electrodeposition process, the quality of the films deposited from this latex were generally poor as a result of the glassy behavior of the polymer at the deposition conditions. Films deposited with this latex showed poor coalescence on the substrate and generally cracked or flaked off of the substrate upon drying. Alternatively, analysis of the electrodeposition behavior of the Epon and Emerez mixture was found to be complicated by the concurrent heteroflocculation between the two components and the crosslinking reaction occurring at the particle - particle interface. As a result of these various phenomena, it was decided to investigate the possibilities of developing a single - component latex system which would form reasonably good films in the cathodic electrodeposition process, and would require no post-deposition curing. Vanderhoff et al [54], Matsunaga [32], and Woo [62], indicated that tough protective

coatings of high gloss could be obtained from aqueous single - component polyurethane dispersions, thus it was on this system that efforts to develop a suitable cationic latex were concentrated.

3.1.2 Latex Preparation and Characterization

3.1.2.1 Preparation

The latex system under investigation consisted of a polyurethane acrylic copolymer; a sample recipe used for the preparation of this latex is shown in Table 3-1. The latex was prepared in a three step process involving a solution polymerization step, an emulsification step, and subsequent emulsion polymerization. This process is very similar to that described by Vanderhoff et al [54]; the major difference in the polymer obtained results from the unique structure and reactivity of the diisocyanate monomer used. In the first stage, a solution of isophorone diisocyanate (3-isocyanatomethyl-3,5,5-trimethyl cyclohexyl isocyanate, Veba Chemie, AG), 2-hydroxy propyl methacrylate (2-HPMA), butyl acrylate (BA), and isobutyl methacrylate (IBMA) was prepared. Isophorone diisocyanate contains two differently combined isocyanate groups, with the aliphatic isocyanate approximately ten times as reactive as the cycloaliphatic one [55]. Consequently, the more reactive isocyanate could be reacted somewhat selectively with the active hydrogen of the 2-HPMA, while leaving the second (cycloaliphatic) isocyanate group available

Table 3-1: Polyurethane Acrylic Latex Recipe

CATIONIC POLYURETHANE - ACRYLIC LATEX

<u>Component</u>	<u>Moles</u>	<u>Unit Wt. %</u>
2-Hydroxy Propyl Methacrylate	1	4.0
Isophorone Diisocyanate	3	17.5
Polyol PCP-0200	2	27.8
Butanol	1	2.1
Butyl Acrylate	4.6	15.4
Isobutyl Methacrylate	8.4	31.2
Acrylic Acid	1.1	2.0

Distilled Deionized H₂O = 400 gm.

Hexadecyl Trimethyl Ammonium Bromide - 3 gm.

Hexadecane - 2 gm.

for further reaction. This was accomplished by adding dibutyl tin dilaurate, a low temperature catalyst, to the above described solution and agitating at 60 °C. for 1/2 hour. Prior to raising the temperature the system was inhibited with phenothiazine to prevent bulk free - radical polymerization of the acrylic monomer (BA, IBMA, 2-HPMA) at this stage. Following the reaction of a portion of the isophorone diisocyanate with the 2-HPMA, a caprolactone diol (Polyol PCP-0200, Union Carbide), was added to the solution and reacted with the isophorone diisocyanate for one hour at 80 °C. Butanol was then added to the solution and allowed to react for another hour at 80 °C. in order to "block" any residual isocyanate groups and prevent further growth of the polyurethane chain. This solution then consisted ideally of urethane prepolymer with a molecular weight of approximately 2000 terminated at one end with a reactive vinyl group, dissolved in a monomer solution of BA and IBMA. It must be noted that the isocyanate reactions were not completely specific, thus along with the urethane prepolymer described above the solution contained a significant fraction of higher molecular weight polyurethane containing no vinyl groups as well as polyurethane terminated at both ends with reactive vinyl groups (leading to crosslink sites in the final polymer; the development of crosslinking during the free - radical polymerization of this system has been observed by other workers in this laboratory [36]).

The second stage of the polyurethane acrylic latex synthesis

route involved emulsification of the prepolymer solution by essentially the same technique used in the formulation of the commercial resin emulsions (Ref. Experimental), and consisted of preparation of a crude emulsion by standard techniques using the hexadecane / hexadecyl trimethyl ammonium bromide mixed emulsifier system, followed by sonification and homogenization to yield a stable prepolymer emulsion.

The final preparation stage consisted of free - radical emulsion polymerization of the acrylic monomer in the resulting emulsion. Two alternative methods of initiating polymerization were used. In the first of these a water - soluble azo - type initiator, V-50 (2-2'-Azobis(2-amidino-propane)HCl, Crescent Chemical Co.) and a small quantity of surfactant were dissolved in water, and the prepolymer emulsion was added to this solution with agitation at 60 °C. over a period of four hours. Following addition of the emulsion, the reaction was continued at 60 °C. for another 12 hours in order to obtain a high conversion. Finally the latex was vacuum stripped at 50 °C. in a Buchler rotary evaporator to remove any residual monomer and adjust the solids to the desired level. Analysis of the amount of monomer collected during stripping indicated that conversions of greater than 95% were obtained.

The second method of initiating polymerization employed used an oil - soluble initiator, lauroyl peroxide. In this method of

initiation the initiator was dissolved in the prepolymer emulsion prior to emulsification. In the emulsion polymerization step a surfactant solution was prepared, and the prepolymer emulsion containing the dissolved initiator was added to the solution, polymerized, and stripped under conditions identical to those employed with the V-50 initiated system. Analysis of the amount of monomer collected during stripping indicated that high conversions were also obtained using the lauroyl peroxide initiator.

The lauroyl peroxide and V-50 initiators were observed to result in latexes with considerably different electrodeposition behavior; this difference resulted from the nature of the radical fragment generated during polymerization with the different initiator systems. The radical fragment generated with the V-50 initiator was cationic, thus a positive bound charge (in addition to the charge resulting from the adsorbed surfactant) was imparted to the latex particles; this charge was observed to be very pH dependent (ionized at pH of less than 6), which would be expected to affect the electrodeposition behavior of the latex. The lauroyl peroxide radical fragment was nonionic, thus polymerization with this initiator did not affect the surface charge or pH stability of the latex particles. However, it was observed that during polymerization with the lauroyl peroxide the pH tended to drift downwards from approximately 6.5 at the beginning of polymerization to about 4.0 following polymerization. A possible mechanism for the

drop in pH during polymerization has been suggested by Ghosh and Maity, who examined the polymerization of acrylic monomer with acyl peroxide initiator in the presence of quaternary ammonium salts [19]. Their results indicated the occurrence of an interaction between the acyl peroxide and the quaternary ammonium components during polymerization, leading to the generation of hydrogen ions.

Several variations on the polymerization process were examined, including elimination of the post-emulsification sonification and homogenization steps, and addition of the aqueous V-50 initiator solution directly to the monomer emulsion. However, with both of these modifications large amounts of coagulum were obtained during polymerization, and the original process outlined above appeared to be the most effective in preparing stable polyurethane acrylic latex. Along with variation of the polymerization process, the composition of the acrylic (main) polymer chain was varied, while the ratio of acrylic to polyurethane was held constant at 1:1 (W:W). Early formulations of the polyurethane acrylic latex yielded glassy, brittle films that did not adhere well to the steel electrodeposition substrate. Acrylic acid (2% based on the total monomer) was added to the formulation and the adhesion was observed to improve considerably. Wessling et al [57] have reported that the glass transition temperature (T_g) of a polymer greatly affects its electrodeposition behavior, and that for optimal performance the polymer should be marginally film forming at the deposition

temperature. Humayun [25] observed that a glassy polymer resulted in electrodeposited films that were thick (indicating poor current cut-off behavior), poorly coalesced, and cracked upon drying. In order to vary the T_g of the polyurethane acrylic polymer, the ratio of butyl acrylate to isobutyl methacrylate was varied, and good films (flexible, tough, not tacky or glassy) were obtained with a 27 wt. percent BA, 63 wt. percent IBMA composition.

Finally, in order to observe the effect on electrodeposition, a sample of polyurethane acrylic latex was prepared using the V-50 initiator and subsequently "cleaned" of adsorbed surfactant; this latex was then stabilized primarily by the cationic V-50 initiator fragments bound to the latex particles. Removal of the adsorbed surfactant was accomplished using serum replacement; this technique involved separation of the latex serum from the bulk latex by pumping deionized water through the latex sample confined in a Plexiglas[™] cell with a 0.2 micron pore size Nuclepore[™] filter. The conductivity of the exit stream was monitored and cleaning considered to be essentially complete when the conductivity did not vary greatly with time. The conductivity of the cleaned latex at 15% solids was 180 $\mu\text{S}/\text{cm}$, compared with a value of 1100 $\mu\text{S}/\text{cm}$ prior to cleaning.

A summary of the variations in the polymerization process and recipe is provided in Table 3-2.

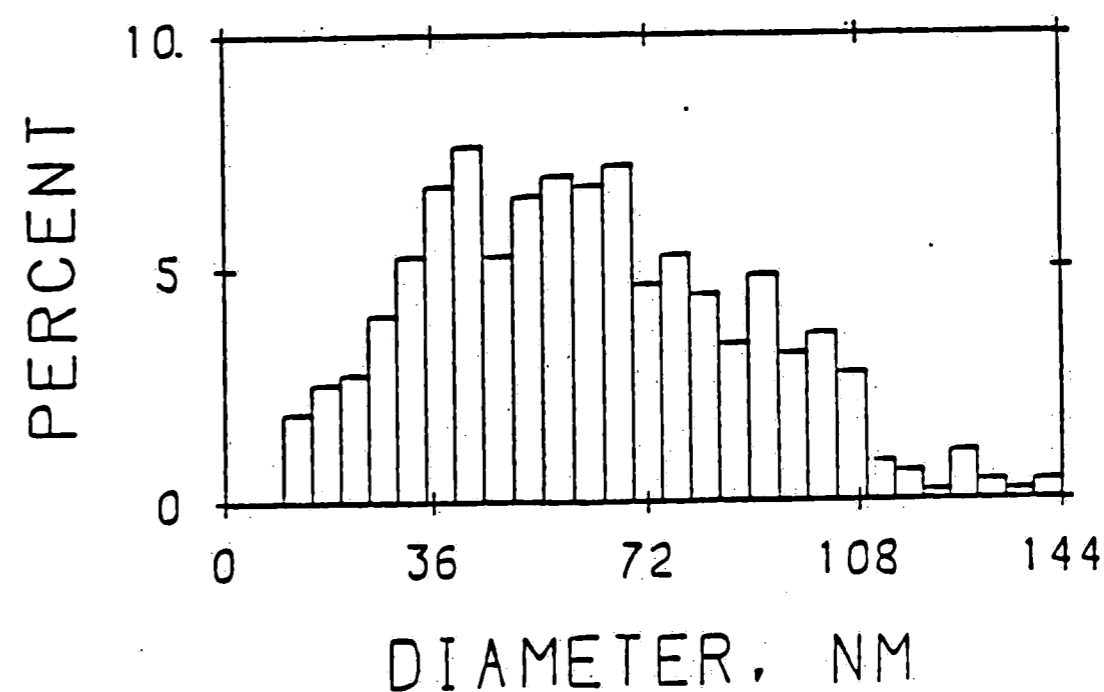
Table 3-2: Polyurethane acrylic latex polymerization process and recipe variations.

LATEX SAMPLE	FORMATION	LATEX PROPERTIES	ELECTRO-DEPOSITION BEHAVIOR
JAH-1	(first attempt; V-50 initiator; no acrylic acid)	tacky film; poor adhesion	extensive gassing; poor film; low coulombic efficiency
JAH-3	increased IBMA fraction; acrylic acid added	brittle(glassy) film; poor coalescence	increased gassing; slow current cut-off; low coulombic efficiency
JAH-4	decreased IBMA fraction slightly	tough, flexible film, not tacky or glassy; good coalescence and adhesion	reduced gassing; thinner film; low coulombic efficiency
JAH-6	eliminated homogenization (latex coagulated during polymerization)	-----	-----
JAH-7	substituted Lauroyl Peroxide for V-50 initiator	same behavior as sample JAH-4	decreased gassing; good film; higher coulombic efficiency
JAH-8	added V-50 solution directly to monomer emulsion (latex coagulated during polymerization)	-----	-----
JAH-9	reduced surfactant concentration	same behavior as sample JAH-4	further reduced gassing; very smooth film; increased coulombic efficiency
JAH-11	V-50 initiator; following polymerization latex "cleaned" using Serum Replacement	same behavior as sample JAH-4	little gassing; very thin, smooth film; extremely high coulombic efficiency (5 times that of JAH-9)

3.1.2.2 Characterization

Characterization of the polyurethane acrylic latex properties was essential to the understanding of the electrodeposition behavior of this system. As a first step in this characterization, average particle size and particle size distribution were determined using cold - stage transmission electron microscopy. As the acrylic portion of the polymer was transparent to electrons, it was necessary to "stain" the samples using phosphotungstic acid prior to examination in the TEM. The results of the particle size analysis are shown in Figure 3-1; it is evident from this analysis that the latex had a fairly broad distribution (PDI= 1.49), which was typical of emulsions prepared using the direct emulsification process.

Differential scanning calorimetry (DSC) was used to determine the T_g of an air-dried sample of the polyurethane acrylic latex. The sample was scanned from 200 K. to 400 K., at heating rates of 20 °C./min. and 10 °C./min. on a Perkin-Elmer DSC-1B system. Essentially identical scans profiles were obtained for the two runs. A broad T_g was observed, spanning from approximately 260 K. (-13 °C.) to 320 K. (47 °C.). This broadened T_g indicated that some phase separation may have been occurring in the polymer; thus further examination of the thermal properties was made using dynamic mechanical spectroscopy (DMS). In this technique a direct - reading viscoelastometer (Rheovibron) was used to apply a sinusoidal strain of fixed frequency to one end of a dried film of the polymer. The



$$D_n = 63 \text{ nm}$$

$$D_w = 93 \text{ nm}$$

$$\text{P. D. I.} = 1.49$$

Figure 3-1: Particle size analysis for polyurethane acrylic latex.

response (stress) was then measured at the opposite end of the sample as a function of temperature, and the storage modulus (E') and tan delta (the ratio of energy dissipated to energy stored, a measure of damping) determined. The polyurethane acrylic sample was scanned from $-100\text{ }^{\circ}\text{C.}$ to $50\text{ }^{\circ}\text{C.}$ at a frequency of 100 Hz. ; the resulting values of E' and tan delta are shown in Figure 3-2. In agreement with the results of the DSC analysis, the polymer exhibited a broad glass transition, as indicated by the wide temperature range of decreasing modulus and increasing damping (approximately $-25\text{ }^{\circ}\text{C.}$ to $50\text{ }^{\circ}\text{C.}$). A similarly broad transition region has been reported by Allen et al [1] for composites formed by interstitial polymerization of vinyl monomers in polyurethane elastomers. The broad transition behavior may be taken to indicate that extensive but incomplete mixing of the polymer components had occurred, similar to that found by Sperling [46] in semicompatible latex interpenetrating polymer networks. While the polyurethane acrylic copolymer cannot be considered to be a true interpenetrating polymer network, the crosslink sites generated during the prepolymer reaction (polyurethane oligomers with two vinyl functional groups) would be expected to lead to a polymer with properties similar to those of IPNs. From a practical point of view, this broad T_g is very desirable, as the mechanical behavior of the polymer consequently remains relatively constant over a broad temperature range, and such problems as coating bath temperature control become

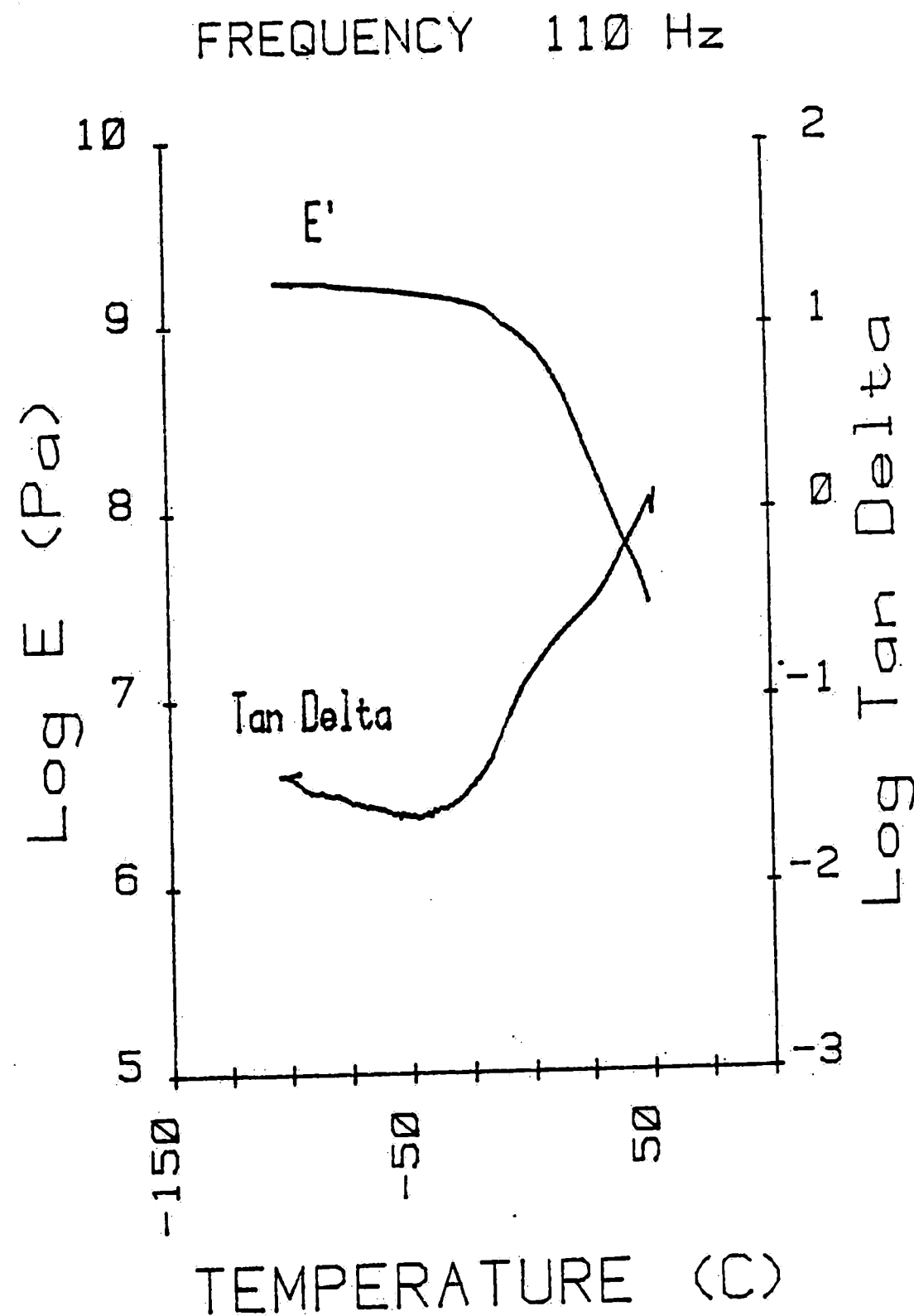


Figure 3-2: Dynamic mechanical spectroscopy results; polyurethane acrylic latex.

less crucial to the electrodeposition behavior. In addition, the damping exhibited by the polymer over a wide temperature range is a very desirable characteristic for a coating to be used on a vibrating (e.g. automobile) or noise reducing surface in a range of application temperatures [47, 48]. It is important to note that this polymer composition gave good electrodeposition behavior, and did not exhibit the undesirable characteristics of the Epon 1001 and Epon / Emerez latexes studied earlier.

3.2 Electrodeposition Behavior

The current - time behavior of the polyurethane acrylic latex deposited until current cut-off (constant residual current) at various applied voltages and live entry may be seen in Figure 3-3. The current - time curves are similar to those reported by Wessling et al [58] for the electrodeposition of latexes prepared with an ammonium surfactant. The shape of the current - time curve obviously depended strongly on the deposition voltage. The initially increasing current was an indication of the increasing electrode area as the sample was lowered into the bath with live entry; at a lowering speed of 3 ft./min. the immersion was completed in approximately 2 seconds. At low voltages the film remained conducting for a longer time, as is evident from Figure 3-3, curve a; the current was relatively constant at 180 mA. for a period of 8 sec., after which it slowly decreased to a constant value of 10 mA. The current - time curve for the highest applied voltage tested (225

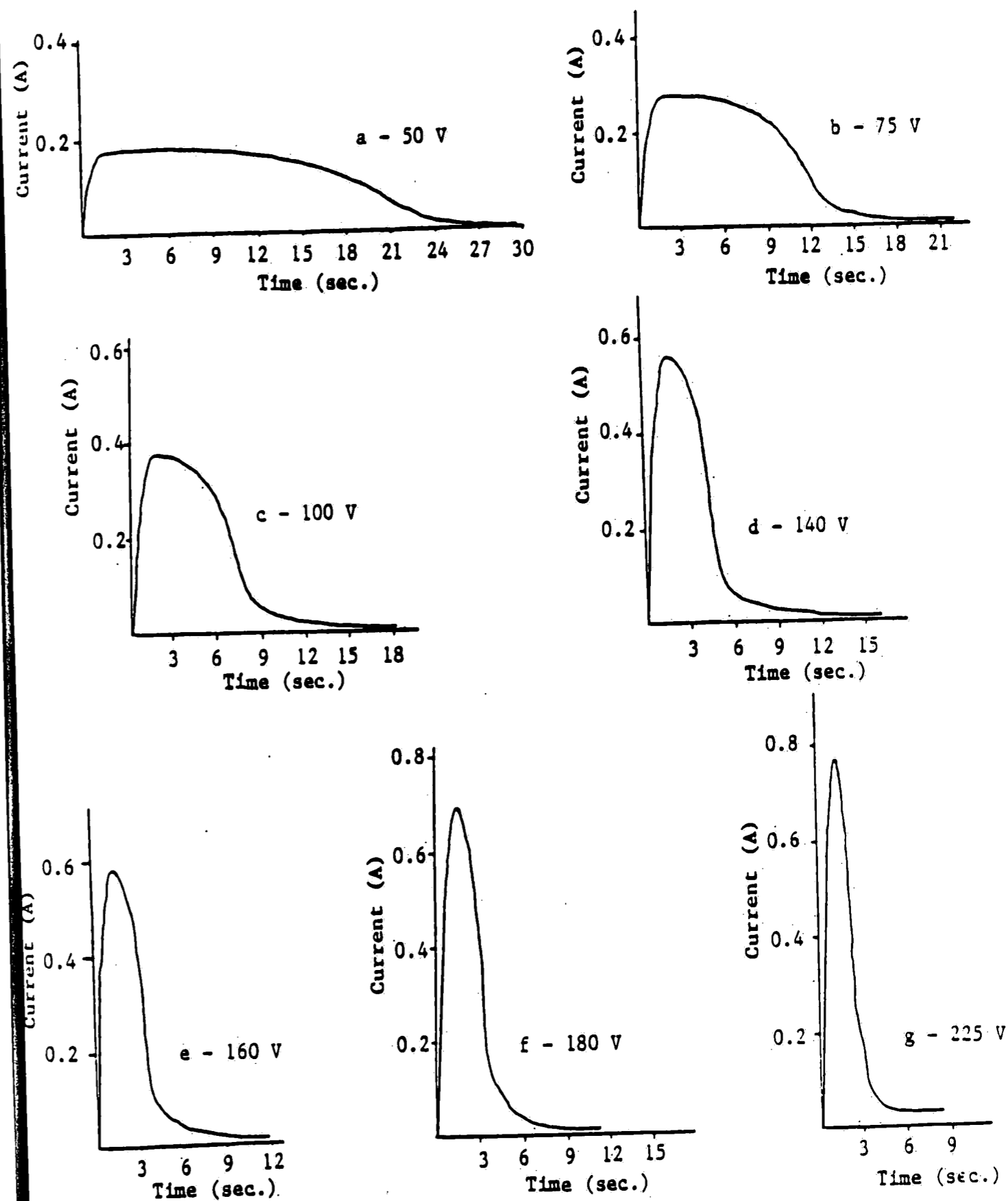


Figure 3-3: Current - time curves for the electrodeposition of polyurethane acrylic latex, varying applied voltage.

V., Figure 3-3, curve g) shows a smooth, rapid current cut-off, thus no film rupture (which would be characterized by a continued increase in the current) occurred. As the applied voltage was increased from 50 to 225 V., the maximum current increased and current cut-off (indicating the formation of an insulating film) was more rapid. As the maximum current depended primarily on the initial bath conductivity (constant) and the applied voltage, the increase in current with applied voltage was as anticipated. For this polyurethane acrylic latex system the optimum coating voltage (over the range tested) would consequently be 225 V.

Scanning electron micrographs of polyurethane acrylic latex films deposited at 75 V. and 200 V. may be seen in Figures 3-4 and 3-5, respectively. It is evident that raising the applied voltage had a profound effect on the film morphology; at low voltage the film was thick and exhibited many gassing defects, while at the higher voltage a smooth, thin film, free of defects was obtained. A similar effect of the applied voltage on the film morphology was reported by Turner and Coler [52] in their study on the electrodeposition of natural rubber latexes.

The current - time curves for the deposition of polyurethane acrylic latex at 160 V. using both dead and live entry are shown in Figure 3-6. While dead entry was useful in performing studies on the rate of film growth, it is evident from Figure 3-6 that the



Figure 3-4: Scanning electron micrograph of polyurethane acrylic latex deposited at 200 V. Magnification = 2000X.

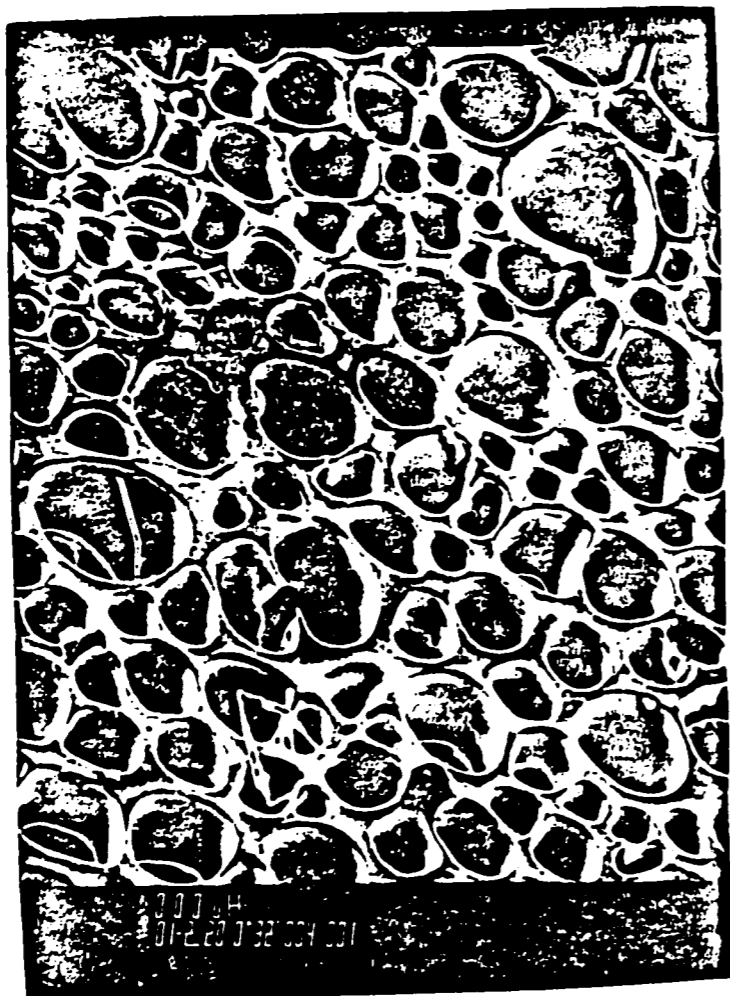


Figure 3-5: Scanning electron micrograph of polyurethane acrylic latex deposited at 75 V. Magnification = 100X.

electrodeposition behavior was not as good as that observed with live entry. The higher current surge that occurred with dead entry resulted in increased gassing and less rapid current cut-off, leading to thicker deposited films with more gassing "pinholes". The varying substrate area during deposition at live entry would not affect the coverage of the test piece thus, as noted by Machu [31], industrial electrocoating processes often utilize live entry to avoid the current surge and gassing that are observed with dead entry.

It should be noted that the current - time behavior of the polyurethane acrylic latex prepared with HDTMAB differed considerably from that observed by Humayun [25] for epoxy latexes prepared with the same surfactant. With the epoxy latexes a distinct period of increasing current followed the immersion of the sample into the bath; this current increase was attributed to the presence of a conducting film. However, a conducting film alone would be expected to result in a constant current, not an increasing one. A similar behavior was observed with the polyurethane acrylic latex, but only for samples deposited at very low voltages (< 30 V.) for long times (> 60 sec.), when the film did not cut off current effectively. It is believed that the increasing current was a direct result of the increasing conductivity of the bath, which arises from the desorption of emulsifier from the depositing polymer particles. In addition, the current cut-off behavior of the

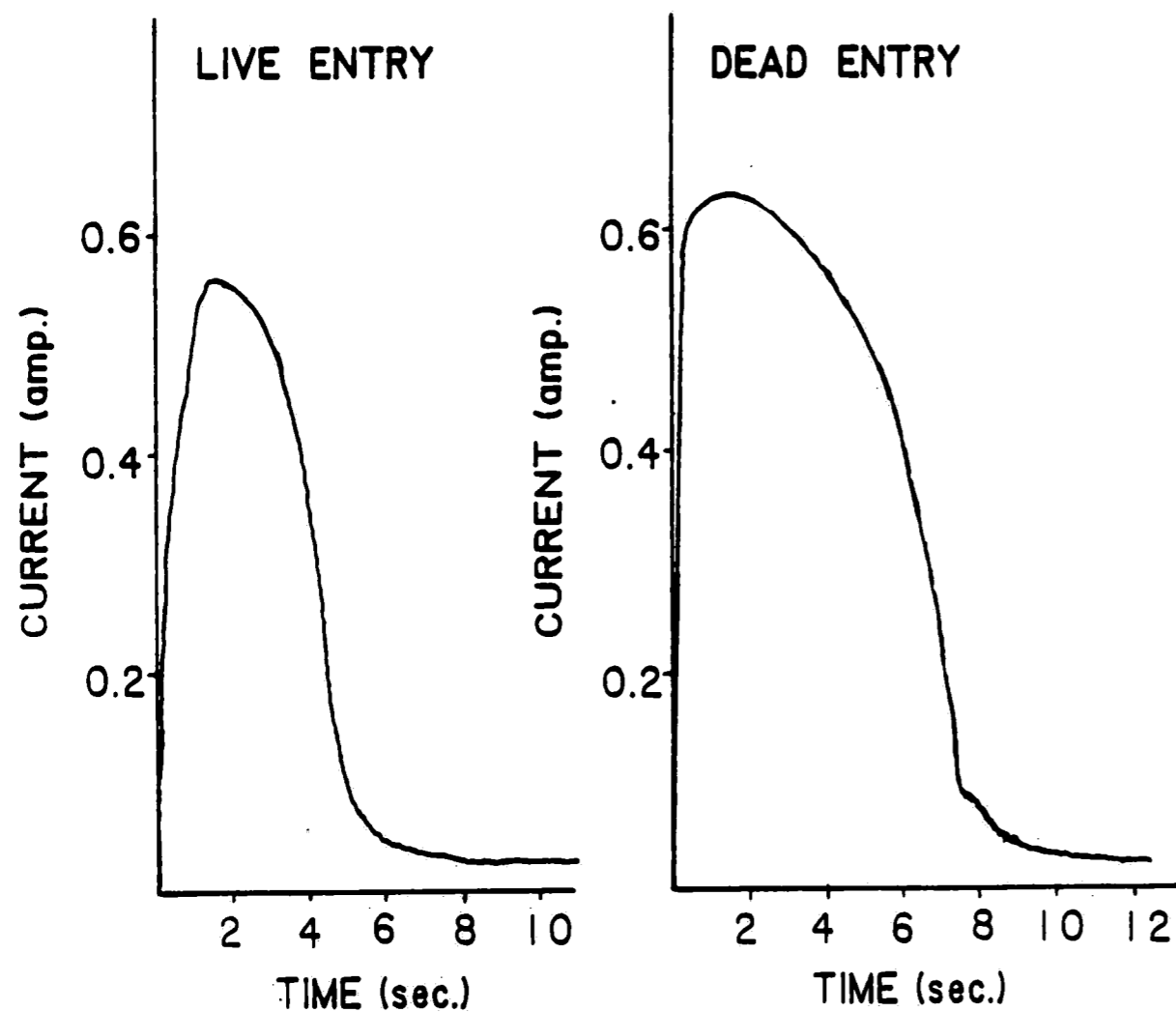


Figure 3-6: Polyurethane acrylic latex, deposition at 160 V., live entry vs. dead entry.

polyurethane acrylic latex deposited over the range 75 - 225 V. was much better than that reported for the epoxy latex. This improvement in current cut-off was the expected result of the less glassy behavior of the polyurethane acrylic polymer during deposition and film formation; similar improvements in electrodeposition performance upon lowering the softening temperature of a polymer were reported by Wessling et al [57].

The current - time voltage relationships for the commercial resin solubilized with acetic acid are shown in Figure 3-7. These curves are similar in nature to those observed for the polyurethane acrylic latex, with generally smoother, more rapid current cut-off behavior. As with the latex system, the form of the current - time curves for the solubilized resin depended very strongly on the applied voltage. With the commercial resin, however, the initial current was somewhat higher than that observed for the latex, indicative of the higher conductivity of the commercial resin (1500 - 1800 μ S./cm. at 15% solids). The effect of the applied voltage on the formation of an insulating film with this resin is very clearly demonstrated in Figure 3-7. As the voltage was raised to 160 V. a "hump" or current surge appeared on the current - time curve, showing that rupture of part of the deposited film had occurred. At 200 V. the current was observed to begin to decrease as a film of the resin began to insulate the electrode, following which the film ruptured and the current increased steadily until the end of the

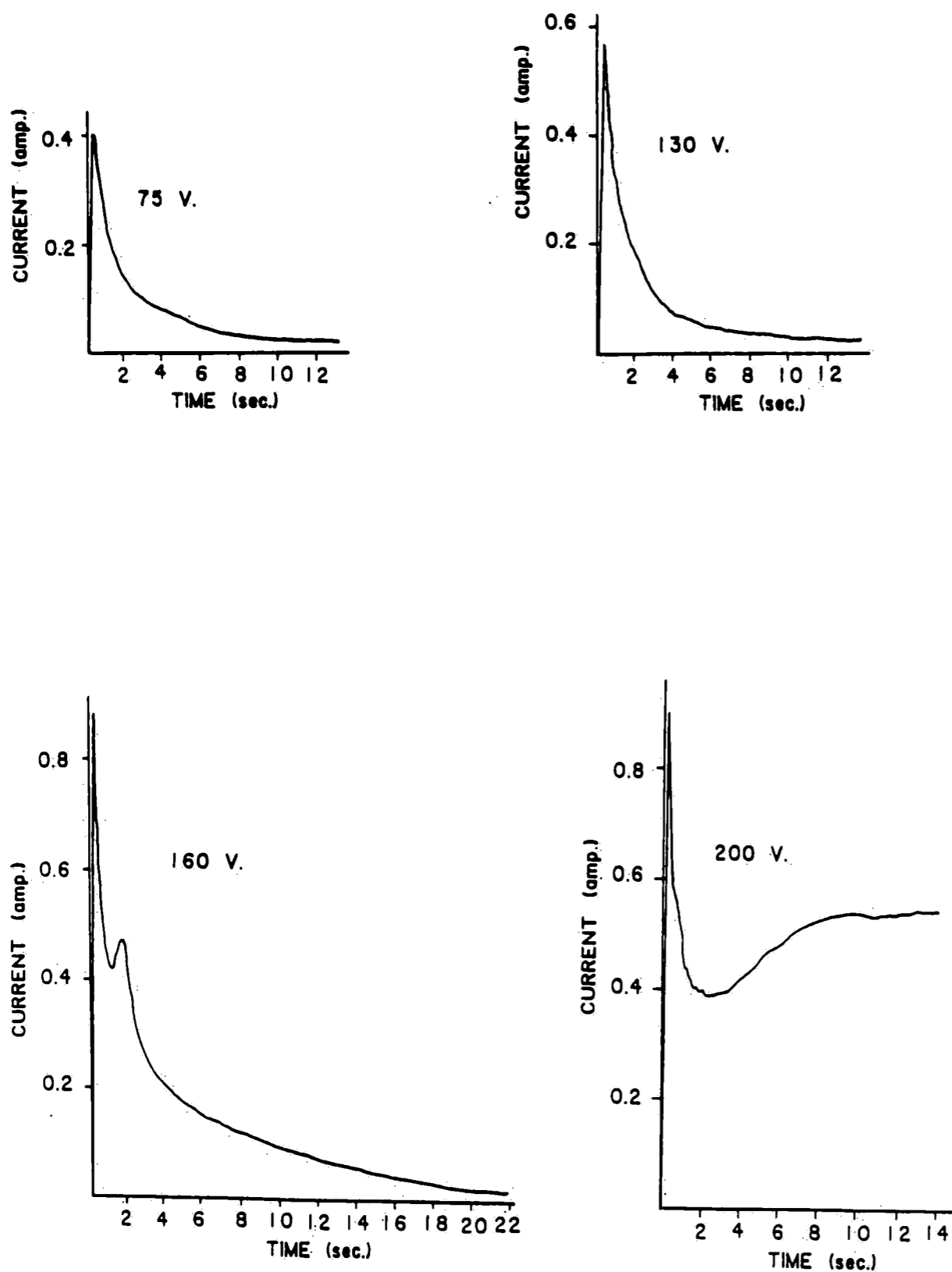


Figure 3-7: Current - time curves, commercial solubilized resin, varying applied voltage.

run; at this voltage it was not possible for the film to become insulating and completely cut off current flow. Film rupture has been attributed to increased gassing and heating of the bath at high current densities [18], and the voltage at which rupture takes place obviously varies significantly depending on the polymer and electrodeposition bath physical properties. From Figure 3-7 it is evident that there was an optimum voltage range (appr. 120 - 140 V.) for efficient electrodeposition of the commercial resin system.

An interesting difference in the effect of applied voltage on the time to current cut-off was noted between the commercial resin and the polyurethane acrylic latex. Comparing Figures 3-3 and 3-7 it is clear that increasing the applied voltage led to a decrease in the time to current cut-off (more rapid film insulation) for the polyurethane acrylic latex, while with the commercial resin increasing the applied voltage resulted in an increase in the time to current cut-off. This opposite behavior would seem to indicate that different mechanisms governed the electrodeposition and film growth for the two systems.

The coulombic efficiency of electrodeposition, defined as the mass of polymer deposited per coulomb of charge passed, was calculated for the deposition of the polyurethane acrylic latex under various conditions. As shown in Table 3-3, the coulombic efficiency increased slightly as the applied voltage was raised from

Table 3-3: Effect of applied voltage on coulombic efficiency; polyurethane acrylic latex.

<u>Applied Voltage</u>	<u>Coulombic Efficiency</u>
50 V.	64. mg/coul.
100 V.	76. mg/coul.
140 V.	78. mg/coul.
180 V.	80. mg/coul.
200 V.	83. mg/coul.

50 to 200 V. While the variation in the data above 100 V. could simply reflect experimental error, below 100 V. the coulombic efficiency decreased significantly. This decrease in efficiency is explained by realizing that at low voltages deposition continued for a much longer period than at higher voltages, with constantly increasing bath conductivity during deposition. This increasing bath conductivity would be expected to lead to a lower coulombic

efficiency, as noted by Fink and Feinleib [17]. The effect of the applied voltage and the bath conductivity on the coulombic efficiency and coating quality is summarized in Table 3-4. These results further verify the relationship proposed by Fink and Feinleib between the bath conductivity and electrodeposition performance.

Table 3-4: Effect of applied voltage and bath conductivity on polyurethane acrylic latex electrodeposition performance.

<u>Sample No.</u>	<u>Applied Voltage</u>	<u>Conductivity</u>	<u>Film Thickness</u>	<u>Efficiency</u>
1	200 V.	800 μ s/cm	1.2 mil	83 mg/coul.
2	200 V.	2000 μ s/cm	28.0 mil	53 mg/coul.
3	75 V.	800 μ s/cm	13.5 mil	51 mg/coul.

The coulombic efficiency of electrodeposition was also determined for the commercial solubilized resin system deposited under conditions similar to those used for the polyurethane acrylic

latex. As can be seen in Table 3-5, the coulombic efficiency was fairly constant

Table 3-5: Effect of applied voltage on coulombic efficiency; commercial resin system.

APPLIED VOLTAGE(V)	COULOMBIC EFFICIENCY (mg/C)
30	17.4
60	25.1
75	27.9
130	31.3
160	32.6
200	28.7

to very low voltages. The stabilizing group (protonated amine) was deposited with the resin in the commercial system, so the bath composition remained essentially constant during deposition and the coulombic efficiency would not be expected to vary with the applied voltage. The unexpected decrease in the coulombic efficiency at low

voltages could be explained by several effects. A certain current "loss" (current passing for which no deposition takes place) is expected for the electrodeposition of solubilized resins, and is generally attributed to the development of a suitable ionic boundary layer around the electrode for deposition to take place, and the diffusion of ions into the bath before the surface of the electrode is coated with a paint film [41]. While the current loss is observed to be constant for a widely varying range of applied voltages [51], the fraction of the current lost in this manner would greatly increase as the total charge passed decreased. For the commercial resin solution, the total current passed during deposition at 30 V. was $1/30^{\text{th}}$ of that passed at 200 V., thus the fraction of the current lost could have been significant at the lower voltage. In addition to the current loss, a portion of the film deposited would be expected to consist of loosely coagulated material, which would be removed from the cathode during post-deposition rinsing. Again, this portion would not vary greatly with the applied voltage for the solubilized resin system, however the fraction of the total film lost would rise and could become significant as the total deposited film mass decreased. Either or both of these factors may have contributed to the lower effective coulombic efficiency observed at low voltages with the solubilized resin system.

Comparison of the coulombic efficiencies obtained for the

polyurethane acrylic latex and commercial resin systems (Tables 3-3 and 3-5) revealed that the efficiency of the latex system was much greater than that of the solubilized resin, verifying the hypothesis of Finn and Mell [18] that the deposition of a latex would be more efficient than the deposition of solubilized resins. It is important to note that the efficiency of electrodeposition for solubilized resins is dependent on the molecular weight of the resin and the quantity of hydrophilic functional groups included in the polymer chain [41], resulting in a fixed electrochemical equivalent weight. Thus, for this type of electrodeposition system, the coulombic efficiency cannot be varied without altering the polymer composition. With a latex system, however, the polymer molecular weight and surface charge can be varied independently simply by changing the amount of surfactant used in the preparation of the polymer. Alternatively, the surface charge (corresponding to an electrochemical equivalent weight) can be varied following formulation by "cleaning" the latex using serum replacement, ion exchange, or dialysis. In this case the polymer system has a variable electrochemical equivalent weight, and the coulombic efficiency can be changed by varying the surface charge of the latex particles. While the increase in electrochemical equivalent weight is limited by an accompanying decrease in throwpower (ability to coat recessed areas) [57] and the decrease in latex stability, theoretically it would be possible to achieve very high coulombic

efficiencies merely by reducing the surface charge of the latex. To test this, a sample of the polyurethane acrylic latex prepared with the V-50 initiator and cleaned of a significant amount of the adsorbed ammonium surfactant was deposited. While the conductivity of the latex was very low (180 $\mu\text{S./cm.}$), which would severely reduce the possible throwpower, the coulombic efficiency observed was 450 mg./coul., over ten times that obtained with the solubilized system, and five times that observed for the same latex prior to cleaning.

A series of electrodepositions was performed at 200 V. with the polyurethane acrylic latex system and reusing the same bath to observe the effect of multiple depositions on the electrodeposition behavior. The current - time curves for these depositions are shown in Figure 3-8. The maximum current and the time to current cut-off both were seen to increase with increasing number of depositions from the bath. In addition, the residual amperage following the current cut-off increased from 20 mA. (first deposition) to 80 mA. (seventh deposition). Film rupture had also begun to occur by the fourth deposition, as shown by the increase in current after the initial current cut-off (curves c and d, Figure 3-8). The rupture of the film was a result of the increased gassing that occurred with multiple depositions from the same bath; the effect of this gassing on the film morphology can be seen by comparing Figures 3-5 and 3-9. The decline in electrodeposition performance with the number of depositions from the bath with the latex system was anticipated; as

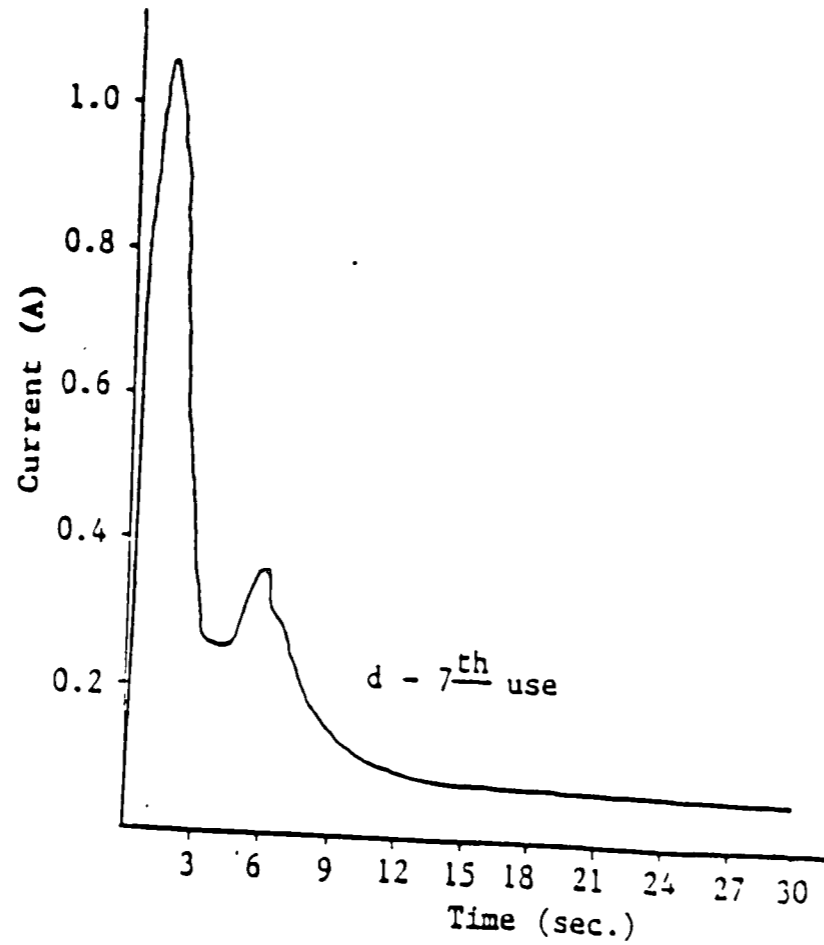
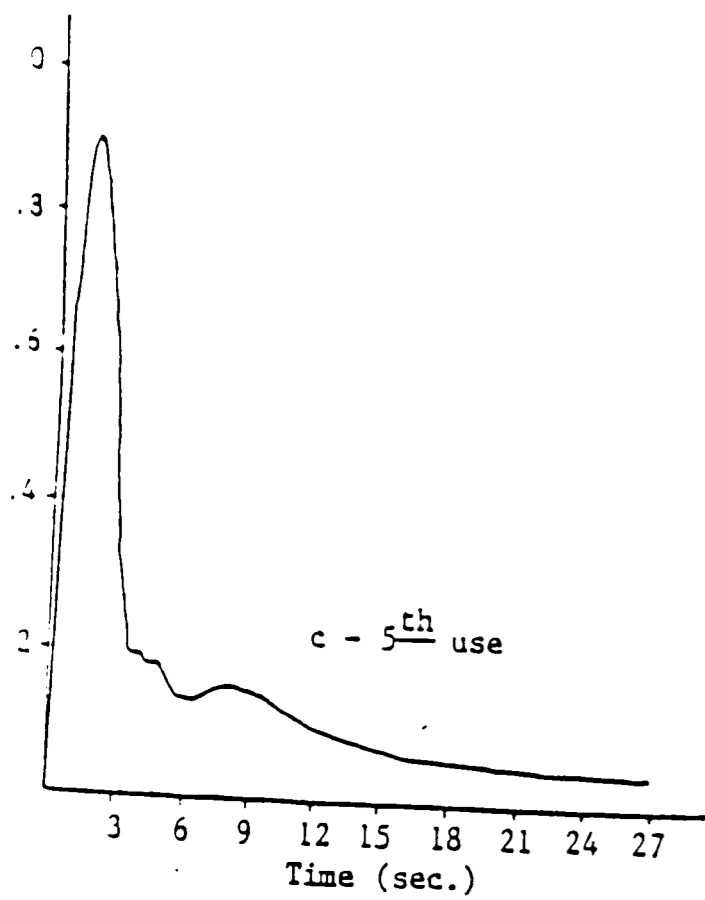
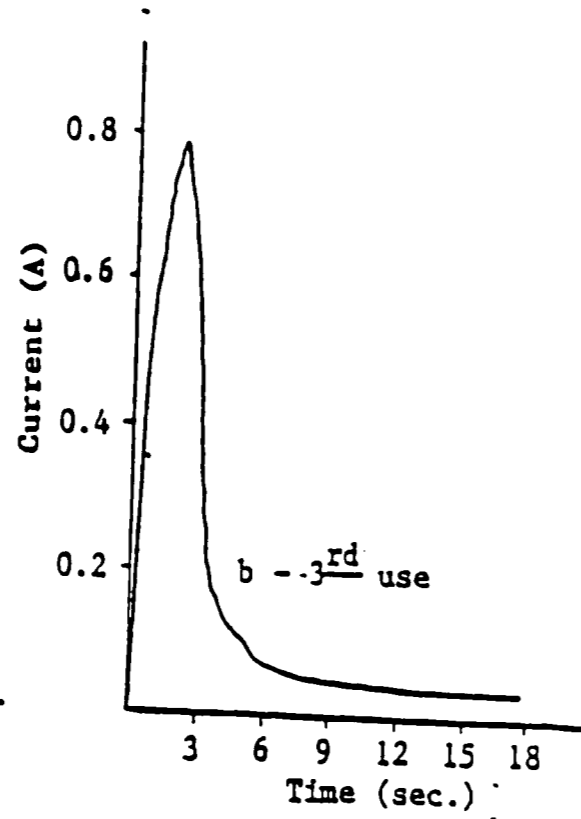
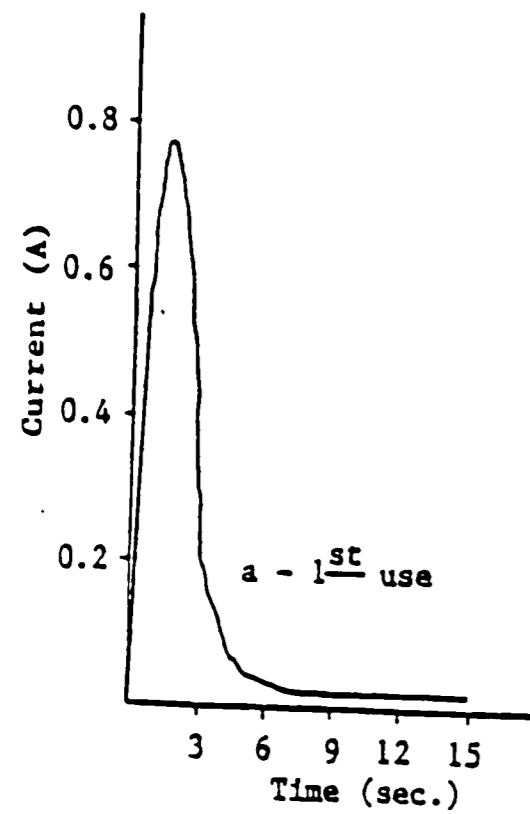


Figure 3-8: Current - time curves for the electrodeposition of polyurethane acrylic latex; multiple depositions from the same bath.



Figure 3-9: Scanning electron micrograph of polyurethane acrylic latex deposited at 200 V.; fourth use of bath.

deposition took place a portion of the emulsifier associated with the depositing particles would desorb and be redispersed, increasing the emulsifier concentration in the bath [25]. The increased gassing, film rupture, and current - time behavior observed with the multiple depositions occurred because of the higher bath conductivity that resulted from this increased emulsifier concentration. To verify that the surfactant was actually being redispersed, the conductivity of the electrodeposition bath was measured before and after the multiple depositions. Initially the conductivity was 1000 μ S./cm., while after seven depositions it had increased to 1400 μ S./cm. While this conductivity could not be correlated directly with the bath emulsifier concentration (due to the adsorption equilibrium between the latex particles and the bath serum), it did clearly indicate an increase in the total amount of surfactant present in the bath. The coulombic efficiency of deposition was measured for the multiple depositions, and is shown in Table 3-6. From these results it is evident that the increasing emulsifier concentration in the bath associated with multiple depositions from the same bath caused a significant reduction in the coulombic efficiency; by the seventh deposition from the same bath the efficiency had dropped to 28% below the initial value.

Multiple depositions from the same bath were also performed using the commercial resin system and the cleaned polyurethane acrylic latex stabilized by V-50 radical fragments. For both of

Table 3-6: Coulombic efficiency vs. number of depositions; polyurethane acrylic latex.

<u>Number of Depositions</u>	<u>Coulombic Efficiency</u>
1	83. mg/coul.
2	80. mg/coul.
3	79. mg/coul.
4	73. mg/coul.
5	67. mg/coul.
6	65. mg/coul.
7	60. mg/coul.

these systems the electrodeposition behavior (current - time curves, film quality) was found to be essentially independent of the number of depositions from the bath. As the stabilizing entity was bound to the polymer and deposited in the coating rather than redispersed

in the bath for both of these systems, the bath composition (and the electrodeposition behavior) would not be expected to vary significantly with the number of depositions. Analysis of the bath before deposition and after ten depositions for these two systems indicated a slight drop in conductivity (e.g. from 1600 μ S./cm. to 1490 μ S./cm. for the commercial resin system); this drop was taken to result from the reduction of charge - carrying molecules as the solids content of the bath was decreased.

The dependence of the electrodeposition process on the applied voltage for the polyurethane acrylic latex is further demonstrated in Figure 3-10, which shows the film mass (mg./cm.^2) at current cut-off plotted as function of the applied voltage. While there is some scatter in the data, a clear trend of decreasing film mass with increasing applied voltage is evident. The results appeared to be in conflict with those presented by Humayun for the deposition of the single - component Epon 1001 epoxy latex [25], as well as the data reported for the deposition of solubilized resins [31, 23, 33]. However, Humayun reported the mass deposited after 60 seconds of electrodeposition; thus the deposition was ended prior to current cut-off, and the reported film masses therefore reflected the different rates of growth at different voltages, not the ultimate film mass (that at current cut-off). As observed with the polyurethane acrylic latex, at higher voltages the film became insulating more rapidly than at lower voltages (see Figure 3-3),

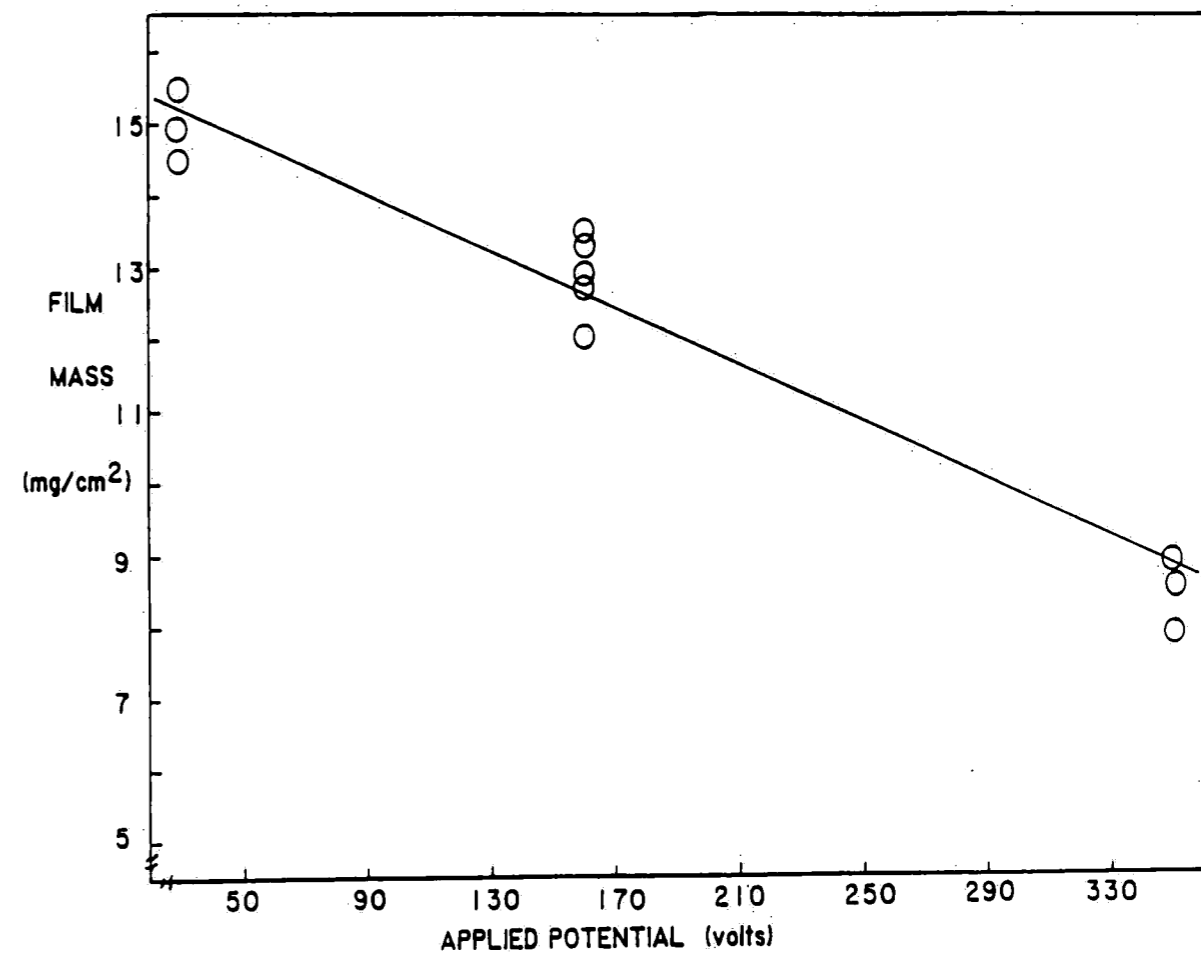


Figure 3-10: Film mass versus applied voltage, polyurethane acrylic latex.

and the ultimate film build was consequently reduced. The decrease in film mass with increasing deposition voltage was also observed by Finn and Mell [18] for the electrodeposition of films which remained somewhat electrically conducting for a period following the beginning of deposition. In light of the nature of the HDTMAB surfactant used in the electrodeposition of the polyurethane acrylic latex, instantaneous charge destruction upon deposition would not occur, and behavior similar to that reported by Finn and Mell would be expected. For comparison, the effect of applied voltage on the film mass obtained upon deposition of the commercial solubilized resin was determined, and is illustrated in Figure 3-11. Again some scatter of the results was observed, however the trend indicated an increasing film mass with increasing applied voltage. Finn and Mell [18] reported the same relationship for the anodic electrodeposition of a solubilized carboxylated polymer system, and attributed the behavior to the rapid formation of an insulating film, and the observed increase in the time to current cut-off with increasing voltage with that system. Reference to Figure 3-7 shows this same increase in time to current cut-off with increasing applied voltage was observed with the commercial resin system, thus the increase in film mass with increasing applied voltage should be expected for this system. It must be noted that this relationship would not be expected to hold at higher voltages (> 180 V.) where film rupture occurred.

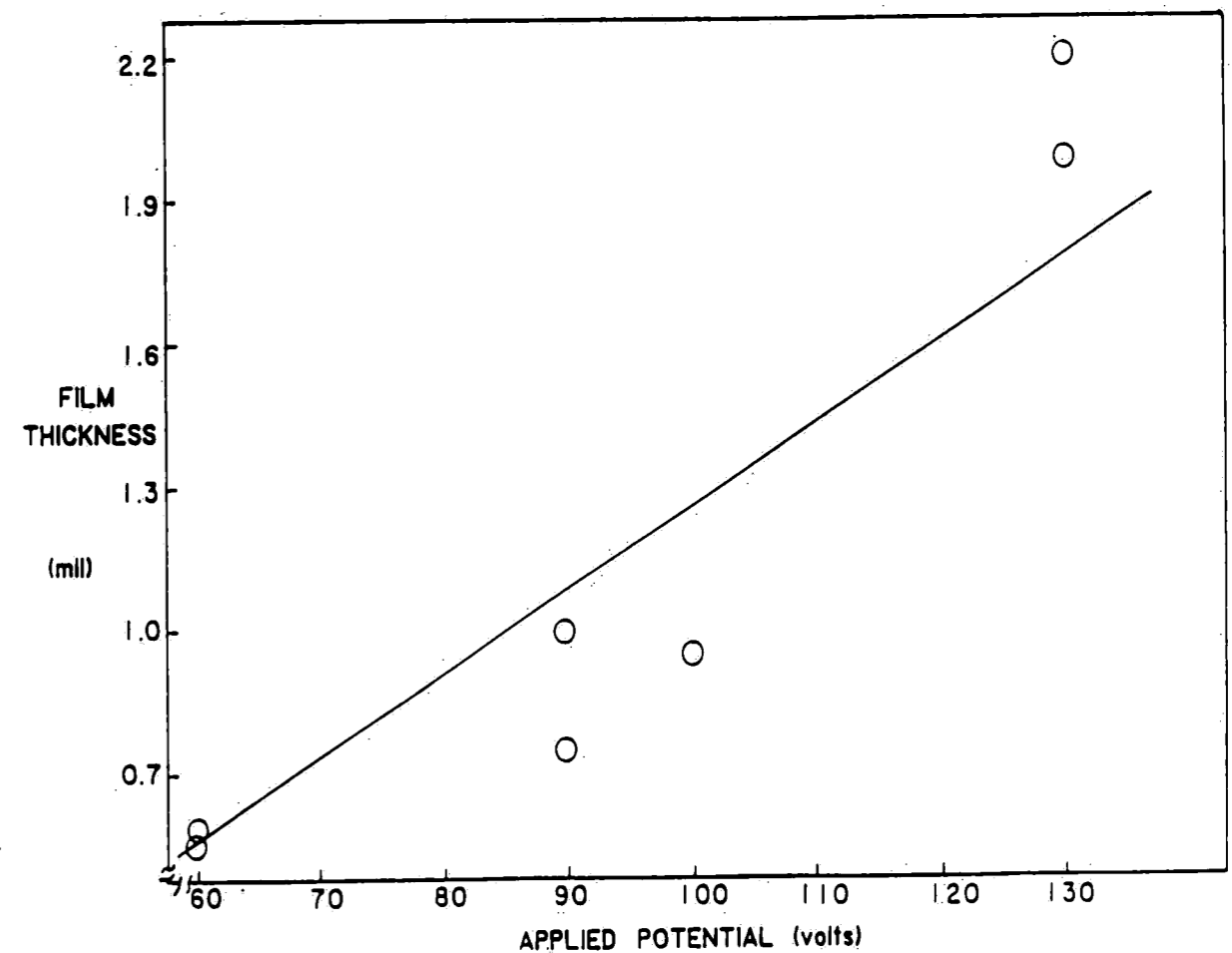


Figure 3-11: Film mass versus applied voltage, commercial resin solution.

In order to observe the relationship between the quantity of charge passed and the amount of polymer deposited for the two systems (polyurethane acrylic latex and commercial solubilized resin), the film mass was plotted against the coulombs of charge passed for a variety of electrodeposition conditions. As can be seen in Figures 3-12 and 3-13, there is a linear relationship between the film mass deposited and the charge passed for both the polyurethane acrylic latex and the solubilized commercial resin systems. In addition, as a good fit was obtained over a wide range of applied voltages and deposition times, further evidence was provided that the coulombic efficiency did not vary greatly with either of these system parameters. These results indicated that Faraday's law was followed in the deposition of the latex and the solubilized resin, and are in agreement with the findings of Saatweber and Vollmert [41], Olsen [35], and Brown and Campbell [11].

3.3 Kinetics of Electrodeposition

3.3.1 Introduction

The study of electrodeposition kinetics involves a theoretical analysis of the deposition process, with the ultimate aim of developing a mathematical model capable of describing the rate of electrodeposition under various conditions. Since the development of electrodeposition as an important industrial process in the early

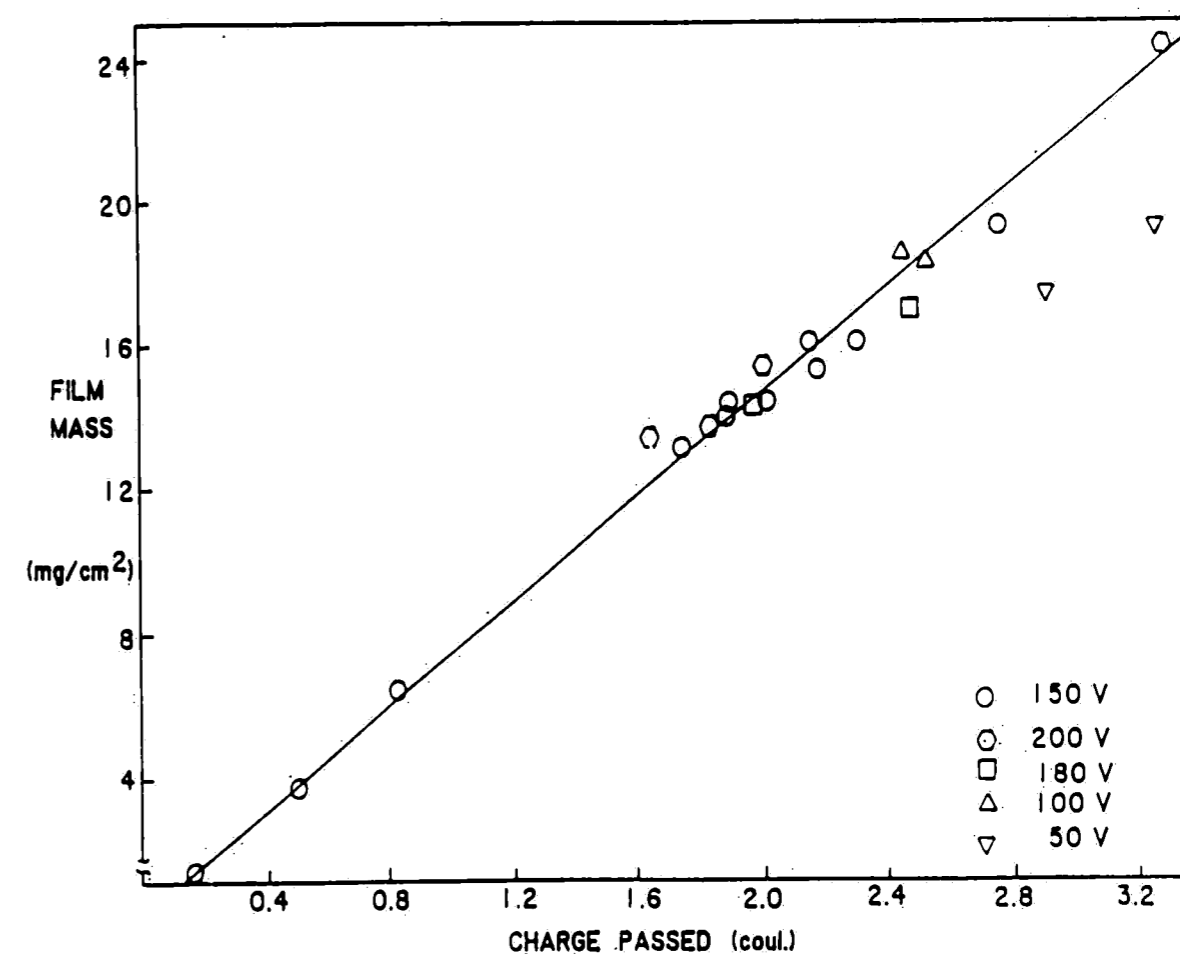


Figure 3-12: Film mass versus charge passed; polyurethane acrylic latex.

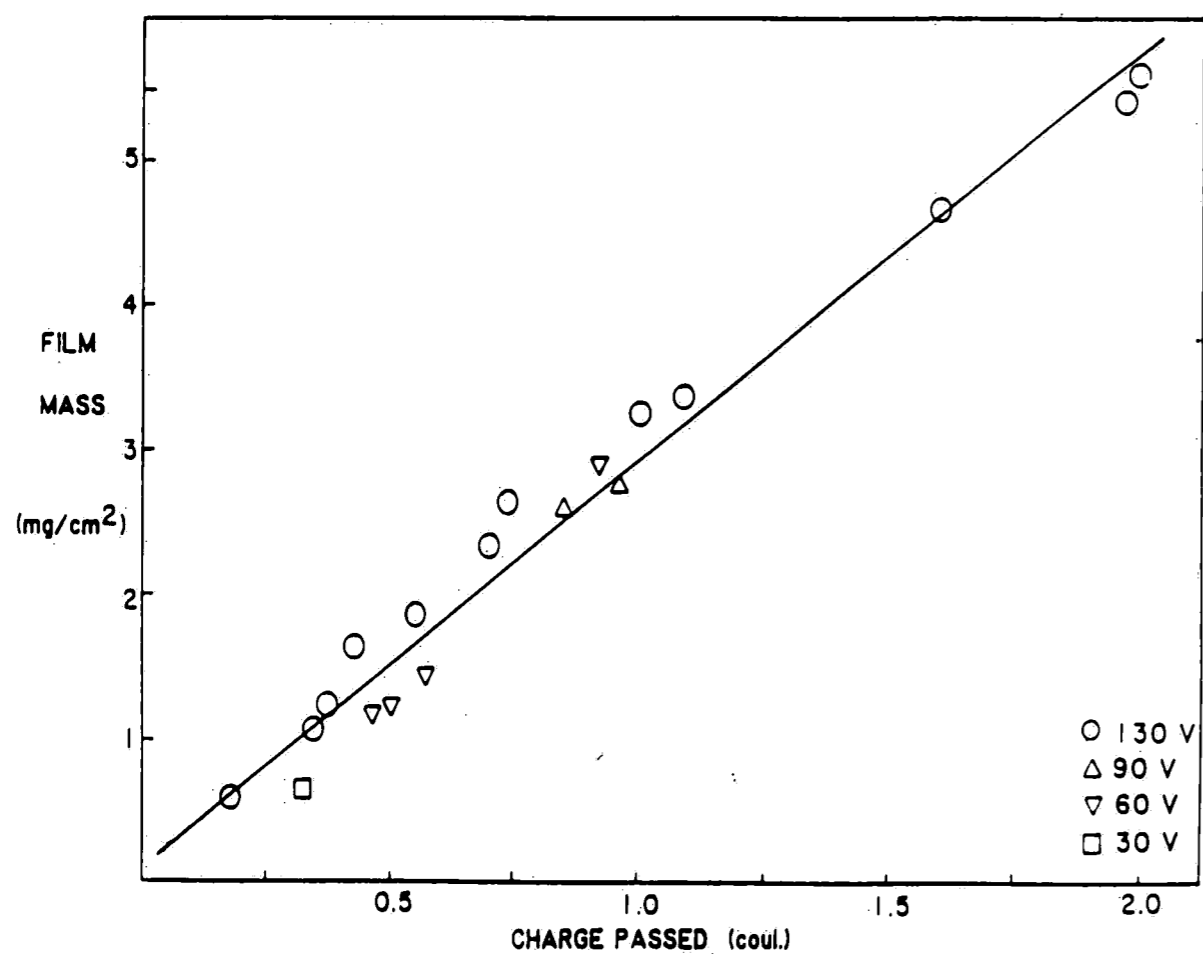


Figure 3-13: Film mass versus charge passed; commercial resin system, 15% solids, varying applied voltage.

1960s, numerous researchers have examined the kinetics of film growth and various models have been proposed. These models have been developed for solubilized resins, and consequently assume a charge - destruction mechanism of deposition. The variables affecting the rate of film growth during deposition from a latex system should differ from those involved in a solubilized resin system, thus a kinetic model developed for a latex system would not be expected to be the same as that for a solubilized system.

Prior to discussion of the kinetic models developed it is necessary to mention that, in each of these models, an induction period (during which no deposition takes place) is considered. This induction period occurs as a consequence of the mechanism of electrodeposition, and as a result would be expected to vary significantly with different parameters, depending on the specific mechanism governing the formation of the film. Consequently, a discussion of the effect of such variables as the applied voltage and the bath properties on the induction period is included in the section dealing with the mechanism of electrodeposition. The kinetic models developed for the electrodeposition process therefore consider only film growth following the induction period.

In one of the earliest quantitative studies on the kinetics of the electrodeposition process, Olsen [35] examined in detail both the migration of components in the bath and the specific reactions

taking place at the electrode. Olsen observed experimentally that the electrodeposition rate appeared to be controlled by other factors than the electrophoretic migration of particles to the electrode, and concluded that the rate determining step in the electrodeposition process involved the diffusion of ions through the deposited film. Upon comparison of the growth of the electrodeposited film to the formation of oxide films on metals, and examination of the rate of film growth, the following expression was derived for constant voltage electrodeposition:

$$ad + d^2 = kt \quad (3.1)$$

where a and k are constants, d is the film thickness, and t is the deposition time. Olsen observed a two - region electrodeposition curve. In the first region, a linear film mass versus time dependence was followed, while in the second region a linear film mass versus square root of time dependence was followed. These dependencies were explained by assuming that in the first region the electrode was not completely covered by the film, thus the deposition reaction was unimpeded. In the second region, diffusion of ions through the film resulted in the observed square root time relation; the two regions then represented limiting cases of Equation (3.1): region 1 where $d \ll 1$, region 2 where $d > 1$. Significantly, Olsen concluded that the first region of deposition covered only a small fraction of the electrodeposition process, and could be considered to have a negligible effect on the overall

kinetics of film growth. Thus the model proposed by Olsen reduced to:

$$d = kt^{1/2} \quad (3.2)$$

Fink and Feinleib [17] proposed a similar relationship for the anodic electrodeposition of natural rubber latex; however they did not verify the kinetic model experimentally with the latex system. With [61] presented experimental evidence for a square root time dependence of film growth in an anodic electrodeposition system, but no attempt was made to model the kinetic data, and the results were somewhat ambiguous as With did not specify the nature of the resin (latex, solubilized, etc.). A more quantitative analysis of the process was performed by Phillips and Damm [37], who also assumed the rate limiting step to be the diffusion of ions through the film, then solved Fick's second law of diffusion for a planar electrode:

$$\frac{\partial C}{\partial t} = D_0 \frac{\partial^2 C}{\partial x^2} \quad (3.3)$$

where C_0 is the concentration of ions within the film, D_0 is the diffusion coefficient of the ions in the film, x is the distance from the electrode, and t is the deposition time. The boundary and initial conditions were chosen to represent diffusion with a moving boundary layer and constant ion flux at $x = 0$, and the solution obtained is of the form:

$$l = (2D_0C_0^* t/m)^{1/2} \\ \text{or} \\ l = kt^{1/2} \quad (3.4)$$

where C_0^* is the concentration of ions at the metal - film interface, m is the concentration of ions within the film, l is the film thickness, and k is a constant. Note that this mathematical expression (Eq. (3.4)) is of the same form as the empirical kinetic model presented by Olsen. Beck [4] applied the expression developed by Phillips and Damm to kinetic results for the anodic electrodeposition of dissolved polyelectrolytes, and found good correlation between experimental data and the model curves.

Recently, Pierce et al [60, 59, 38, 39] have examined the kinetics of the cathodic electrodeposition process in detail, and observed a strong similarity between the growth of electrodeposited organic coatings and oxide films. Of particular interest is the fact that, while the mechanism of electrodeposition was assumed to involve the destruction of the stabilizing charge on the polymer by electrochemical reaction, the kinetic models developed did not rely on this or any assumption concerning the mechanism (unlike the kinetic treatments of Olsen [35], Fink and Feinleib [17], Phillips and Damm [37], and Beck [5]). Rather, the only assumption made in the kinetic models developed by Pierce et al was that the quantity of polymer deposited was directly proportional to the amount of charge passed; i.e. Faraday's Law is obeyed. Thus following the induction period, the rate of growth is given by:

$$\frac{d\delta}{dt} = C_1 j \quad (3.5)$$

where C_1 is the coulombic efficiency, j is the current density, δ is the film thickness, and t is the deposition time. At constant current deposition ($j = \text{constant}$) a linear time dependence of the film growth is predicted, regardless of the characteristics of the film. However, at constant voltage j is time dependent and related to the voltage drop through the deposited film, thus the film characteristics must be considered. Note that this general kinetic model still equates the growth of the film with the transport of ions through the film; however, the transport is important only as it results in current flow. This model (Eq. (3.5)) is then applicable to any electrodeposition system, regardless of the mechanism of electrodeposition assumed to be governing deposition.

In the case of constant voltage deposition it is necessary to determine the relationship between the applied field and the current density. According to Kovac-Kalko [30], the most general relationship between the current density and the field strength in a material is:

$$j = A \sinh(BV/\delta) \quad (3.6)$$

where A and B are constants, V/δ is the instantaneous field strength, and j is the current density. Several important limiting cases of Equation (3.6) can be considered. If the field strength in the material is not exceedingly high:

$$\sinh(BV/\delta) \approx (BV/\delta) \quad (3.7)$$

and therefore

$$j = ABV/\delta \quad (3.8)$$

Equation (3.8) is simply a statement of Ohm's law, and a film in which this relationship holds is considered an ohmic resistor.

Substituting Equation (3.8) into Equation (3.5) and integrating yields:

$$\begin{aligned} \delta &= (2ABC_1Vt)^{1/2} \\ \text{or} \\ \delta &= kt^{1/2} \end{aligned} \quad (3.9)$$

Note that Equation (3.9) is identical in form to the kinetic models presented by Olsen [35] and Phillips and Damm [37]. At higher field strengths Equations (3.7) and (3.8) do not apply, and the film conduction behavior is considered to be non-ohmic. The hyperbolic sine function may then be approximated by an exponential function [38]:

$$j = A \exp(BV/\delta) \quad (3.10)$$

In the case of non-ohmic conduction a numerical solution of Equation (3.5) is necessary. Pierce et al have obtained a numerical solution for this equation in reduced form (dimensionless deposition time and coating thickness), and observed that at long times the solution approached the form of Equation (3.9).

In addition to consideration of the film conduction characteristics, the above model may be modified to include such

effects as excessive gassing at the electrode, or poor coalescence of the film following deposition; both of these phenomena would be expected to result in a porous film. In the case of a porous film in which conduction takes place primarily through the pores, the current density may be written:

$$j = j_0(1-x) \quad (3.11)$$

where j_0 is the initial current density, and x represents the fraction of electrode surface covered. The film mass deposited may be assumed to be proportional to the fractional surface coverage, and Equation (3.5) may be rewritten in terms of the deposited film mass:

$$m = kx \quad (3.12)$$

and

$$\frac{dm}{dt} = C_2j \quad (3.13)$$

Substituting Equations (3.11) and (3.12) into Equation (3.13) and integrating leads to an exponential film growth equation for constant voltage deposition:

$$m = k\{1 - \exp[-kC_2j_0t]\} \quad (3.14)$$

Following complete surface coverage of the electrode, further film growth would be described by Equation (3.9).

Finally, it should be noted that while the basic film growth equation proposed by Pierce et al (Eq. (3.5)) is not based upon a specific mechanism of deposition, different mechanisms of film formation would result in considerably different film characteristics, which would consequently enter into the solution of Equation (3.5). Then, with a complete knowledge of the deposition mechanism (and resulting film characteristics) it should theoretically be possible to model any Faradaic electrodeposition process by solving Equation (3.5). Alternatively, analysis of the film growth behavior for a particular system in terms of Equation (3.5) may be useful in elucidating the mechanism of deposition.

3.3.2 Film Growth Results and Discussion

The kinetics of electrodeposition were obtained by varying the time the sample remained in the bath at a constant applied voltage, and measuring the mass of polymer deposited. Kinetic studies were performed using: (i) the standard polyurethane acrylic latex, (ii) commercial resin in the solubilized form, (iii) an emulsion prepared from the commercial resin, and (iv) "cleaned" polyurethane acrylic latex.

Figures 3-14 - 3-16 illustrate typical kinetic data for the polyurethane acrylic latex deposited at 160 V. In Figure 3-14 is shown the film growth versus deposition time. These data indicate that, following a short induction period, the latex film appeared to

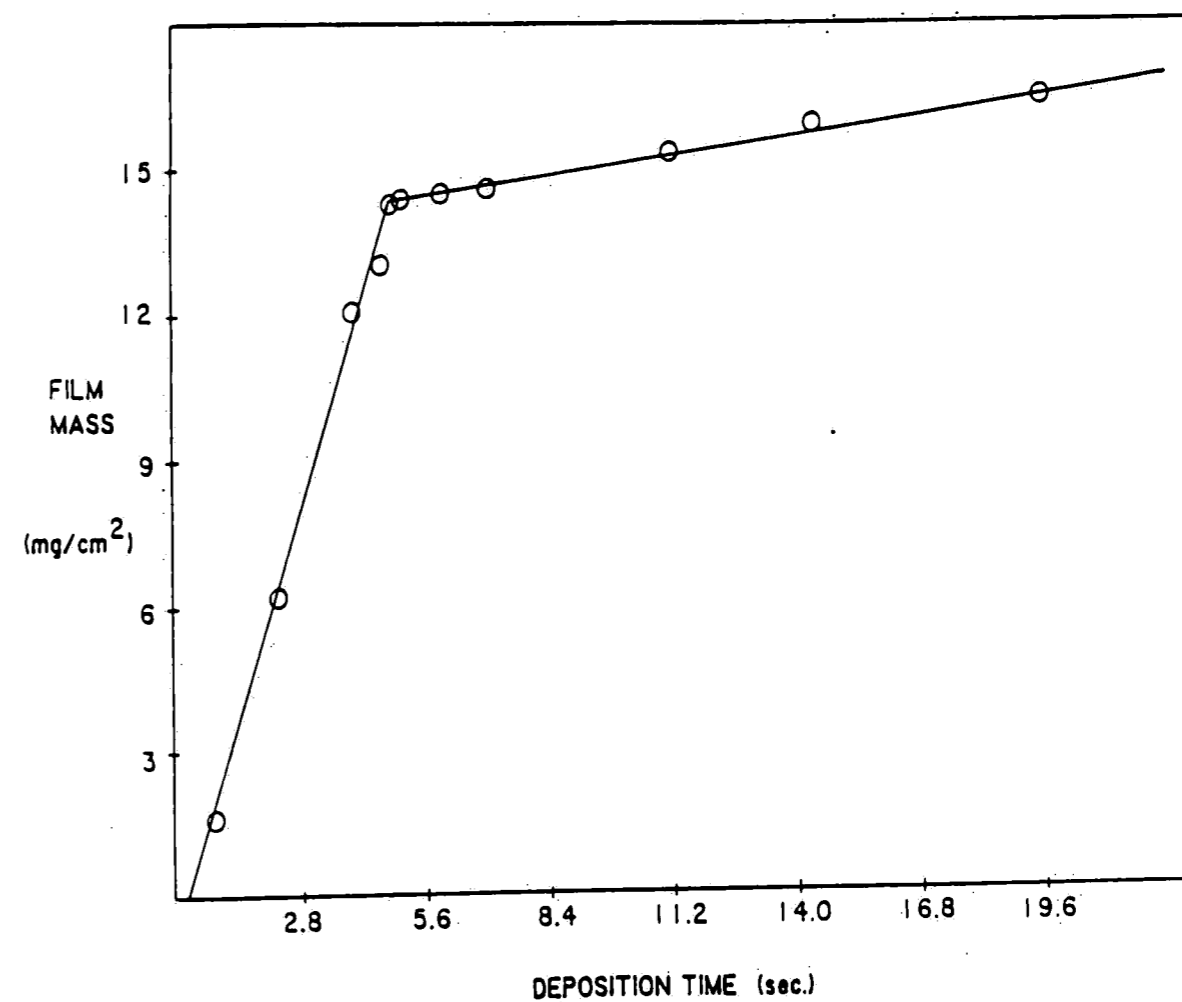


Figure 3-14: Film mass versus deposition time; polyurethane acrylic latex deposited at 160 V.

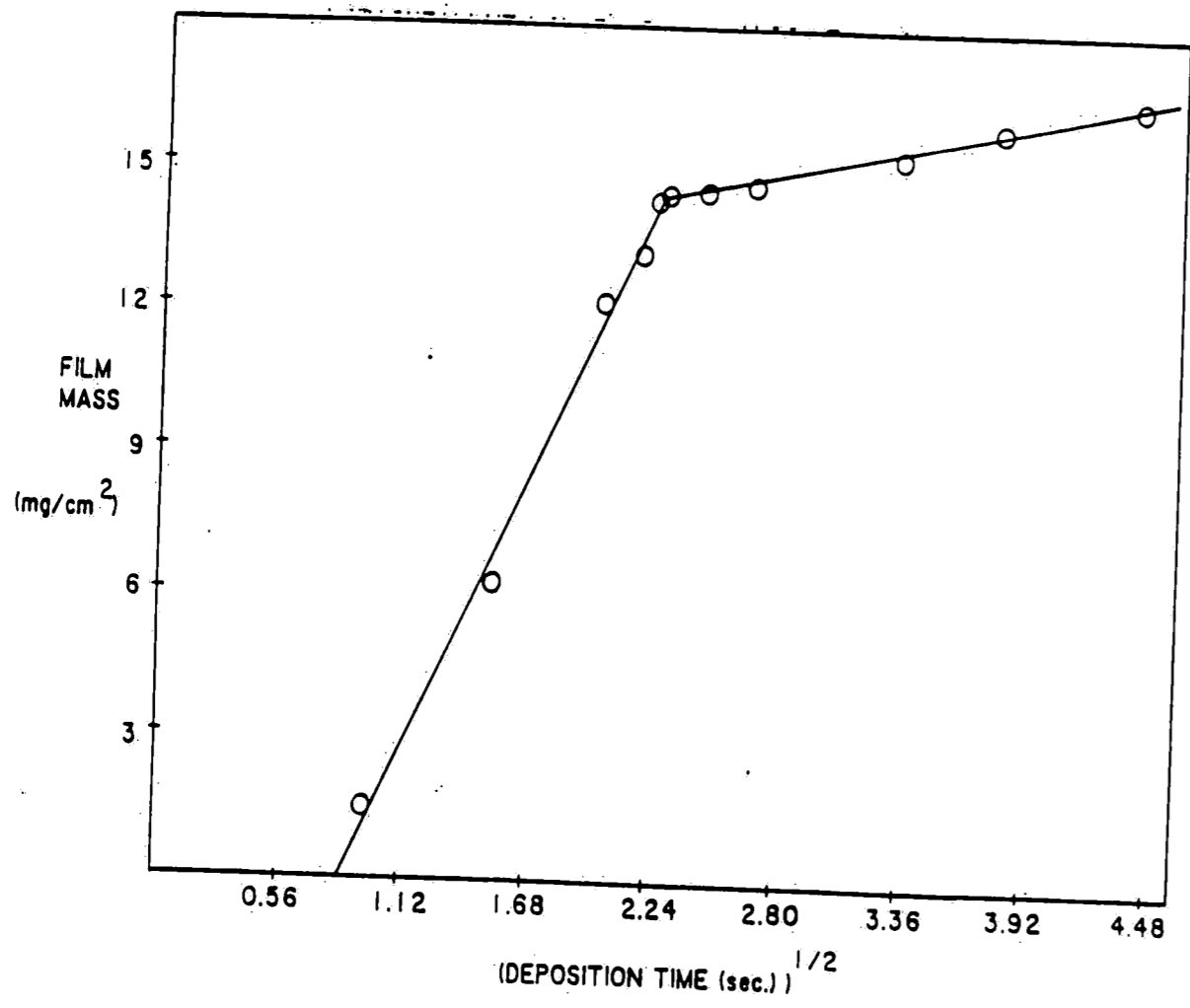


Figure 3-15: Film mass versus square root of deposition time; polyurethane acrylic latex deposited at 160 V.

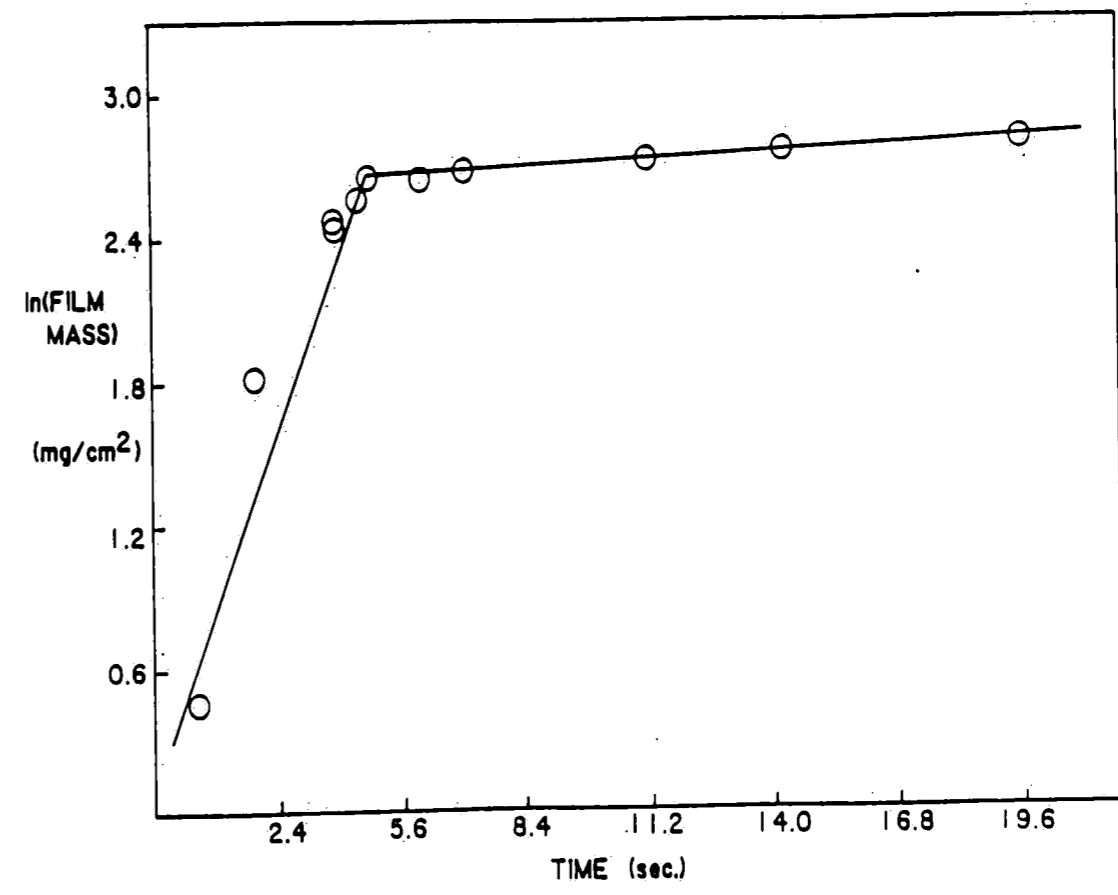


Figure 3-16: Ln{film mass} versus deposition time; polyurethane acrylic latex deposited at 160 V.

grow linearly with time, and at two distinct rates. It was shown in Figure 3-12 that the electrodeposition of the polyurethane acrylic latex obeyed Faraday's law, thus the kinetic expressions developed based on this assumption should be applicable. If an ohmic, insulating film were formed, it is expected that a plot of film mass versus the square root of deposition time would yield a straight line, indicating that the film growth was limited by the migration of ions through the film [17, 61, 37, 38, 35]. This plot is shown in Figure 3-15; the relationship was clearly not linear, so the simple case of deposition of an insulating ohmic film did not occur with the polyurethane acrylic latex. Similarly, if the electrodeposition film growth behavior were a result of the formation of a porous film, a plot of $\ln\{\text{film mass}\}$ versus deposition time should be linear, in accordance with Equation (3.14). Figure 3-16 shows such a plot for the polyurethane acrylic latex; evidently the observed kinetics are not simply a result of the film porosity.

From this analysis it was deduced that a two - stage process with a well-defined inflection point most accurately described the electrodeposition of the polyurethane acrylic latex system. The initial linear period observed (Figure 3-14) indicated that the growth of the film at the cathode was unimpeded as deposition continued. Olsen [35] and Munson [33] considered this initial growth period to result from the phase of the deposition prior to

which the surface of the electrode was covered by a polymer film. The results of Figure 3-14 differ from those of Olsen and Munson in two significant ways. The initial stage of deposition was considered by these researchers to be negligible compared to the overall deposition time (leading to an overall linear square root time dependence); this was clearly not the case in the electrodeposition of the polyurethane acrylic latex system under investigation. Also, if the linear film growth - time relationship occurred due to incomplete coverage of the electrode, examination of the electrode during this period should reveal a "spotty" film [33]. Electrodeposition runs were performed with the polyurethane acrylic latex in which the run was ended and the sample removed from the bath prior to the point at which the second stage growth kinetics occurred. With the exception of samples from runs ended after only a fraction of a second of electrodeposition, the cathode was found to be completely covered with polymer. Thus the linear growth period was a result of other factors than incomplete electrode coverage. It was observed experimentally by Wagener [56], Beck [5], and Wessling [57] that resins stabilized by quaternary ammonium functional groups (either bound or adsorbed) did not undergo charge destruction at the cathode during deposition. This behavior is due to both the tendency of the ammonium group to remain ionized even at very high pH and to its resistance to electrochemical reduction in an aqueous system. Therefore, it is very likely that the HDTMAB

surfactant adsorbed on the latex particles resulted in the deposition of a highly conductive film which initially posed little resistance to current flow and further film growth. This film remained conducting until a sufficient quantity of the surfactant had desorbed and redispersed in the bath through electroosmosis. Additional evidence for this type of deposition was presented by Wessling [58], who found that resins stabilized by bound ammonium functional groups (prevented from desorbing) did not cut off current at all during deposition, indicating that even at long deposition times the film remained conductive. The results reported by Wessling are depicted in Figure 3-17.

While the proposed deposition of a highly conductive film satisfactorily explained the observed initial constant film growth rate, a question arose as to why the desorption of surfactant did not occur continuously during deposition, resulting in a gradually decreasing film growth rate and elimination of the inflection point on the film growth curve. However, as Fink and Feinleib [17] observed, a certain current density and field strength would be reached at which a combination of electroosmotic dehydration and surfactant desorption would bring about a rapid increase in the resistance of the film, and therefore, in the rate of dehydration, surfactant removal, and further insulation. Once this process started it would proceed at a self-accelerating rate until the deposit developed sufficient resistance to completely cut off the

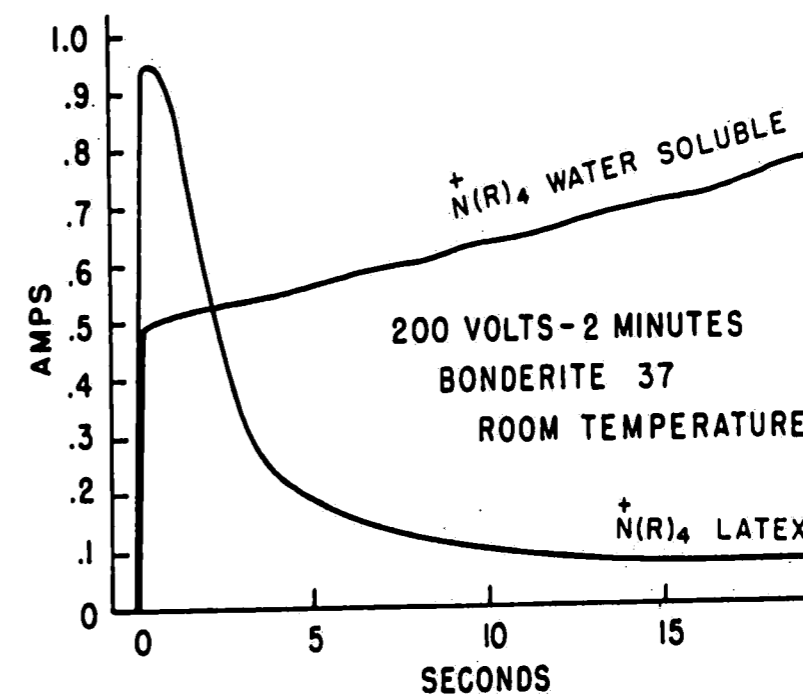


Figure 3-17: Current - time curves for the electrodeposition of ammonium stabilized solubilized and latex systems on Bonderite steel [58].

current flow. Consequently, the inflection point on the kinetic curve (Figure 3-14) may be taken as the point at which this accelerative process occurred. It was observed that, within experimental error, the inflection point corresponded well with the current cut-off point on the current - time curves over the range of voltages examined.

It was initially observed that in the second stage (after the inflection point in Figure 3-14), the film growth apparently depended on the deposition time in a linear fashion, as in the first stage but at a much slower rate [25, 20]. A closer examination of the electrodeposition kinetics in terms of the previously proposed models (pp. 75 - 80) indicated that this observation was not correct. While a linear growth period was explained satisfactorily by the presence of a conductive film, once the film became insulating and posed resistance to ionic transport, a linear film growth - deposition time relationship could not occur. The second stage growth data were replotted as a function of the square root of deposition time, and a linear relationship was observed (Figure 3-18), indicating that further growth of the film (and current flow) after the inflection point was limited by the migration of ions through a resistive film, as described by Equation (3.9). The field strength in the deposited film during the second stage of growth was calculated by dividing the applied voltage by the film thickness (assuming, then, that the potential drop in the film was much greater than that in the bath), and was on the order of 5×10^3 V./cm. This was approximately two orders of magnitude less than the field strength reported in the anodic electrodeposition of solubilized resins, some of which exhibited non-ohmic behavior [61]. Beck [4] reported that films deposited at very high voltages often show deviations from non-ohmic behavior; in this case the current

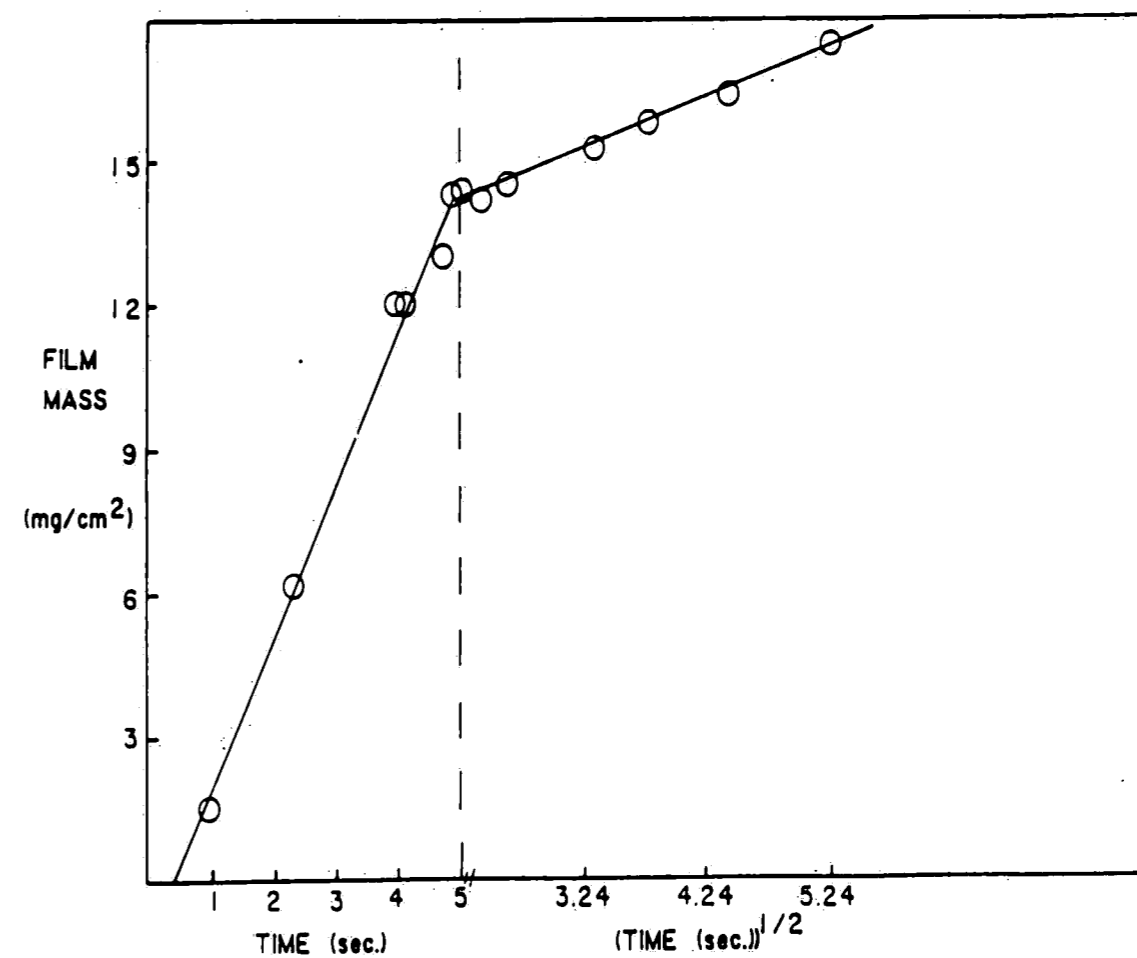


Figure 3-18: Film mass versus deposition time and square root of deposition time; polyurethane acrylic latex deposited at 160 V.

density - field strength relationship would be given by Equation (3.10) and the film growth equation (Equation (3.5)) would require a numerical solution. The linear square root time dependence observed for the polyurethane acrylic latex deposited at 160 V. indicated that the film conduction characteristics during this second stage of deposition were ohmic in nature.

The effect of the applied voltage on the kinetics of film growth for the polyurethane acrylic latex is shown in Figure 3-19, which shows the film mass plotted as a function of time for electrodeposition at 50 V. As in deposition at the higher voltage, a distinct two - stage growth was observed. The initial linear growth rate was much slower for the deposition at 50 V. (1.3 mg./cm.²-sec., compared to 4.0 mg./cm.²-sec. at 160 V.) and the time to the inflection point (current cut-off) was significantly greater (34.0 sec. at 50 V., 4.9 sec. at 160 V.). The longer time required to establish a film of sufficient resistance to initiate the accelerative current cut-off process would be expected to have an effect on the deposited films; this effect was shown in Figure 3-10 and Figures 3-4 and 3-5.

In summary, the kinetics of electrodeposition for the polyurethane acrylic latex over the range of voltages examined were accurately represented by a two-stage growth model. In the first stage the film posed little resistance to current flow and further

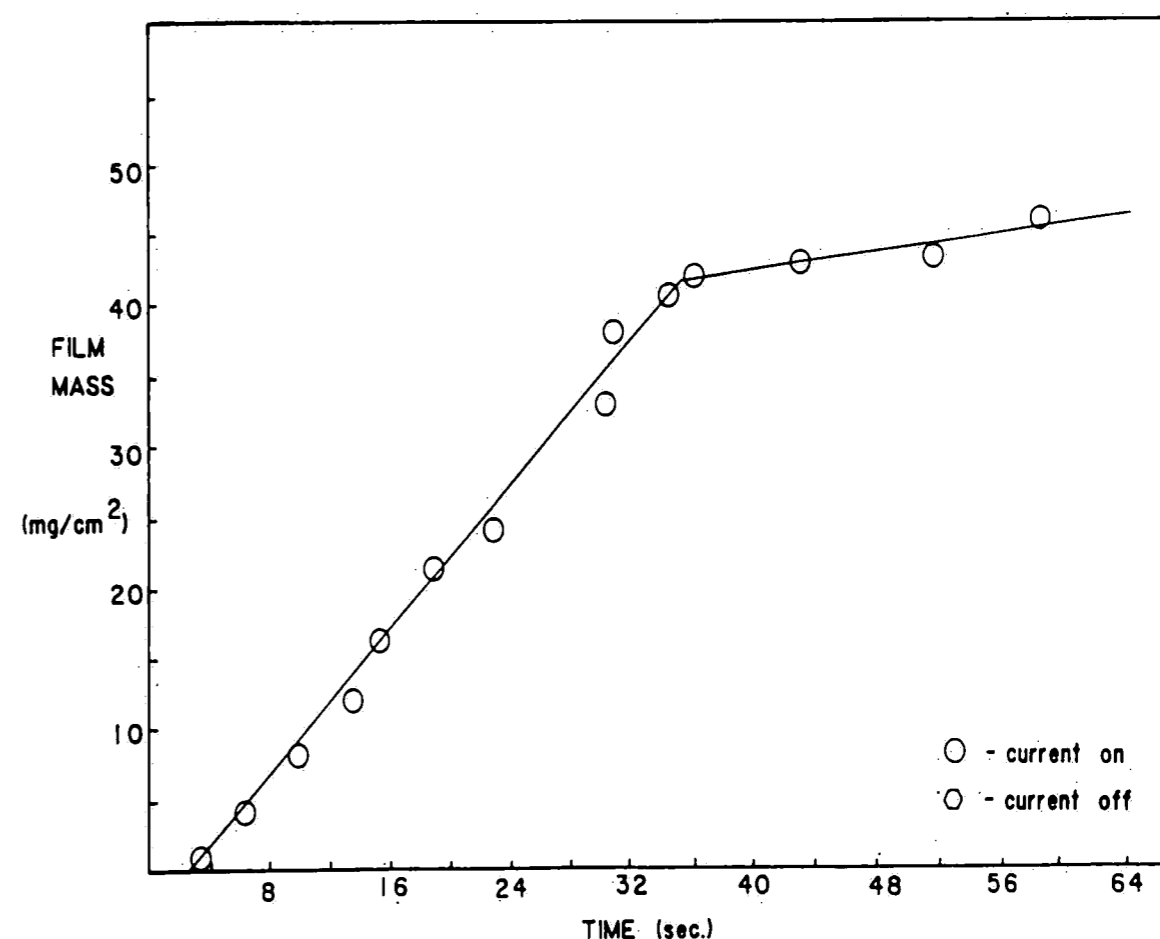


Figure 3-19: Film mass versus deposition time; polyurethane acrylic latex deposited at 50 V.

deposition, and a linear film growth - time relationship was followed. In the second stage, the film became insulating and apparently behaved as an ohmic resistor, thus the film growth depended linearly on the square root of the deposition time. During the first stage the current density, j , remained constant and Equation (3.1) could be integrated to yield:

$$\delta = c_1 j t \quad (\text{Stage 1}) \quad (3.15)$$

During the second stage the film growth was best described by integrating Equation (3.5) for the case of ohmic resistance to yield Equation (3.16):

$$\delta = k t^{1/2} \quad (3.16)$$

For comparison, the kinetics of electrodeposition of the commercial solubilized resin were studied under conditions similar to those used for the electrodeposition of the polyurethane acrylic latex. The deposition of the protonated amine - stabilized type of solubilized resin has been reported to take place by a charge destruction mechanism [29, 58], thus it was expected that the deposited film would show little conductivity from residual charged groups. The formation of an insulating film would limit further growth, and, if the film were ohmic, solution of Equation (3.5) would lead to a linear square root time dependence, Equation (3.9). The results of the kinetic study with the commercial resin in solubilized form are shown in Figures 3-20 and 3-21; depositions

were performed at 130 V. to avoid the complications of film rupture observed at higher voltages. From Figure 3-21 it is clear that the film growth of the solubilized resin was linear with the square root of deposition time over the entire deposition period. A slight deviation from this straight line occurred at very short deposition times; this deviation was also observed by Kovac-Kalko [30] during constant voltage deposition of solubilized resin, and was attributed to the high current density that occurred at the beginning of electrodeposition before the film developed any significant resistance to current flow.

Kinetic studies were also performed with polyurethane acrylic latex stabilized primarily with V-50 initiator radical fragments ("cleaned" of ammonium surfactant) and emulsified commercial resin samples in order to determine whether the kinetic results described above could be attributed to the physical nature (particulate latex versus solubilized polymer) of the system. If the two - stage growth observed with the polyurethane acrylic latex were a result simply of the particulate nature of the system, it would be expected that the latex stabilized with the V-50 radical fragments (which undergo rapid charge destruction in an alkaline medium) would also exhibit this two - stage growth. The kinetic data obtained with the V-50 stabilized polyurethane acrylic latex deposited at an initial pH of 4.0 are shown in Figures 3-22 and 3-23. From the plot of film mass versus deposition time (Figure 3-22) it is evident that a two

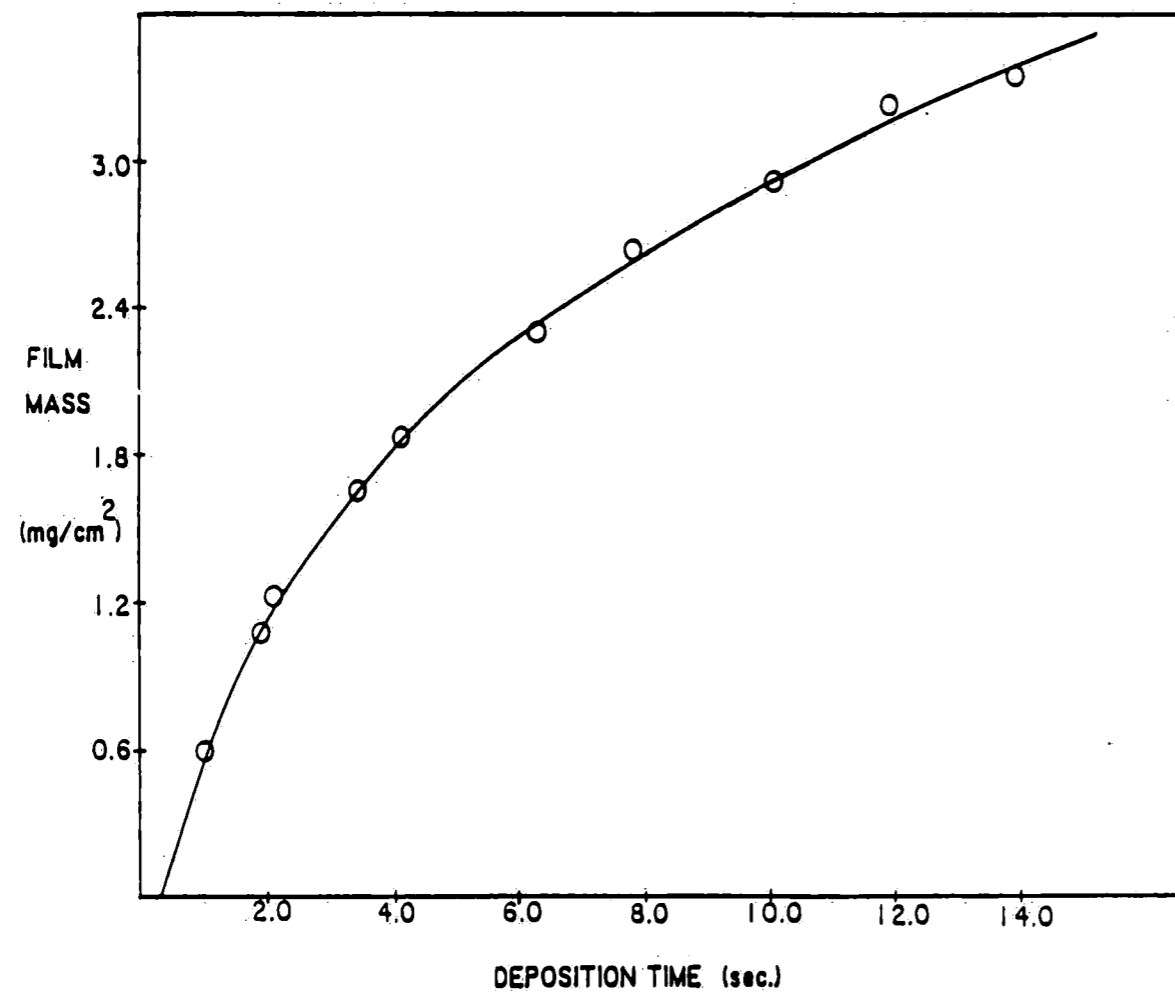


Figure 3-20: Film mass versus deposition time, commercial resin in solubilized form.

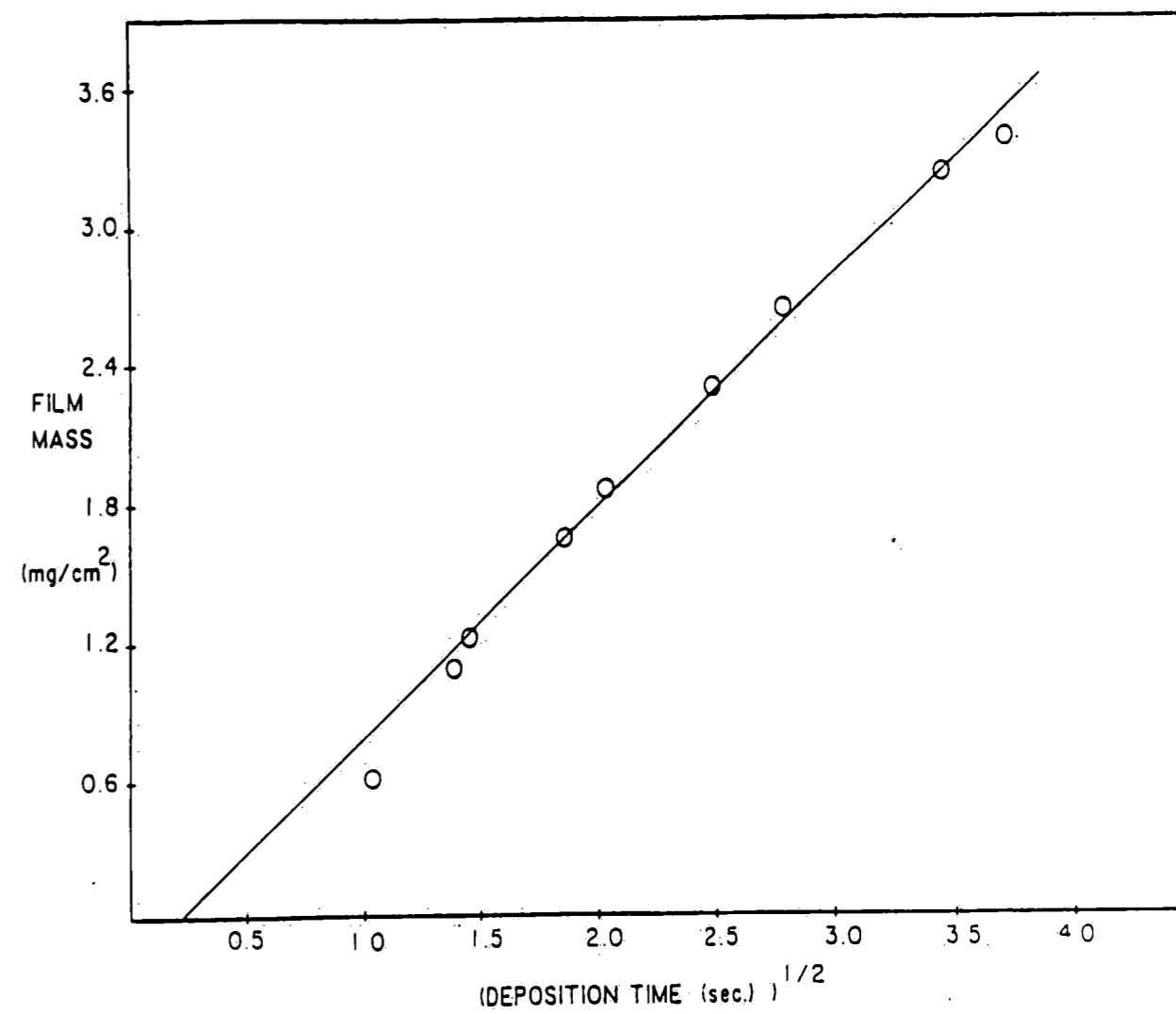


Figure 3-21: Film mass versus square root of deposition time, commercial resin in solubilized form.

- stage growth pattern was not observed with the V-50 stabilized latex. In Figure 3-23 the film mass is plotted as a function of the square root of the deposition time, and a straight line, similar to that found with the commercial solubilized resin, is observed. These data indicated that the polyurethane acrylic latex stabilized with the V-50 radical fragments rapidly formed an insulating film and that the deposition rate was governed by the transport of ions through this film. This behavior was clearly significantly different from that observed with the polyurethane acrylic latex stabilized by adsorbed HDTMAB surfactant, and indicated that the deposition kinetics were not strictly a result of the particulate nature of the latex system.

In Figures 3-24 and 3-25 are shown the film mass versus deposition time and square root of deposition time curves for an emulsion prepared from the commercial amino-functional resin using the HDTMAB surfactant rather than acetic acid solubilizer. As reported in section 2.1, this sample had a well defined particle size (with a broad PSD), and hence would be expected to exhibit the deposition behavior of a particulate system. The data in Figures 3-24 and 3-25 for this emulsion deposited at 160 V. showed considerable experimental scatter and indicated generally that the film growth did not appear to follow a linear dependence on either the deposition time or the square root of the deposition time. This may have been an indication that both the bound amino functional

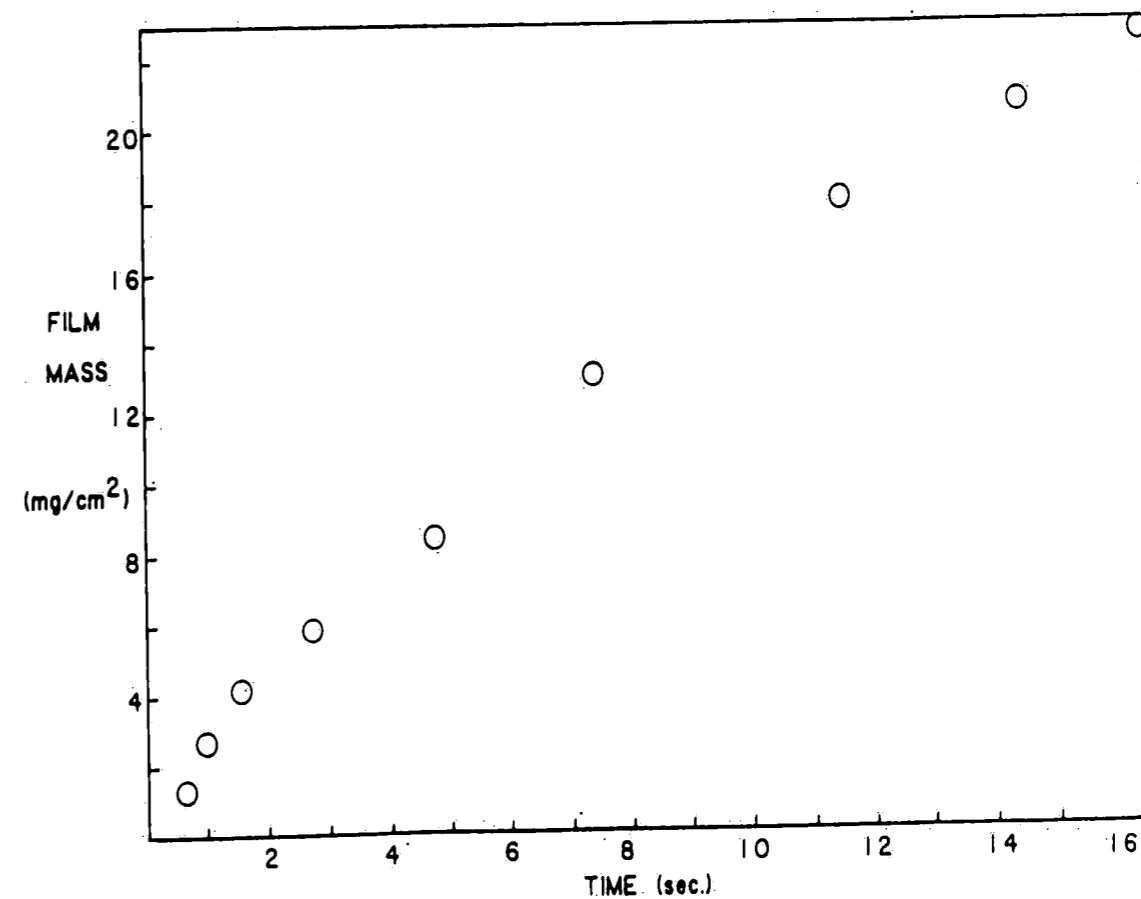


Figure 3-22: Film mass versus deposition time; V-50 stabilized polyurethane acrylic latex deposited at 160 V.

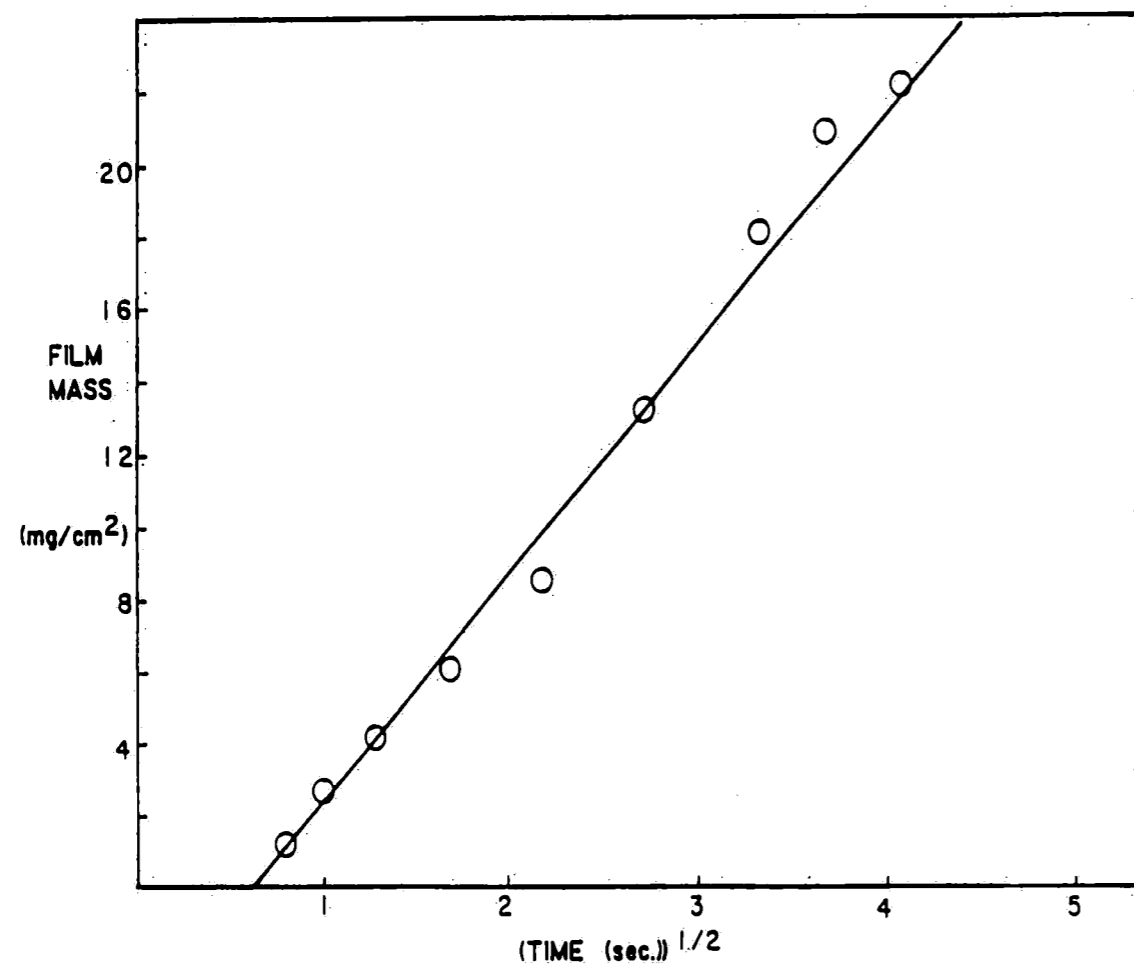


Figure 3-23: Film mass versus square root of deposition time; V-50 stabilized polyurethane acrylic latex deposited at 160 V.

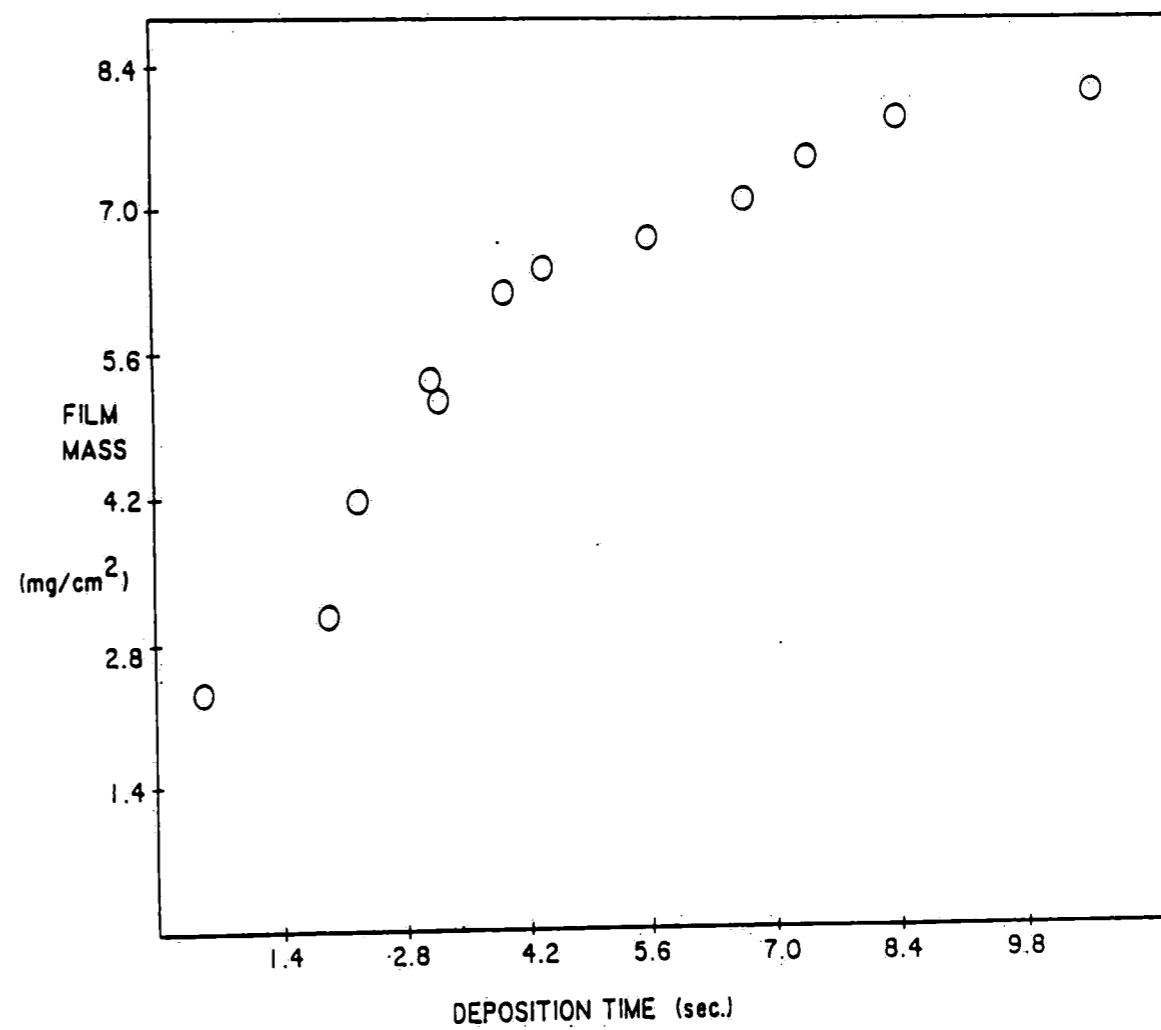


Figure 3-24: Film mass versus deposition time; commercial resin emulsion sample I-3 deposited at 160 V.

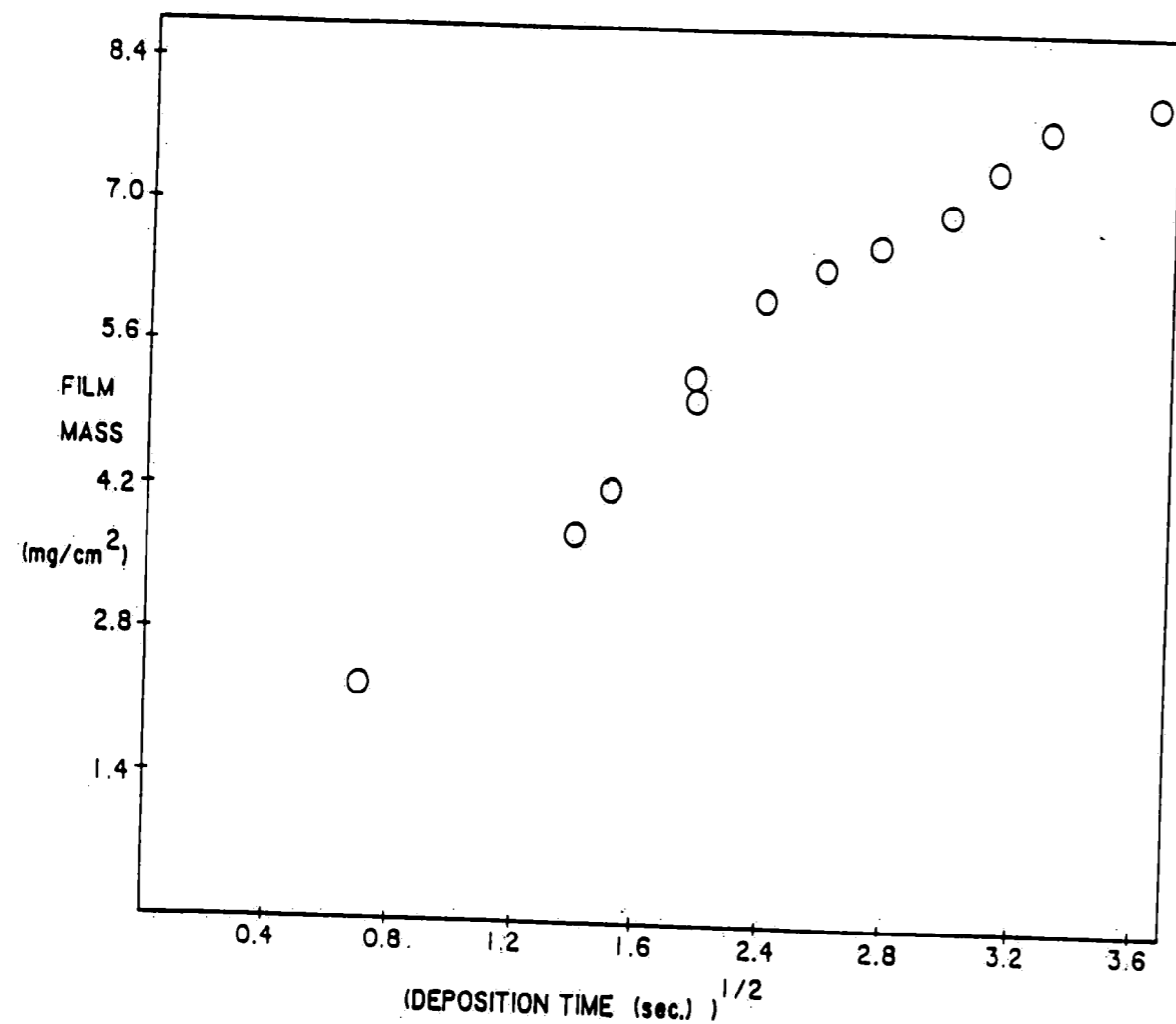


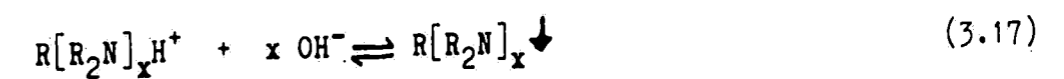
Figure 3-25: Film mass versus square root of deposition time; commercial resin emulsion I-3 deposited at 160 V.

groups and the adsorbed ammonium surfactant were involved in the stabilization of the emulsion, and that some charge destruction (and resulting variation of film conductivity) occurred during deposition. Consequently, no attempt was made to describe the kinetics of film growth in terms of the previously developed models for this emulsion.

3.4 Mechanism of Electrodeposition

3.4.1 Introduction

The mechanism of polymer destabilization and deposition during the cathodic electrodeposition process has been extensively examined by a number of investigators including Pierce [38, 39], Wessling [57], Wagener [56], Beck [4, 5], and Wismer [60]. The consensus reached by these investigators is that deposition takes place primarily by a charge destruction mechanism, at least with the protonated amine stabilized resins examined in each of these studies [10]:



Unlike anodic electrodeposition, in cathodic electrodeposition electrode reactions involving the resin have little effect on the deposition process.

In addition to the charge destruction mechanism which has been demonstrated to play the major role in the deposition of polymers

which are able to undergo reactions similar to that described in Equation (3.17), two other mechanisms have been proposed to describe the electrodeposition of polymeric systems onto the cathode. These are the flocculation mechanism and the accumulation, or concentration coagulation mechanism. As noted by Wagener [56], these latter two mechanisms may play an important part in the destabilization and deposition of a film, particularly in systems in which the charge destruction reaction does not take place.

The flocculation mechanism, originally proposed by Koelmans and Overbeek [27], and developed further by Koelmans [28], is based upon the destabilization of the polymer by increasing electrolyte concentration in the vicinity of the electrode. The electrolyte concentration increases as the result of the electrolytic decomposition of water (see Equation 1, Figure 1-2); as the concentration of electrolyte increases, the electrical double layer responsible for particle - particle repulsion is depressed, which results in a reduced energy barrier to flocculation. At a certain critical electrolyte concentration particle attraction will overcome repulsion, and irreversible flocculation and deposition onto the electrode will occur. The time required for the concentration of the electrolyte to increase to a level sufficient to initiate deposition is known as the critical time or the induction period; prior to this time current will pass with no accompanying deposition taking place. An expression for the electrolyte concentration as a

function of time (prior to the beginning of deposition) is found by solving Fick's second law of diffusion using the appropriate boundary conditions; this solution is outlined in Appendix I. The resulting expression is:

$$C_L = C_0 + (1-t_1)(2j/F)(t/(\pi D_0))^{1/2} \quad (3.18)$$

where C_L is the electrolyte concentration, C_0 is the initial bath electrolyte concentration, j is the current density, t_1 is the hydroxyl ion transport number, D_0 is the diffusion coefficient of the hydroxyl ion, and t is the time. Rearranging Equation (3.18) to solve for the critical time yields:

$$t^* = D_0((\Delta C)/(2j(1-t_1)))^{1/2} \quad (3.19)$$

where ΔC is the increase in electrolyte concentration required to bring about flocculation ($C_L - C_0$). From Equation (3.19) it is seen that the critical time is inversely proportional to the square of the current density. Prior to the deposition of a resistive film, the current density is directly proportional to the product of the field strength and the bath conductivity:

$$j = aVk \quad (3.20)$$

where a is a constant dependent on the cell geometry, V is the applied voltage, and k is the conductivity of the bath. For a system in which deposition is governed by the flocculation mechanism, the critical time is then found to be inversely proportional to the square of both the bath conductivity and the

applied voltage [28].

The third mechanism which may play a role in the formation of a film of polymer on the electrode during electrodeposition is the accumulation mechanism. This mechanism was first proposed by Hamaker and Verwey in 1939 to explain the development of an irreversibly coagulated deposit on an electrode upon applying an electrical potential across an otherwise stable suspension [21]. Hill, Lovering, and Rees [24] analyzed the electrodeposition of powdered barium strontium carbonate from a non-aqueous suspension, and found that their results could be explained by a model based on the accumulation mechanism. The mechanism proposed by Hamaker and Verwey considers the formation of an insulating film during electrodeposition to be analogous to the sedimentation and coagulation observed, for example, during the centrifugation of a colloiddally stable suspension. It is proposed that the actual destabilization mechanisms occurring in sedimentation and electrodeposition are identical, with the gravitational force exerted during sedimentation replaced by a coulombic electrical force during electrodeposition. Significantly, Hamaker and Verwey noted that if this mechanism governs electrodeposition, the electrostatic charge on the particles in the bath does not play an important part in the destabilization of the polymer and the formation of a film, and no electrochemical discharge of the stabilizing ions is necessary. In this case, the role of the

electrical field is to exert a force on the charged particles, and electrodeposition becomes primarily a mechanical process.

As noted by Del Pico [14], in sedimentation particles undergoing destabilization may be considered in two categories; those which have already coagulated, and those which are simply concentrated in the vicinity of the deposit and not yet coagulated. This will result in the formation of two layers, referred to as the "fixed" and "fluid" layers, respectively, which will exhibit considerably different properties. The fixed layer, being irreversibly coagulated, cannot be redispersed upon agitation or other mechanical influence, whereas the fluid layer, having not coagulated, can be redispersed upon stirring, etc. It is expected that fixed and fluid layers would be observed in electrodeposition if the accumulation mechanism were the cause of deposition; a schematic of these fixed and fluid layers at an electrode surface is shown in Figure 3-26.

A qualitative analysis of the sedimentation process can be made by considering the energy of interaction of particles which have moved to a surface (e.g. the bottom of a container) under the influence of gravity; this energy of interaction, as presented by Hamaker and Verwey [21], is shown in Figure 3-27, and represents the summation of the attractive and repulsive energies acting on the particles. The repulsive energy is provide by the electrical double

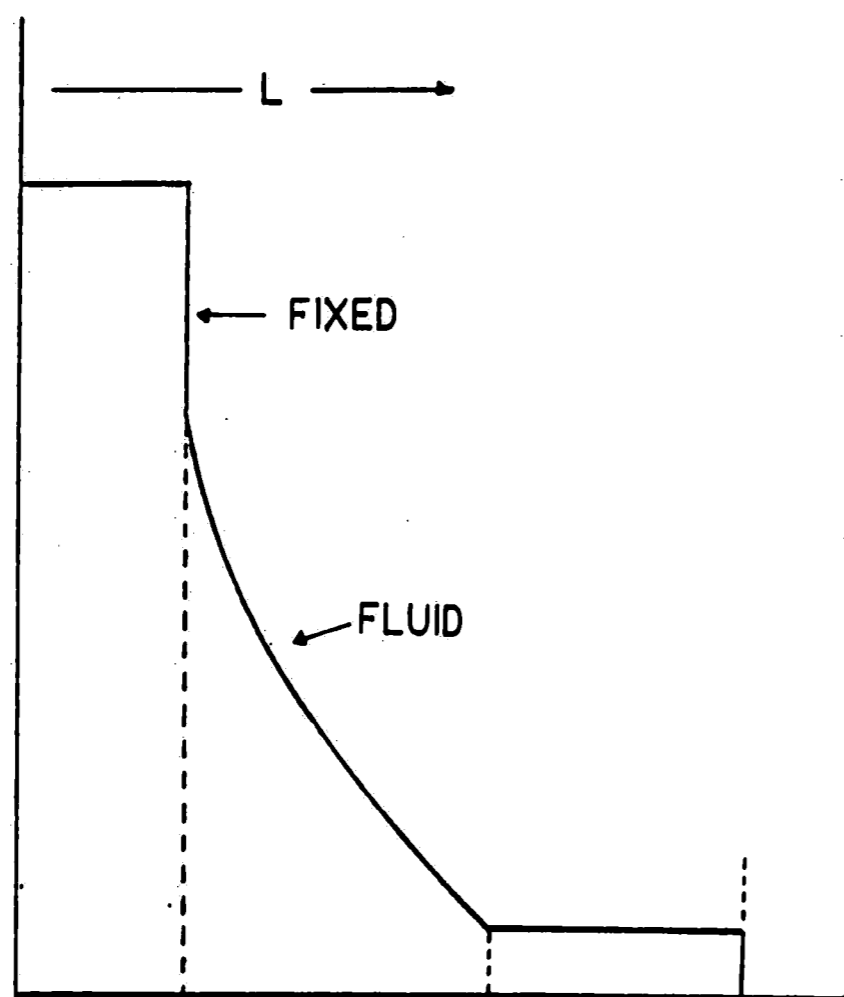


Figure 3-26: Schematic of the fixed and fluid layers expected with the accumulation mechanism of electrodeposition.

layer surrounding the particles, and, as indicated in Figure 3-27, is a function of the distance between the particles. The particles are not able to move together as a result of this repulsive energy, consequently they will be separated by a distance such that the repulsive force and the attractive forces (including Van der Waals forces and any force pushing the particles together) are in equilibrium. As the sedimentation process progresses, additional particles will settle onto those initially settled, and act upon these lower particles with a pressure which is schematized in Figure 3-27 by curve c; this pressure is due to the gravitational force exerted on the accumulated particles, and is independent of the particle separation. The energy of interaction between the particles is then no longer represented by curve a, but rather by the sum of curves a and c. The sum of these curves results in a local energy minimum, as can be seen in Figure 3-28. The particles will then be separated by the distance at which this local energy minimum occurs, and the total repulsive energy between the particles is given by the difference between S and M in Figure 3-28. Further settling of particles results in the the development of a concentrated fluid layer, and an increased pressure on the lower particles; this increased pressure is represented in Figure 3-28 by an increasing slope of curve c. Notice that as the slope of curve c increases both the particle separation distance (R_m) and the energy barrier to flocculation ($S - M$) decrease. At some critical fluid

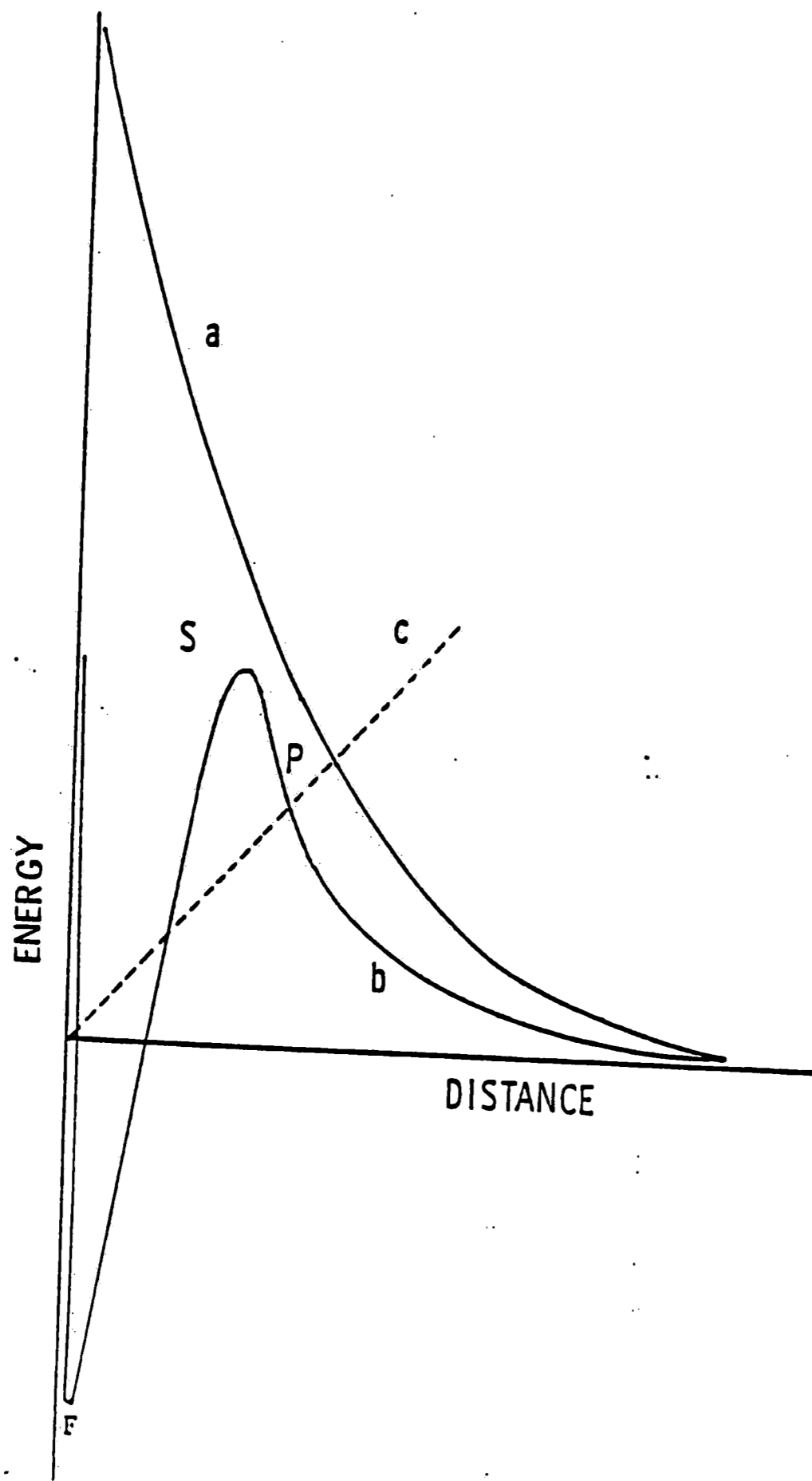


Figure 3-27: Potential energy curve for a colloidally stable system.

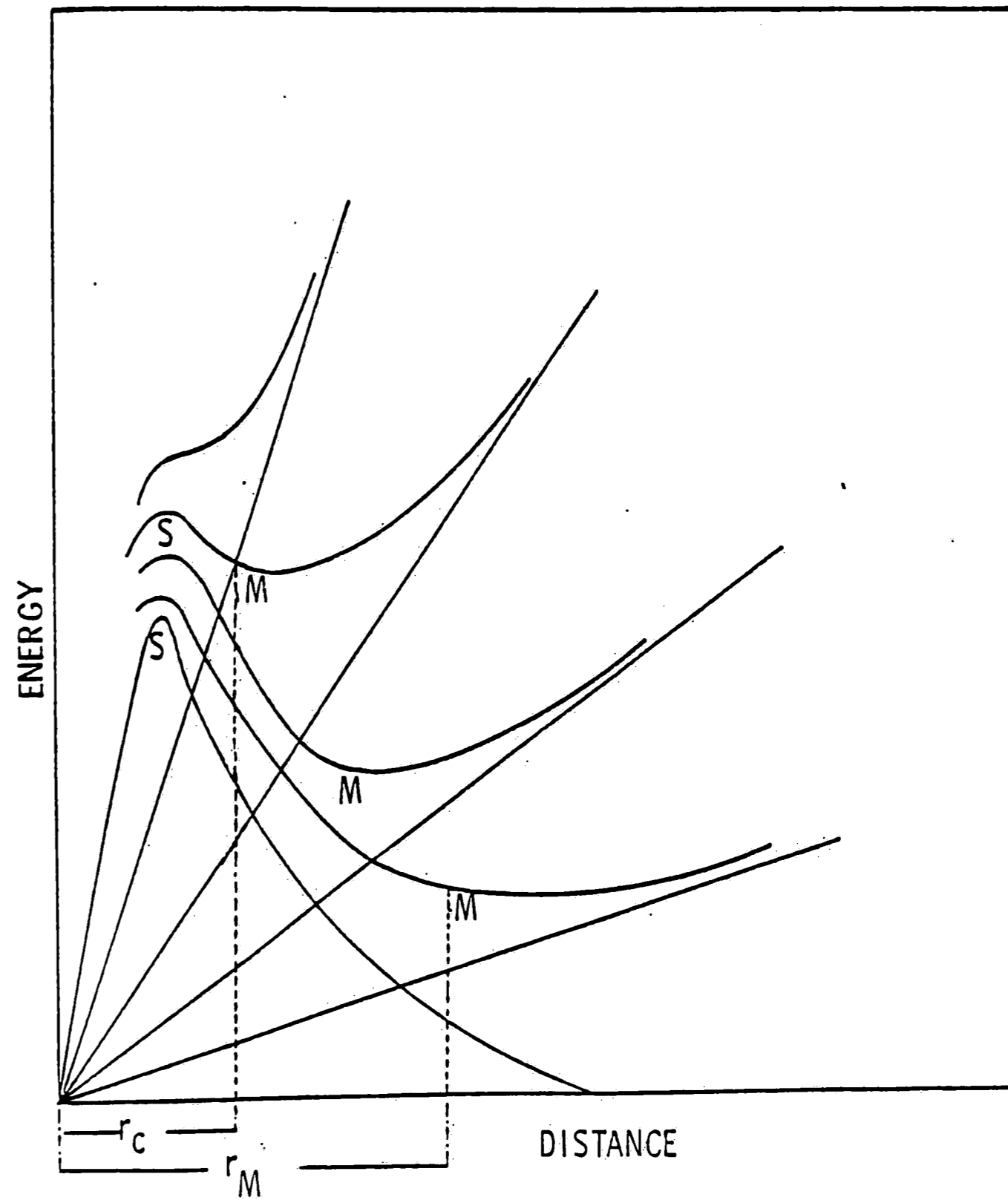


Figure 3-28: Summation of repulsive, attractive and pressure forces acting on the particles.

layer thickness sufficient force will be exerted upon the initially settled particles to "push" them over the potential energy barrier into the potential energy well F (Figure 3-17), where attractive energy is predominant, resulting in irreversible coagulation and formation of a fixed layer of polymer. As settling continues, the fixed layer grows, while the fluid layer remains at the required critical thickness.

In electrodeposition the situation is similar to that described for sedimentation, with the container surface replaced by the electrode, and the gravitational force exerted on settling particles replaced by a coulombic electrical force exerted on electrophoretically migrating charged particles [14]. The "electrical pressure" that results from the force exerted upon a layer of particles may be depicted in the same way as the gravitational pressure, thus the curves in Figures 3-27 and 3-28 apply to electrodeposition as well as sedimentation.

The experimentally observed induction period or critical time is explained in the accumulation mechanism as the time required to the development of a fluid layer of sufficient thickness for initiate irreversible coagulation and deposition. This explanation is considerably different than that proposed for the flocculation mechanism (ref. page 103), consequently an examination of the effect of various electrodeposition parameters on the induction period

would be expected to yield information concerning the deposition mechanism. A mathematical analysis of the accumulation mechanism was performed (similar to that of Hill, Lovering, and Rees [24]), and is presented in Appendix II. From this analysis the following expression for the critical time expected with the accumulation mechanism was obtained:

$$t^* = (4\pi\eta\sigma_1^*) / (a\epsilon^2\xi^2 (V/L)^2 C_0) \quad (3.21)$$

where η is the bath kinematic viscosity, σ_1^* is the normal stress (pressure) required to initiate coagulation, a is the particle radius, ϵ is the dielectric constant of the bath, ξ is the zeta potential of the particle double layer, C_0 is the concentration of particles in the bath, and (V/L) is the electric field strength. From Equation (3.21) it can be seen that, as with the flocculation mechanism, the critical time is predicted to be inversely proportional to the applied voltage for the accumulation mechanism. However, with the accumulation mechanism the induction period is also inversely proportional to the bath particle concentration, and independent of the bath conductivity. A summary of the effect of electrodeposition and bath parameters on the induction period for the two mechanisms is presented in Table 3-7. From this table it is evident that careful measurement of the effect of particle concentration and bath conductivity on the induction period should provide information concerning the mechanism governing deposition. Also, with the flocculation mechanism the film deposited would not

Table 3-7: The effect of electrodeposition and bath parameters on the critical time.

	<u>Voltage</u>	<u>Conductivity</u>	<u>Latex Concentration</u>
Accumulation Theory	V^{-2}	indep.	C^{-1}
Flocculation Theory	V^{-2}	K^{-2}	indep.

be expected to exhibit the two - layer (fluid and fixed) behavior predicted if deposition were result of particle accumulation; thus, analysis of the film characteristics during deposition should aid in the determination of the mechanism of electrodeposition.

3.4.2 Results and Discussion

For the electrodeposition of the polyurethane acrylic latex stabilized with an adsorbed quaternary ammonium surfactant, the current - time behavior, kinetic data, and film thickness - applied voltage data (ref. Figures 3-3, 3-14, and 3-10) all pointed toward the formation (initially) of an electrically conductive film. In

addition, as noted earlier, Beck [5] and Wagener [56] observed that the quaternary ammonium group showed little tendency to undergo charge destruction at the cathode either as a result of alkaline deprotonation or electrochemical reduction. Consequently it was concluded that the first mechanism of deposition discussed (charge destruction) did not occur in the cathodic electrodeposition of the polyurethane acrylic latex system under investigation.

3.4.2.1 Film Characterization

In order to observe the film characteristics during deposition, a series of electrodepositions was carried out in which the cathode was left in the bath for varying times after the end of the deposition run; this differed from the usual procedure in which the sample was removed from the bath immediately following deposition. As reported by Del Pico and Botsaris [15], the presence of a fluid layer would be indicated by a decreasing film mass with increasing "waiting time" in the bath after the electric field was removed. Humayun [25] reported a decreasing film mass as a function of waiting time for the cathodic electrodeposition of epoxy latexes, however it is possible that the observed trend in that study resulted from the poor coalescence of the glassy polymer on the cathode, rather than the occurrence of the accumulation mechanism. In Figures 3-29 and 3-30 are shown the results obtained with the polyurethane acrylic latex system deposited at two different voltages (50 V. and 160 V.). It was desired to measure the waiting

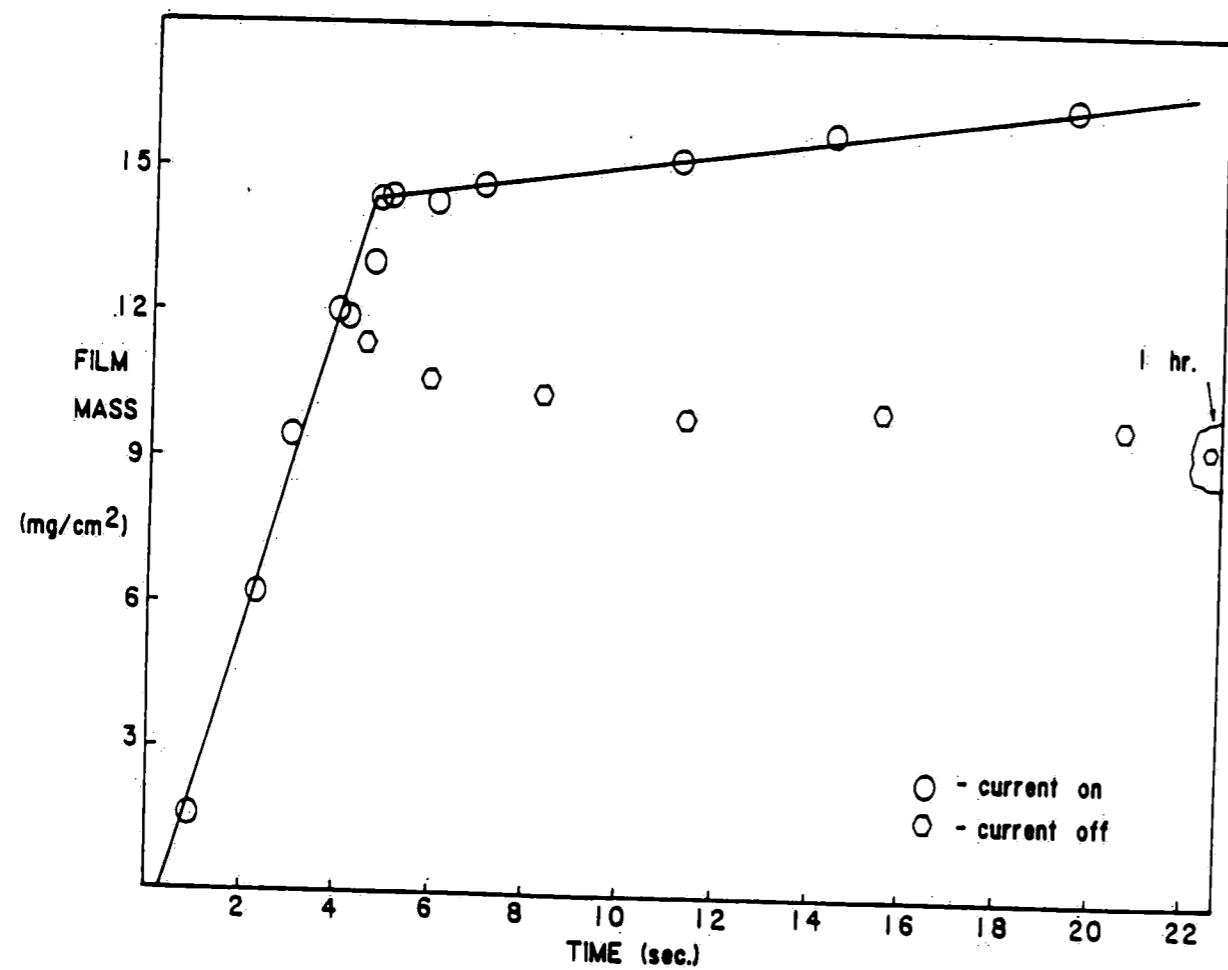


Figure 3-29: Film mass as a function of waiting time; polyurethane acrylic latex deposited at 160 V.

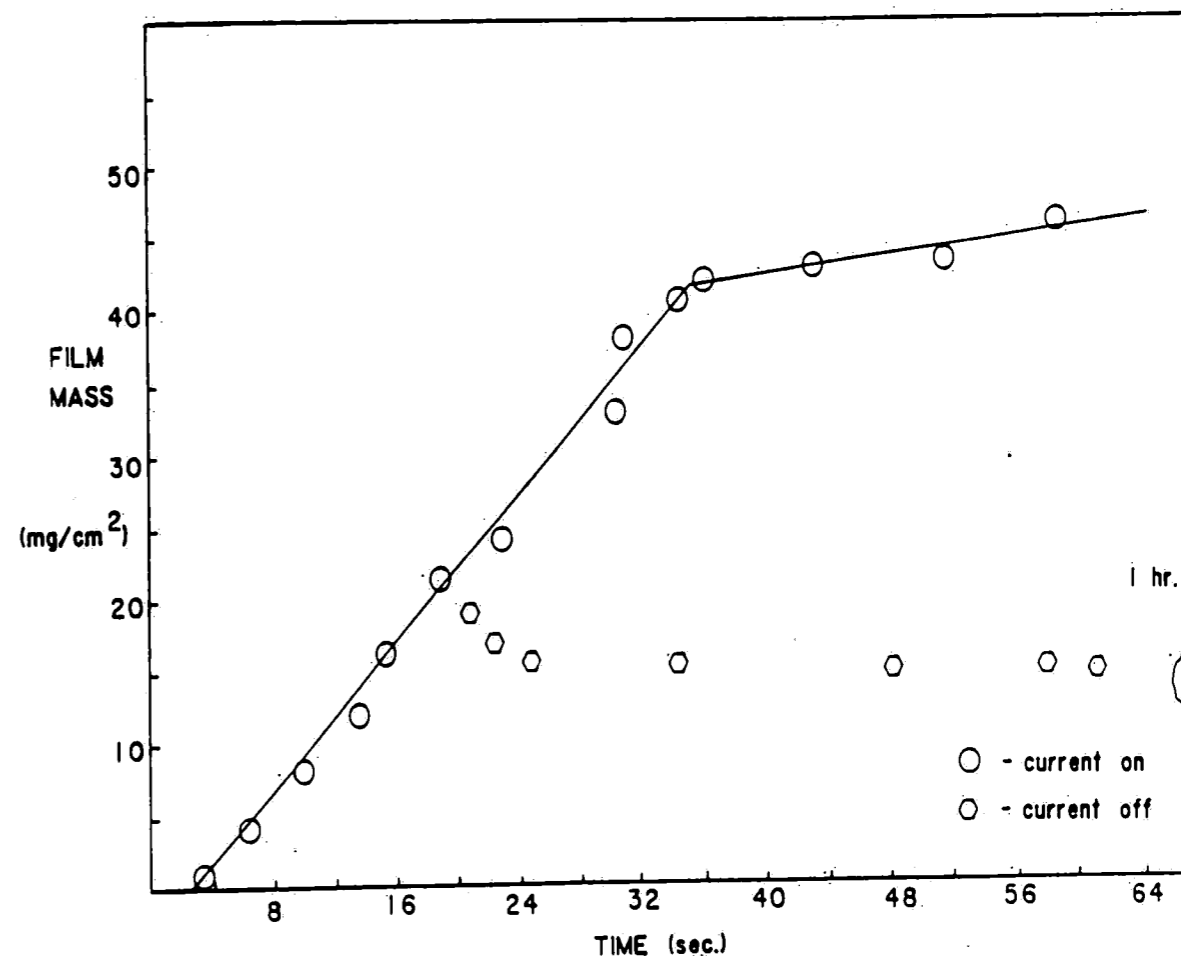


Figure 3-30: Film mass as a function of waiting time; polyurethane acrylic latex deposited at 50 V.

time from a point before current cut-off occurred, as after this point the fluid layer would be difficult to detect; consequently, deposition was stopped after 4 seconds at 160 V., and after 20 seconds at 50 V. From Figures 3-29 and 3-30 it is evident that the deposited film mass did decrease with increased waiting time in the bath following deposition, thus indicating the presence of a fluid layer in addition to the irreversibly coagulated fixed layer. The percent decrease in film mass after "infinite" waiting time (1 hour) for deposition at 160 V. was approximately 18%, while for deposition at 50 V. the percent decrease was approximately 25%. This increase in the fluid layer thickness with decreasing voltage can be explained by the accumulation mechanism; as the voltage was decreased the force on the particles in the fluid layer decreased, and a thicker fluid layer was required to exert sufficient pressure on the particles next to the electrode to initiate deposition (see Appendix II).

The data obtained for the film mass as a function of waiting time could then be satisfactorily explained in terms of the accumulation mechanism, and provided evidence for the occurrence of this mechanism in the cathodic electrodeposition of the polyurethane acrylic latex.

3.4.2.2 Induction period

An attempt was made to measure the induction period as a function of latex solids at constant conductivity; as indicated in Equations (3.20) and (3.21), the induction period should be inversely proportional to the latex solids if the accumulation mechanism were predominant, and independent of the latex solids if deposition took place by the flocculation mechanism. However, the critical times measured were extremely short (0.5 - 1.5 sec.) and reflected considerable experimental error (0.3 sec.), thus no conclusions could be drawn concerning the effect of the latex solids on this critical time. Kovac-Kalko [30] and Pierce [39] observed similarly short induction periods with constant voltage electrodeposition, and attributed the rapid initiation of deposition to the high current densities present at the beginning of deposition, where the current is limited only by the bath resistance. Consequently, it appears that in order to accurately determine the effect of the latex solids and the bath conductivity on the induction period, and thereby unambiguously specify the mechanism of electrodeposition for the quaternary ammonium stabilized polyurethane acrylic latex system, constant current density electrodepositions must be performed. At constant current density the rate of development of the conditions necessary to initiate deposition (either the accumulation of a sufficiently thick fluid layer of particles or an increase in the electrolyte

concentration to the critical level) could be controlled at a level low enough to permit accurate measurement of the critical time.

4. Conclusions

A cationic polyurethane acrylic latex was synthesized which showed unique physical properties, similar to those observed with latex interpenetrating polymer networks. This behavior resulted from extensive but incomplete mixing of the polymer components, and was reflected in a broadened glass transition and increased damping over a wide temperature range. Of the variations on the polymerization recipe, the best electrodeposition results were obtained with the lauroyl peroxide initiated polyurethane acrylic latex system. This latex deposited much better films than the previously examined epoxy latexes, primarily as a consequence of the improved physical properties of the polyurethane acrylic polymer.

Cathodic electrodeposition of the polyurethane acrylic latex over the range 30 - 225 V. showed that no film rupture occurred in this voltage span during deposition, indicating that the optimum electrodeposition voltage for this system was 225 V. The current time behavior and film morphology of the polyurethane acrylic latex showed that, with proper optimization of the electrodeposition and bath parameters, it was possible to deposit a high quality, thin, glossy film from an ammonium stabilized latex. In the cathodic electrodeposition of a commercial resin in solubilized form, rupture occurred at applied voltages greater than 140 V. While the commercial resin generally deposited more rapidly, resulting in a

thinner film than obtained with the latex system, the coulombic efficiency of deposition with the latex was much greater than that of the commercial resin. With proper formulation of the latex it was possible to obtain coulombic efficiencies ten times greater than those obtained with the commercial resin in the solubilized form.

The film thickness at current cut-off decreased with increasing applied voltage for the polyurethane acrylic latex, while with the commercial resin system the ultimate film thickness increased with increasing applied voltage. This opposite behavior indicated different deposited film properties, and a different mechanism of deposition for the two systems. Both the polyurethane acrylic latex and the solubilized commercial resin system obeyed Faraday's Law during deposition (after an initial induction period); that is, the amount of polymer deposited was directly proportional to the quantity of charge passed at any applied voltage and any deposition time.

A study of the kinetics of electrodeposition at constant applied voltage with the polyurethane acrylic latex showed that the film growth occurred in two distinct stages. In the first stage the film growth was linear with the deposition time, and strongly dependent on the applied voltage, thus the film growth was unimpeded at the cathode and a conductive film was being formed. During the second stage the conductivity of the film rapidly decreased as a

result of an accelerating process of electroosmosis and removal of the adsorbed surfactant from the deposited polymer. In the second stage the film growth was most accurately modelled by a linear dependence on the square root of time, indicating that transport of ions through the deposited film was the rate limiting step in this stage of deposition. Electrodeposition of the solubilized resin occurred in a single stage following an induction period, and a linear dependence of film growth on the square root of the deposition time was found for the entire growth period. Therefore, an insulating, ohmic film was rapidly formed, and transport of ions through the film controlled the deposition rate during the entire deposition with the commercial solubilized resin. The electrodeposition of a polyurethane acrylic latex stabilized by functional groups able to undergo charge destruction showed a film growth behavior similar to that found with the commercial solubilized resin; the film growth was accurately described by a linear dependence on the square root of the deposition time throughout the deposition process. From these results it may be concluded that the electrodeposition behavior of the ammonium stabilized polyurethane acrylic latex was a result of the inability of the ammonium functional group to experience charge destruction at the cathode, and was not due simply to the particulate nature of the latex system. Additional evidence for the lack of charge destruction during electrodeposition of the ammonium stabilized

latex was provided by the observed increasing bath conductivity during electrodeposition, the decrease in film thickness with increasing applied voltage, and the erratic film growth behavior observed with commercial resin emulsion samples prepared with the ammonium surfactant.

It was shown that the films deposited from the polyurethane acrylic latex consisted of two layers, a "fixed" layer of irreversibly coagulated polymer, and a "fluid" layer in which the polymer was concentrated but not coagulated. The fluid layer was observed to increase in thickness with decreasing applied voltage. The existence of a two - layer film provided a clear indication that the accumulation mechanism proposed by Hamaker and Verwey [21] governed the deposition of the ammonium stabilized latex. A mathematical analysis of the flocculation and accumulation mechanisms showed that the measurement of the induction period prior to the initiation of deposition would indicate which mechanism was actually taking place; however, attempts to measure this induction period were unsuccessful, and the mechanism of deposition was therefore not proven unambiguously.

5. Recommendations for Future Work

During the research performed for this report it became apparent that several areas of the cathodic electrodeposition process with the latex system warranted examination beyond that possible in this study. These areas are outlined briefly below.

- Latex Particle Size Distribution. While Hamaker indicated that the particle size would not be expected to exert a profound effect on the electrodeposition process [22], it was postulated that the particle size might affect the electrodeposition process in such areas as gassing, deposition rate, and current cut-off behavior by affecting the packing of the particles during the first stage of film growth. In addition, fractionation of the particles in the bath could conceivably occur, which would affect the electrodeposition behavior after multiple depositions from the same bath.
- Constant Current Deposition. As mentioned in section 4, a study of the induction period at constant current density would be expected to provide evidence indicating the predominance of either the accumulation or the flocculation mechanism of electrodeposition.
- Effect of Stirring Rate. While all of the depositions performed in this study were done in an unstirred bath, it was realized that agitation of the bath would affect the development of either a boundary region of increased electrolyte concentration or a boundary layer of increased particle concentration. Thus if either the accumulation mechanism or the flocculation mechanism governs deposition, the deposition behavior would be expected to be altered significantly with bath agitation. Beck [4] examined the effect of agitation on the deposition of solubilized resins; thus far no work has been done on the effect of agitation on the deposition of latexes that do not experience charge destruction at the electrode.
- Effect of the Surfactant Structure. The results of this study clearly indicated that the stabilizing functional group may play a predominant role in the electrodeposition behavior of a polymer latex; however the surfactant was not systematically varied, and no general relationship

between the electrodeposition performance of the latex and such parameters as the pH stability and electrochemical reactivity of the surfactant could be deduced. Wagener et al [56] have reported preliminary data in this area, and found that varying the electrochemical reactivity of the ammonium surfactant by the alteration of substituent groups bound to the nitrogen resulted in dramatic changes in electrodeposition performance. It would be useful to extend this work to the polyurethane acrylic latex developed in this study.

- Refinement of the Mathematical Analysis of the Electrodeposition Process. While preliminary models describing the kinetics and mechanism of the cathodic electrodeposition of the latex system were developed in this study, considerable refinement of these models would be useful to allow broader application and a more quantitative treatment of the effects of such variables as the applied voltage, bath temperature, agitation rate, and latex properties on the overall electrodeposition process.

References

- [1] Allen, G., Bowden, M., Blundell, D., Hutchinson, F., Jeffs, G., and Vivoda, J.
Polymer 14(597), 1973.
- [2] Anderson, D., Murphy, E., and Tucci, J.
J. Coatings Tech. 50(646):38, 1978.
- [3] Beal, C.
Ind. Eng. Chem. 25(6):609, 1933.
- [4] Beck, F.
Prog. Org. Coatings 4(1), 1976.
- [5] Beck, F.
Farbe und Lack 73(298), 1968.
- [6] Bobalek, E., and Fischer, W., ed.
Organic Protective Coatings.
Reinhold Publishing Corp., New York, 1973.
pp.2-6.
- [7] Bosso, J., and Wismer, M.
U.S. Patent # 3,936,679.
- [8] Brewer, G., ed.
Advances in Chemistry. Volume 119: Electrodeposition of Coatings.
American Chemical Society, 1972.
- [9] Brewer, G.
Metal Finishing 50, 1976.
- [10] Brewer, G.
J. Paint Tech. 45(37), 1973.

- [11] Brown, W., and Campbell, G.
Variables Affecting the Kinetics of Polymer Deposition.
In Brewer, G. (editor), Electrodeposition of Coatings, pages
166-177. American Chemical Society, 1972.
- [12] Clayton, Sumner, Morse, and Johnson (Crosse and Blackwell,
Ltd.
British Pat. # 455,810.
1936.
- [13] Davey, W.
U.S. Patent # 1,294,627.
1919.
- [14] Del Pico, J.
The Mechanism of Electrodeposition Through a Low Polarity
Liquid.
PhD thesis, Tufts University, 1972.
- [15] Del Pico, J., and Botsaris, G.
Trans. IEEE 1-A(16):303, 1980.
- [16] Feinleib, M.
Trans. Electrochem. Soc. 88(11), 1945.
- [17] Fink, C., and Feinleib, M.
Trans. Electrochem. Soc. 94(309), 1948.
- [18] Finn, S., and Mell, C.
J. Oil Color Chem. 47(219), 1964.
- [19] Ghosh, P., and Maity, S.
Eur. Polym. J. 14(855), 1978.
- [20] Hadley, J.
Graduate Research Progress Report.
Technical Report 19, Emulsion Polymers Institute, Lehigh
University, 1983.
pp. 199-212.
- [21] Hamaker, H., and Verwey, J.
Trans. Far. Soc. 30(180), 1940.

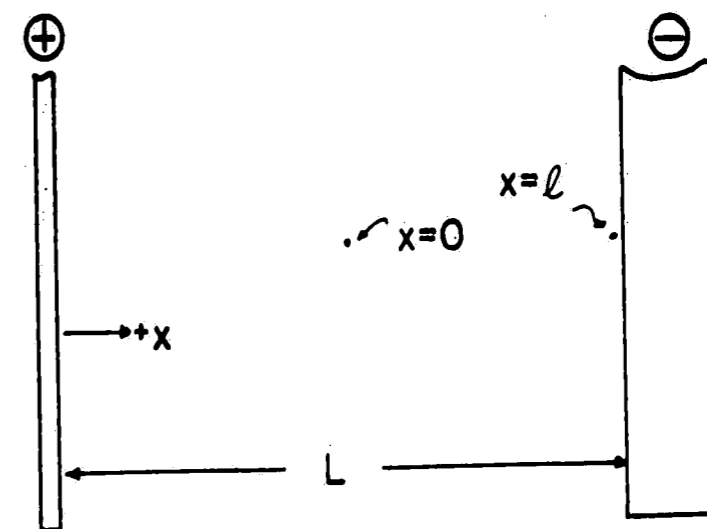
- [22] Hamaker, H.
Trans. Far. Soc. 30:279, 1940.
- [23] Hays, D., and White, C.
J. Paint Tech. 41(535):461, 1969.
- [24] Hill, C., Lovering, P., and Rees, A.
Trans. Far. Soc. 43(407), 1947.
- [25] Humayun, A.
The Kinetics and Mechanism of the Cathodic Electrodeposition
of Epoxy Latexes.
Master's thesis, Lehigh University, 1982.
- [26] Indian Patents # 33,058 and # 33115.
1946.
- [27] Koelmans, H., and Overbeek, J.
Trans. Far. Soc. 18(52), 1954.
- [28] Koelmans, H.
Philips Res. Rep. 10(181), 1955.
- [29] Kordomenos, P., and Nordstrom, J.
J. Coatings Tech. 54(696):33, 1982.
- [30] Kovac-Kalko, Z.
Electrochemistry of Polymer Deposition.
In Brewer, G. (editor), Electrodeposition of Coatings, pages
149-165. American Chemical Society, 1972.
- [31] Machu, W.
Handbook of Electropainting Technology.
Electrochemical Publications (1978).
- [32] Matsunaga, Y., Hoshino, Y., and Kobayashi, Y.
U.S. Patent # 3,823,118 (1974).
- [33] Munson, L.
J. Coatings Tech. 44(570):83, 1972.

- [34] Murphy, E.
Plating and Surf. Finish 24, 1978.
- [35] Olsen, D.
J. Paint Tech. 38(499):429, 1966.
- [36] Abbeywardena, P.
Graduate Research Progress Report.
Technical Report 19, Emulsion Polymers Institute, Lehigh University, 1983.
- [37] Phillips, S., and Damm, E.
J. Electrochem. Soc., Electrochem. Sci. 118(12), 1971.
- [38] Pierce, P.
J. Coatings Tech. 53(672):52, 1981.
- [39] Pierce, P., Kovac-Kalko, Z., Higginbotham, C.
Ind. Eng. Chem. Prod. Res. Dev. 17(4):317, 1978.
- [40] Saatweber, D., and Vollmert, B.
Angew. Makromol. Chem. 8(1), 1969.
- [41] Saatweber, D., and Vollmert, B.
Ang. Makromol. Chem. 9(93):61, 1969.
- [42] Schenck, H., and Stoelting, J.
J. Oil Color Chem. 12(482), 1980.
- [43] Shanmugam, N., and Guruswamy, S.
Metal Finishing (62), 1977.
- [44] Sheppard, S., and Eberlin, L.
Ind. Eng. Chem. 17(711), 1925.
- [45] Sheppard, S.
Trans. Am. Electrochem. Soc. 52(711), 1927.

- [46] Sperling, L., Chiu, T., and Thomas, D.
J. Appl. Polymer Sci. 17(2443), 1973.
- [47] Sperling, L., and Thomas, D.
U.S. Patent # 3,833,404 (1973).
- [48] Sperling, L., Chiu, T., Thomas, D., and Hartman, C.
Intern. J. Polym. Mater. 1(331), 1972.
- [49] Sumner, C.
Trans. Far. Soc. 35(272), 1940.
- [50] Sumner, C.
Chemistry and Industry 2072, 1967.
- [51] Tawn, A., and Berry, I.
J. Oil Color Chem. 48(790), 1965.
- [52] Turner, W., and Coler, M.
Ind. Eng. Chem. 30(11):1282, 1938.
- [53] Vanderhoff, J., El-Aasser, M.S., and Ugelstad, J.
U.S. Pat. # 4,177,177.
1979.
- [54] Vanderhoff, J., El-Aasser, M.S., and Hoffmann, J.
U.S. Patent # 4,070,323 (1978).
- [55] Veba Chemie, AG Technical Bulletin #22-ME-871-6.
- [56] Wagener, E., Kurowsky, S., Gibbs, D., and Wessling, R.
Effect of Surfactant Structure on the Electrodeposition of Cationic Latexes.
In Piirma, I. (editor), Emulsion Polymerization. Academic Press, N.Y., 1982.
- [57] Wessling, R.
The Cathodic Electrodeposition of Polymer Colloids.
In Parfitt, G., and Patsis, V. (editors), Advances in Organic Coatings Science and Technology. Technomic Publ. Co., Westport, Ct., 1980.

- [58] Wessling, R., Gibbs, D., Settineri, W., and Wagener, E. Studies in Cathodic Electrodeposition. In Brewer, G. (editor), Electrodeposition of Coatings. American Chemical Society, 1972.
- [59] Wismer, M. Organic Coatings and Plastics Chemistry 45, 1981.
- [60] Wismer, M., Pierce, P., Bosso, J., Christenson, R., Jerabek, R., and Zwack, R. J. Coatings Tech. 54(688):35, 1982.
- [61] With, A. The Basic Principles of Electrophoretic Coating. In Chapman, B., and Anderson, J. (editors), Science and Technology of Surface Coating. Academic Press, N.Y., 1974.
- [62] Woo, L. U.S. Patent # 4,241,200 (1980).

I. Mathematical Analysis of Flocculation Mechanism



This mechanism assumes that deposition of the polymer takes place as a result of double-layer depression, which is caused by the generation of OH^- ions at the cathode. A critical time is expected prior to which a build up of OH^- ions occurs with no deposition taking place. With this assumed mechanism of deposition, the effect of various system parameters on the critical time, t^* , may be determined in a manner similar to that applied by Koelmans [28].

There are various fluxes of OH^- ions:

1. Electrophoretic migration:

$$J_1 = It_{\text{OH}}/(FA) \quad (5.1)$$

where J_1 is the electrophoretic ion flux, I is the current, F is Faraday's number, A is the cross-sectional area, and t_{OH} is the ion transport number.

2. Diffusion:

$$J_2 = -D \frac{\partial C_{OH^-}}{\partial x} \quad (5.2)$$

where J_2 is the diffusive ion flux, D is the diffusion coefficient, and $\frac{\partial C_{OH^-}}{\partial x}$ is the concentration gradient.

(This assumes that convective transport = 0 for our unstirred system). Thus the total OH^- flux is:

$$J = J_1 + J_2 \quad (5.3)$$

$$J = -D \frac{\partial C_{OH^-}}{\partial x} + (t_{OH^-} I / FA) \quad (5.4)$$

The accumulation of OH^- is given by the divergence of J :

$$\frac{\partial C_{OH^-}}{\partial t} = \nabla \cdot J \quad (5.5)$$

or, expanding:

$$\frac{\partial C_{OH^-}}{\partial t} = \frac{\partial}{\partial x} (D_{OH^-} \frac{\partial C}{\partial x}) + \frac{\partial}{\partial x} (\frac{I}{FA} t_{OH^-}) \quad (5.6)$$

Assuming that D , I , t_{OH^-} are not a function of the x position, we may write:

$$\frac{\partial C_{OH^-}}{\partial t} = D_{OH^-} \frac{\partial^2 C}{\partial x^2} \quad (5.7)$$

The boundary and initial conditions are:

1. At $t = 0$, $\frac{\partial C}{\partial x} = 0$
2. At $x = 1$, $J_{x=1} = D_{OH^-} (\frac{\partial C_{OH^-}}{\partial x})_{x=1} + \frac{I}{FA} t_{OH^-}$
3. At $x = 0$, $\frac{\partial C_{OH^-}}{\partial x} = 0$

A solution to the differential equation with this set of boundary and initial conditions, developed by Rosebrugh and Miller is:

$$\frac{C(x) - C_0}{Kl} = \frac{x}{l} - \frac{8}{\pi^2} \sum \frac{1}{m^2} \exp(-m^2 at) \cos mgj \quad (5.8)$$

where C_0 is the OH^- concentration in the bulk solution, $C(x)$ is the OH^- concentration at point x ,

$$K = (I/FA)(1 - t_{OH^-}) / D_{OH^-}$$

$$a = \pi^2 D_{OH^-} / 4l^2$$

$$g = \pi/2l$$

$$j = 1 - x$$

$$m = 2n + 1$$

An approximation to Equation (5.8) developed by Thompson and Cayley for $at < 1/2$ and $x = 1$ is:

$$\frac{C_l - C_0}{Kl} \approx (4/\pi^{3/2})(at)^{1/2} \quad (5.9)$$

Substituting in K and a , and rearranging leads to:

$$C_l = C_0 + \frac{2j(1 - t_{OH^-})}{F} \sqrt{\frac{t}{\pi D_{OH^-}}} \quad (5.10)$$

In the electrodeposition work performed in this study this approximation is very good, as error only arises for long deposition times and thin boundary (diffusion) layers, neither of which occurred in these experiments.

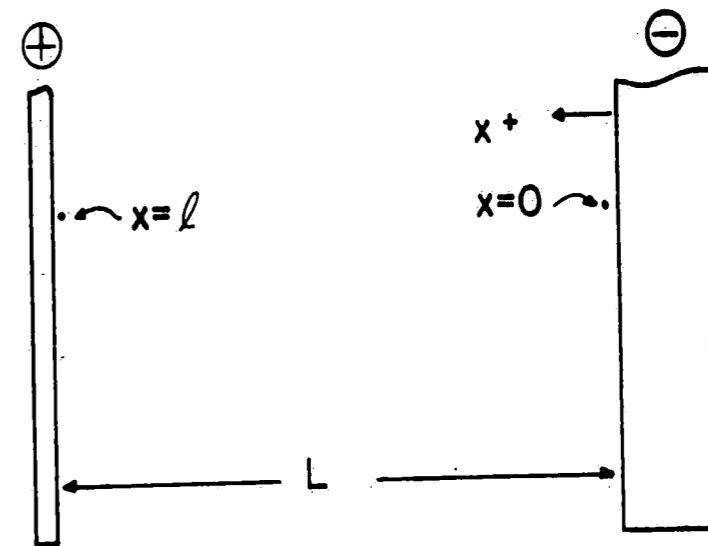
From the above equation ((5.10)) the following relationships are evident:

$$t^* \propto I^{-2}$$

$$t^* \propto V^{-2} k^{-2}$$

where V is the applied potential, and k is the conductivity of the suspending medium.

II. Mathematical Analysis of Accumulation Mechanism



With the accumulation mechanism, deposition takes place by the exertion of sufficient electrical force on the latex particles.

The initial voltage drop (prior to any deposition) is linear across the deposition cell. In this case the following expression may be written:

$$\frac{dV}{dx} = \frac{V}{L} \quad (5.1)$$

where V is the applied voltage, and L is the electrode separation in the x direction.

The velocity of the particles in the deposition bath may then be calculated from the Smoluchowski equation:

$$v = \frac{\epsilon \psi \left(\frac{d\psi}{dx} \right)}{4\pi\eta} \quad (5.2)$$

where v is the velocity in the x direction, ϵ is the dielectric constant of the medium, ζ is the zeta potential of the particle, and η is the kinematic viscosity of the medium. Substituting Equation (5.1) into Equation (5.2) leads to:

$$v = \frac{\epsilon \zeta (v)}{4\pi \eta L} \quad (5.3)$$

It should be noted that for a constant potential gradient the velocity of the particle is constant:

$$v = -dx/dt = \text{constant} = C_1 \quad (5.4)$$

If a cross-sectional area, A (parallel to the face of the electrode and normal to the x axis), is chosen at an arbitrary distance x_b from the electrode, the number of particles crossing the area A per second may be determined. Assuming that no particle depletion in the vicinity of A occurs, this flux is given by:

$$N_1 = C_0 v A \quad (5.5)$$

where C_0 is the bulk concentration of latex particles.

According to the accumulation model, a certain concentration of particles, C_p^* , at a thickness x_b would be required before deposition would start. At a "filling rate" of $C_0 v A$ the time required to raise the concentration to C_p^* may be determined:

$$\text{Initial concentration} = C_p^* x_b A$$

$$\text{Final (required) concentration} = C_p^* x_b A$$

$$\text{"Filling rate"} = C_0 v A$$

Therefore the time required is:

$$t^* = (C_p^* x_b A - C_0 x_b A) / (C_0 v A) \quad (5.6)$$

or

$$t^* = (x_b (C_p^* - C_0)) / (C_0 v) \quad (5.7)$$

Assuming that the initial bulk particle concentration is much less than that required to initiate destabilization and deposition ($C_0 \ll C_p^*$) Equation (5.7) may be rewritten:

$$t^* = (x_b C_p^*) / (C_0 v) \quad (5.8)$$

In the accumulation mechanism model, the thickness of particles of concentration C_p^* is required in order to exert the sufficient force on the particles next to the electrode to overcome repulsion and initiate deposition. The force on a single particle of radius a in an applied field dV/dx is [24]:

$$F = \epsilon \zeta a (dV/dx) \quad (5.9)$$

The force exerted on a layer of particles next to the electrode (at $x = 0$) by all of the particles from $x = 0$ to $x = x_b$ in the electrical field is given by the number of particles multiplied by

the force per particle. The number of particles is given by:

$$N_3 = A \int_{x=0}^{x=x_b} C_p(x) dx \quad (5.10)$$

Then the force exerted is:

$$F_t = a \epsilon \xi (dv/dx) A \int_{x=0}^{x=x_b} C_p(x) dx \quad (5.11)$$

Assume:

1. Linear voltage gradient across cell prior to beginning of deposition (ignores polarization of the electrode).
2. An average value of C_p may be substituted for $C_p(x) \approx \hat{C}_p$.

Then, integrating Equation (5.11) from $x = 0$ to $x = x_b$ yields:

$$F_t = a \epsilon (V/L) A \xi x_b \hat{C}_p \quad (5.12)$$

F_t is the force exerted on the particles next to the cathode, i.e. those particles which would deposit first. Note that a normal stress (force per unit area) would be exerted on this layer, given simply by:

$$\sigma_I = a \epsilon (V/L) \xi x_b \hat{C}_p \quad (5.13)$$

A certain critical stress will be required to overcome the repulsive forces exerted between the particles by electrostatic interaction. σ_I^* is defined as the force per unit area which must be applied to the layer of particles next to the electrode to induce coagulation and deposition. The thickness of the concentrated layer causing this stress may then be written:

$$x_b = \sigma_I^* / (a \epsilon (V/L) \xi \hat{C}_p) \quad (5.14)$$

Substituting Equation (5.14) into Equation (5.8) yields:

$$t^* = (\sigma_I^* L) / (a \epsilon \xi V \hat{C}_p) (C_p^* / C_0 \nu) \quad (5.15)$$

Noting that

$$\hat{C}_p \cong C_p^*$$

and

$$\nu = (\epsilon \xi V) / 4 \pi \eta L$$

the following expression for the critical or induction time is obtained:

$$t^* = (4 \pi \eta \sigma_I^*) / a \epsilon^2 \xi^2 E^2 C_0 \quad (5.16)$$